NASA CR-145186

EVALUATION OF HYDROGEN AS A CRYOGENIC WIND TUNNEL TEST GAS

By

Richard C. Haut

April 1977

Prepared under Grant No. NGR 47-003-052

By

OLD DOMINION UNIVERSITY

Norfolk, VA 23508

for

National Aeronautics and Space Administration

1. Report No	2. Government Accession No.	3. Recipient's Catalog No.
NASA CR-145186		

4 Title and Subtitle	5. Report Date
EVALUATION OF HYDROGEN AS A CRYOGENIC WIND TUNNEL TEST GAS	April 1977
	6 Performing Organization Code

7 Author(s)	8. Performing Organization Report No
Richard C. Haut	
	10. Work Unit No.

9 Performing Organization Name and Address	11. Contract or Grant No.
Old Dominion University Norfolk, VA 23508	NGR 47-003-052
	13. Type of Report and Period Covered
12 Sponsoring Agency Name and Address	Contractor Report
National Aeronautics and Space Administration Washington, DC 20546	14 Sponsoring Agency Code

15. Supplementary Notes Langley Technical Monitor: Jerry B. Adcock
Final Report - R. C. Haut is a doctoral student in the Mechanical Engineering and Mechanics Department at Old Dominion University (ODU). This contractor Report is based on his Doctoral dissertation, submitted to the School of Graduate Studies at ODU.

16. Abstract A theoretical analysis of the properties of hydrogen has been made to determine the suitability of hydrogen as a cryogenic wind tunnel test gas. By using cryogenic hydrogen, instead of air or cryogenic nitrogen, as the wind tunnel test gas, a significant increase in the test Reynolds number may be achieved without increasing the aerodynamic loads. Under sonic conditions, for example, compared to air at ambient temperature, cryogenic hydrogen at a pressure of one atmosphere produces an increase in Reynolds number of a factor of approximately fourteen while cryogenic nitrogen, at the same pressure, produces an increase of only a factor of about six.

The theoretical saturation boundary for parahydrogen is well defined. Thus, any possible effects caused by the liquefaction of the test gas can easily be avoided by knowing the maximum local Mach number on the model.

The nondimensional ratios used to describe various flow situations in hydrogen were determined and compared with the corresponding ideal diatomic gas ratios. The results were used to examine different inviscid flow configurations. This investigation concluded that the relatively high value of the characteristic rotational temperature causes the behavior of hydrogen, under cryogenic conditions, to deviate substantially from the behavior of an ideal diatomic gas in the compressible flow regime. Therefore, if an ideal diatomic gas, is to be modeled, cryogenic hydrogen is unacceptable as a wind tunnel test gas in a compressible flow situation.

However, at low Mach numbers where the assumption of incompressibility is valid, the deviations in the isentropic flow parameters for cryogenic parahydrogen from the

17. Key Words (Suggested by Author(s))		18. Distribution Statement
Real Gas	Normal Shock	Unclassified - Unlimited
Hydrogen	Prandtl-Meyer Flow	
Cryogenics	Power	
Wind Tunnel	Transport Properties	
Isentropic Flow		

19. Security Classif. (of this report)	20. Security Classif. (of this page)	21. No. of Pages	22. Price*
Unclassified	Unclassified	147	$6.00

* For sale by the National Technical Information Service, Springfield, Virginia 22161

Continuation of Item 16. Abstract
corresponding flow parameters for an ideal diatomic gas are negligible. Thus, in the incompressible flow regime, cryogenic hydrogen is an acceptable test gas.

Hydrogen properties and fan drive-power requirements related to a hydrogen wind tunnel were also examined. The drive power requirements were found to decrease with decreasing temperature and may be adequately predicted by using modified versions of the ideal gas equations. Since gaseous hydrogen is capable of penetrating and degrading the mechanical characteristics of numerous materials, materials known to be compatible with hydrogen must be used exclusively in the design of a hydrogen wind tunnel to avoid problems as a result of exposure to gaseous hydrogen.

A literature survey resulted in the conclusion that although hydrogen is a highly combustible substance, safety codes exist which, when followed, minimize the risk involved in handling hydrogen.

NATIONAL AERONAUTICS AND SPACE ADMINISTRATION

EVALUATION OF HYDROGEN AS A CRYOGENIC WIND TUNNEL TEST GAS

By Richard C. Haut*

Old Dominion University

Norfolk, Virginia

SUMMARY

A theoretical analysis of the properties of hydrogen has been made to determine the suitability of hydrogen as a cryogenic wind tunnel test gas. By using cryogenic hydrogen, instead of air or cryogenic nitrogen, as the wind tunnel test gas, a significant increase in the test Reynolds number may be achieved without increasing the aerodynamic loads. Under sonic conditions, for example, compared to air at ambient temperature, cryogenic hydrogen at a pressure of one atmosphere produces an increase in Reynolds number of a factor of approximately fourteen while cryogenic nitrogen, at the same pressure, produces an increase of only a factor of about six.

The theoretical saturation boundary for parahydrogen is well defined. Thus, any possible effects caused by the liquefaction of the test gas can easily be avoided by knowing the maximum local Mach number on the model.

The nondimensional ratios used to describe various flow situations in hydrogen were determined and compared with the corresponding ideal diatomic gas ratios. The results were used to examine different inviscid flow configurations. This investigation concluded that the relatively high value of the characteristic rotational temperature.

---

*Graduate Student, Department of Mechanical Engineering and Mechanics, Old Dominion University, Norfolk, Virginia.

causes the behavior of hydrogen, under cryogenic conditions, to deviate substantially from the behavior of an ideal diatomic gas in the compressible flow regime. Therefore, if an ideal diatomic gas, is to be modeled, cryogenic hydrogen is unacceptable as a wind tunnel test gas in a compressible flow situation.

However, at low Mach numbers where the assumption of incompressibility is valid, the deviation in the isentropic flow parameters for cryogenic parahydrogen from the corresponding flow parameters for an ideal diatomic gas are negligible. Thus, in the incompressible flow regime, cryogenic hydrogen is an acceptable test gas.

Hydrogen properties and fan drive-power requirements related to a hydrogen wind tunnel were also examined. The drive power requirements were found to decrease with decreasing temperature and may be adequately predicted by using modified versions of the ideal gas equations. Since gaseous hydrogen is capable of penetrating and degrading the mechanical characteristics of numerous materials, materials known to be compatible with hydrogen must be used exclusively in the design of a hydrogen wind tunnel to avoid problems as a result of exposure to gaseous hydrogen.

A literature survey resulted in the conclusion that although hydrogen is a highly combustible substance, safety codes exist which, when followed, minimize the risk involved in handling hydrogen.

TABLE OF CONTENTS

PAGE

LIST OF SYMBOLS

A	area
b	constant ($b = \theta_r \times k_B$)
B	constant
c	speed of sound
C_D	drag coefficient
C_L	lift coefficient
C_p	specific heat at constant pressure
C_v	specific heat at constant volume
D	supersonic wave drag
E_j	statistical energy of the state j
g	statistical weight of a degenerate state
g_n	nuclear degeneracy
h	Planck's constant ($h = 6.55 \times 10^{-27}$ erg-sec^{-1})
H	enthalpy
I	moment of inertia ($I = 4.67 \times 10^{-41}$ g-cm^2 for hydrogen)
j	rotational state
k	thermal conductivity
k_B	Boltzmann constant ($k_B = 1.373 \times 10^{-16}$ erg-sec^{-1})
ℓ	length of airfoil
L	total length of the diverging section of the nozzle
m_n	nuclear spin quantum number
$\dot{m}$	mass flow rate
M	Mach number
M_L	saturation local Mach number
M_w	molecular weight

LIST OF SYMBOLS (Continued)

n	number of moles
N_j	fraction of molecules in rotational state j
N_t	total number of molecules
p_j	statistical weight of the state j
P	pressure
Pr	Prandtl number
Pwr	Power
Q_{rot}	rotational partition function
R	gas constant
S	entropy
t	airfoil thickness
T	temperature
u	velocity
u_1	upstream velocity component normal to an oblique shock wave
u_2	downstream velocity component normal to an oblique shock wave
v	velocity component tangential to an oblique shock wave
w_1	velocity upstream of an oblique shock wave
w_2	velocity downstream of an oblique shock wave
x	distance downstream from the nozzle throat
y	nozzle summation constants
Z	compressability factor
α	angle of attack
β	concentration ratio of parahydrogen to orthohydrogen
	shock wave angle (in diamond-airfoil study)
γ	specific heat ratio

LIST OF SYMBOLS (Continued)

δ	small incremental value (e.g. δu small increment of velocity) deflection angle (in diamond-airfoil study)
Δ	increment (e.g. ΔT increment of temperature)
ε	energy required to produce a unit mass of liquid hydrogen (nitrogen)
η	viscosity
θ	local flow angle, Prandtl-Meyer function
θ_r	characteristic rotational temperature (θ_r = 84.837 K for hydrogen)
μ	Mach angle
ξ	local isentropic expansion coefficient
ρ	density
σ	mass of liquid hydrogen required to cool a unit mass of material through a given temperature range
ϕ	diamond-shaped airfoil half angle

Subscripts:

a	conditions upstream of an expansion or shock wave
b	conditions downstream of an expansion or shock wave
i	iteration value
k	summation index
n	normal component
o	values used in subprogram ISENT
s	constant entropy process
t	tangential component (in Prandtl-Meyer flow solution) total conditions (in other solutions)

LIST OF SYMBOLS (Concluded)

Subscripts (continued):

T	total conditions (in Prandtl-Meyer flow solution)
1	upstream conditions
2	downstream conditions

Superscripts:

*	ideal gas value (in Prandtl-Meyer flow solution)
'	calculated value (in normal shock solution)
*	sonic conditions

INTRODUCTION

The wind tunnel has been the primary tool for experimental aerodynamic research and development for many decades. Because of the increase in size and speed of proposed aircraft configurations, a need has developed over the years for improved ground testing capabilities in terms of Reynolds number. The need has been well documented, for example, in references 1 and 2. Programs aimed at the development of efficient transport aircraft and maneuvering fighter aircraft to operate at transonic speeds have demonstrated some of the deficiencies in the testing capabilities of present day wind tunnels, especially with respect to adequate Reynolds number simulation. In the transonic region, one of the major problems is the inability to adequately determine the effect of Reynolds number on the boundary layer - shock wave interactions, and in turn, on the performance, stability, and trim characteristics of the aircraft.

The test Reynolds number at a given Mach number may be increased by using a heavy gas rather than air as the test gas, by increasing the size of the model and tunnel, by increasing the operating pressure of the tunnel, and by reducing the test temperature. The dynamic pressure, mass flow rate, and power consumption of the tunnel will, in general, be affected by the method chosen to increase the Reynolds number.

The use of a heavy gas, such as Freon-12, is a well-known method of achieving high Reynolds numbers. However, when compressibility effects become significant, the difference between the ratios of specific heats between the heavy gas and air leads to an improper flow

simulation, thus making the use of a heavy gas unsuitable for tests at transonic speeds.

The more common approaches of increasing the size and increasing the stagnation pressure in order to increase the Reynolds number involve serious problems concerning the cost of construction and operation, the model and support loads, and the difficulty of providing continuous-flow capability due to the large power requirements.

The fourth method of increasing the test Reynolds number, reducing the test temperature, offers an attractive solution to many of the preceding problems. However, as the test temperature is reduced the properties of the test gas may begin to deviate significantly from the properties of air, which, for all practical purposes under the conditions encountered in flight, behaves like an ideal diatomic gas. The real gas effects may become appreciable at cryogenic temperatures and may alter the aerodynamic test results. Therefore, an analysis must be performed to determine if a particular gas at cryogenic temperatures and anticipated operating pressures is acceptable for wind tunnel research.

A cryogenic wind tunnel concept has evolved at the NASA Langley Research Center in which liquid nitrogen is sprayed directly into the tunnel circuit to cool the tunnel structure, remove the heat input from the drive fan, and balance the heat conducted into the stream through the tunnel walls. Nitrogen is the resulting test gas using this cooling procedure. Throughout the development of the concept, experimental and theoretical studies have been performed to assess the suitability of cryogenic nitrogen as a test gas. By analyzing real gas isentropic and normal shock solutions, and by measuring the surface

pressures on an airfoil, Adcock, Kilgore, and Ray, in reference 3, concluded that the real gas effects of nitrogen at cryogenic temperatures pose no problem in its application in a cryogenic transonic wind tunnel operating at stagnation pressures up to five atmospheres.

Nitrogen is, of course, not the only gas that may be considered for use at cryogenic temperatures. In theory, any diatomic gas will do. One of the most promising diatomic gases in addition to nitrogen is hydrogen. Because of the lower vapor temperature, even higher test Reynolds numbers may be obtained by using cryogenic hydrogen rather than nitrogen. For example, at a pressure of one atmosphere, when compared to ambient air, cryogenic nitrogen and hydrogen, produce increases in Reynolds number by factors of approximately six and fourteen respectively for sonic flows. Alternatively, in a given size wind tunnel, it is possible to achieve a desired test Reynolds number at a lower total pressure by using hydrogen instead of nitrogen, thereby reducing the model, sting, and balance loads.

This thesis contains a theoretical analysis of those properties of hydrogen needed to determine if, in fact, it is suitable for use as a wind tunnel test gas. The thesis is divided as follows: In Chapter I, some of the fundamental properties essential to understand hydrogen are presented. In Chapters II, III, and IV some of the nondimensional ratios used to describe various flow situations in hydrogen are determined and compared with the corresponding ideal diatomic gas ratios. Chapters V and VI present inviscid flow examples to illustrate the deviations studied in Chapters II through IV. Hydrogen properties and fan drive-power requirements related to a hydrogen wind tunnel are

presented in Chapter VII. Finally, recommendations are made concerning the use of hydrogen as a possible wind tunnel test gas.

CHAPTER I

PROPERTIES OF GASEOUS HYDROGEN

I.1. Introduction.

Hydrogen is a homonuclear diatomic molecule having a relatively high characteristic rotational temperature. Because of its molecular composition hydrogen demonstrates various anomalies in its properties affecting its suitability as a wind tunnel test gas. The purpose of this chapter is to introduce the reader to the major peculiarities.

I.2. Ortho-, Para-, Normal-, and Equilibrium Hydrogen.

Hydrogen consists of a mixture of two different types of molecules having different optical and thermal properties. These two distinct forms of hydrogen are known as parahydrogen ($p\text{-}H_2$) and orthohydrogen ($o\text{-}H_2$). The parahydrogen molecules have antiparallel nuclear spins and even rotational quantum numbers, while the orthohydrogen molecules possess parallel nuclear spins and odd rotational quantum numbers. Figure 1 illustrates the difference between ortho- and parahydrogen.

The thermodynamical equilibrium between ortho- and parahydrogen is governed by Boltzmann's distribution law as presented in reference 4. According to this law the fraction of the molecules, N_j, of the total number of molecules, N_t, in the rotational state j is given by the equation

$$N_j = N_t p_j \exp\left(\frac{-E_j}{k_B T}\right) \tag{1.1}$$

where

p_j = statistical weight of the state j

E_j = statistical energy of the state j

k_B = Boltzmann's constant

T = temperature

and where N_t may be taken as equal to one. Since all parahydrogen molecules have even rotational quantum numbers and all orthohydrogen molecules have odd rotational quantum numbers, the ratio, β, of the concentration of the two forms is given by

$$\beta = \frac{\left[p - H_2\right]}{\left[o - H_2\right]} = \frac{\sum_{j=even} p_j \exp\left(\frac{-E_j}{k_B T}\right)}{\sum_{j=odd} p_j \exp\left(\frac{-E_j}{k_B T}\right)} \tag{1.2}$$

Or, considering the energy of the state j and the statistical weight as governed by the quantum statistics applicable to the nuclei

$$E_j = j(j+1)\frac{h^2}{8\pi^2 I} = j(j+1)b$$

$$p_j = g_{nucl.} g_j = \begin{cases} 2j+1 & \text{for } j = \text{even} \\ 3(2j+1) & \text{for } j = \text{odd} \end{cases}$$

where

I = moment of inertia

h = Planck's constant

g = statistical weight of a degenerate state

then

$$\beta = \frac{\sum_{j=\text{even}} (2j+1) \exp\left\{\frac{-j(j+1)b}{k_B T}\right\}}{\sum_{j=\text{odd}} 3(2j+1)\exp\left\{\frac{-j(j+1)b}{k_B T}\right\}} \tag{1.3}$$

or

$$\beta = \frac{1 + 5 \exp\left(\frac{-6\theta_r}{T}\right) + 9 \exp\left(\frac{-20\theta_r}{T}\right) + 13 \exp\left(\frac{-42\theta_r}{T}\right) + \ldots}{3\left\{3 \exp\left(\frac{-2\theta_r}{T}\right) + 7 \exp\left(\frac{-12\theta_r}{T}\right) + 11 \exp\left(\frac{-30\theta_r}{T}\right) + \ldots\right\}} \tag{1.4}$$

where

$$\theta_r = b/k_B = 84.837 \text{ K (from reference 4)}$$

since

$$h = 6.55 \times 10^{-27} \text{ erg/sec}$$

$$I = 4.67 \times 10^{-41} \text{ g-cm}^2$$

$$k_B = 1.373 \times 10^{-16} \text{ erg/K}$$

Equation 1.4 gives the composition of equilibrium hydrogen as a function of temperature and is illustrated in figure 2. At high temperatures (around room temperature) the constant b is much less than $k_B T$ causing the equilibrium ratio to approach the ratio

$$\beta \to 1/3 \quad \text{(high temperature limit)} \tag{1.5}$$

The high temperature equilibrium mixture, consisting of twenty-five percent parahydrogen molecules and seventy-five percent orthohydrogen molecules, is classified as normal hydrogen and is the equilibrium composition of hydrogen at room temperature and above.

The value of b becomes much greater than $k_B T$ as the temperature approaches absolute zero, and from equation 1.4 the equilibrium ratio approaches the limit

$$\beta \to \infty \text{ (low temperature limit)} \qquad (1.6)$$

Thus, at very low temperatures equilibrium hydrogen consists of essentially all parahydrogen molecules. Hydrogen at the lower temperature limit consists of pure parahydrogen because as the temperature is lowered all molecules gradually pass into the lowest state having the quantum number zero, which is a parahydrogen state.

However, according to reference 4, the rate of conversion from parahydrogen to orthohydrogen, that is, the rate at which equilibrium between the two species is approached, is extremely slow unless the hydrogen is heated in the presence of a suitable catalyst, such as oxygen or charcoal. In general the self conversion rate (no catalyst present) is a function of temperature. For example at liquid air temperatures the half life, defined as the time required to convert one half of the excess ortho- or para composition present at the starting time, of the conversion is greater than a year while at 923 K and 0.0657 atmospheres the half life is only on the order of ten minutes. Since the hydrogen that would be used as a wind tunnel test gas would probably be stored in liquid

form, and considering that the experimental run times are relatively short compared to the para-ortho conversion time, the simplifying assumption will be made that the hydrogen gas being used in the wind tunnel is pure parahydrogen.

I.3 Characteristic Rotational Temperature.

As previously mentioned, the characteristic rotational temperature for hydrogen is relatively high. Because of this high value, hydrogen can exist in the gaseous state for temperatures lower than the characteristic rotational temperature. A range of influence associated with the characteristic rotational temperature can be expected so that at the lower temperature limit hydrogen should behave like an ideal monotomic gas and at the higher temperature limit (around room temperature) hydrogen should behave like an ideal diatomic gas.

The range of influence may be analyzed by considering the rotational partition function for a homonuclear diatomic molecule given as (see, for example, reference 5)

$$Q_{rot(odd)} = \frac{g_n(g_n-1)}{2} \sum_{j=even} (2j+1)\exp\left\{-j(j+1)\frac{\theta_r}{T}\right\} + \frac{g_n(g_n+1)}{2} \sum_{j=odd} (2j+1)\exp\left\{-j(j+1)\frac{\theta_r}{T}\right\} \qquad (1.7a)$$

or

$$Q_{rot(even)} = \frac{g_n(g_n+1)}{2} \sum_{j=even} (2j+1)\exp\left\{-j(j+1)\frac{\theta_r}{T}\right\} + \frac{g_n(g_n-1)}{2} \sum_{j=odd} (2j+1)\exp\left\{-j(j+1)\frac{\theta_r}{T}\right\} \qquad (1.7b)$$

where g_n is the nuclear degeneracy. Equations 1.7a and 1.7b are for odd and even mass number homonuclear molecules, respectively.

In most cases the characteristic rotational temperature, θ_r, is near absolute zero (for example, θ_r is 2.1 K for oxygen and 2.9 K for nitrogen). Thus, the temperatures at which the gaseous phase exists are much greater than the characteristic rotational temperature. Under these conditions equations 1.7a and 1.7b both reduce to the form

$$\left(Q_{rot}\right)_{T>>\theta_r} = \frac{1}{2} g_n^2 \sum_{j=0}^{\infty} (2j+1) \exp\left\{-j(j+1)\frac{\theta_r}{T}\right\} \qquad (1.8)$$

The sum for $\theta_r << T$ is essentially equal to the area under a curve of $(2j+1)\exp\{-j(j+1)\theta_r/T\}$ versus j and the summation may be replaced with an integral

$$\left(Q_{rot}\right)_{T>>\theta_r} = \frac{1}{2} g_n^2 \int_o^{\infty} (2j+1) \exp\left\{-j(j+1)\frac{\theta_r}{T}\right\} dj \qquad (1.9)$$

from which

$$\left(Q_{rot}\right)_{T>>\theta_r} = \frac{1}{2} g_n^2 \frac{T}{\theta_r} \qquad (1.10)$$

Because the value of the characteristic rotational temperature for hydrogen is large (θ_r = 84.837 K for hydrogen), equation 1.10 does not hold throughout the gaseous region of hydrogen. Equation 1.7a must be used to determined the rotational partition function of hydrogen because it has an odd mass number (equal to one). The nuclear degeneracy is given by

$$g_n = 2m_n + 1 \tag{1.11}$$

where m_n is the nuclear spin quantum number ($m_n = \frac{1}{2}$ for hydrogen). Substituting into equation 1.7a yields

$$Q_{rot} = Q_{rot,para} + Q_{rot,ortho} = \sum_{j=even} (2j+1)\exp\left\{-j(j+1)\frac{\theta_r}{T}\right\} + 3\sum_{j=odd} (2j+1)\exp\left\{-j(j+1)\frac{\theta_r}{T}\right\} \tag{1.12}$$

where the first summation represents the contribution from the para-states and the second summation represents the contribution from the ortho-states.

Figure 3 illustrates the influence range of the characteristic rotational temperature for parahydrogen. At temperatures well below the characteristic rotational temperature the rotational partition function, $Q_{rot,para}$, is approximately equal to one, signifying that the rotational mode is unexcited and that the gas should behave similar to an ideal monatomic gas. For parahydrogen this occurs for temperatures below approximately 75 K. For temperatures well above the characteristic rotational temperature the rotational partition function should approach the ideal diatomic gas rotational partition function given by equation 1.10. For parahydrogen, the rotational partition function must be multiplied by four since at higher temperatures equilibrium hydrogen consists of only twenty-five percent parahydrogen. Thus, for temperatures above approximately 200 K, the rotational contribution is the dominant factor and parahydrogen may be treated

as an ideal diatomic gas. Therefore, parahydrogen may be expected to behave similar to an ideal monatomic gas for temperatures less than 75 K and similar to an ideal diatomic gas for temperatures greater than 200 K.

The main part of this thesis will be concerned with how the characteristic rotational temperature influences the properties of gaseous hydrogen and the resulting deviations of hydrogen from the behavior of an ideal diatomic gas.

I.4 Parahydrogen Equation of State.

There are literally hundreds of "equations of state" which have been developed to describe parahydrogen. For example, references 6, 7, 8, 9, and 10 describe some of the equations of state to be found in the literature.

Today there are four general methods developed by the National Bureau of Standards (NBS) used to computerize the thermodynamic properties of fluids. These are: linear interpolation; thirty-three term modified Benedict Webb Rubin (MBWR); polynomial interpolation; and a twenty term MBWR. The linear interpolation method is an interpolation on a table of property values stored in computer. The method is fast but not very accurate (average of 1%) and requires more computer core storage than the other methods. The most accurate method, better than 0.1% average, is the polynomial interpolation method. The major disadvantage of the polynomial method is that the computations are slow relative to the other methods.

A good compromise, and a widely used method, is the thirty-three term modified Benedict Webb Rubin equation of state. The method is

faster than the polynomial interpolation and has an accuracy only slightly worse (0.1% average). The major disadvantage of the MBWR is the great inaccuracies near the critical region (20% error in density and 5% in temperature).

On a recommendation from the personnel of the NBS Cryogenics Division, the polynomial interpolation equation of state for para-hydrogen was selected for use in this study and a computer program was obtained directly from them. The program gives the thermodynamic and related properties of parahydrogen from the triple point to 300 K at pressures to 1000 bar.

I.5 Saturation Boundary.

The minimum total temperature which could conceivably be used in a hydrogen wind tunnel depends on several factors, but is basically dependent upon the onset of condensation. The assumption is made that condensation must be avoided under all conditions to be encountered during the testing of a model in the wind tunnel and that condensation is most likely to occur in localized low pressure regions near the model. These low pressure regions may be thought of in terms of high local Mach numbers encountered near the model. To calculate the theoretical saturation boundary, the assumption is made that the test gas expands isentropically from the total conditions to the maximum local Mach number.

Using the vapor pressure equation for parahydrogen given in the NBS program, along with the above assumptions, the theoretical minimum total temperatures have been calculated for a range of total pressures and maximum local Mach numbers, and are presented in

figure 4. For example, if a hydrogen wind tunnel was operating at a total pressure of five atmospheres and a maximum local Mach number of 0.5, the minimum total temperature which could be used to avoid condensation would be approximately 28 K. However, if the maximum local Mach number was increased to 1.5, the total temperature would have to be increased to approximately 37 K.

Total conditions may be selected to avoid any possible errors in the data caused by condensation by using figure 4 and by knowing the maximum local Mach number expected during a test. The theoretical total conditions necessary to avoid any possible errors due to condensation are believed to be conservative since the test gas remains at the high local Mach numbers for only very short periods of time. If the localized high Mach number regions are small, a nonequilibrium frozen flow would exist where the test gas is supersaturated.

As previously mentioned, the Reynolds number will increase with decreasing temperature. Thus the maximum test Reynolds number which can be achieved at a given total pressure is determined by the saturation boundary. This will be discussed in greater detail at the end of this chapter.

I.6 Thermal and Caloric Imperfections.

The need to consider the effects of thermal and caloric imperfections on flow characteristics for parahydrogen at cryogenic temperatures is apparent from figures 5 and 6 where the compressibility factor, Z, and the ratio of specific heats, C_p/C_v, as obtained from reference 11, are shown over a range of temperatures. Departure of Z from the ideal gas value of unity is designated as a thermal imperfection

whereas a departure of C_p/C_v from the ideal diatomic gas value of 1.4 is designated as a caloric imperfection.

Figure 6 illustrates how the specific heat ratio is affected by the characteristic rotational temperature. For temperatures above 200 K the specific heat ratio for parahydrogen is approximately the same as the ideal diatomic gas value of 1.4 whereas, for temperatures less than 75 K the specific heat ratio corresponds more closely to the ideal monatomic gas value of 1.67.

To evaluate the significance of the nonideal behavior, real-gas isentropic and real-gas normal-shock flow solutions, along with other flow situations, have been obtained for parahydrogen for a range of pressures and temperatures down to saturation. The calculation procedure and discussion of the results for these flow situations are presented in the following chapters.

I.7 Transport Properties.

The two transport properties that are of most concern in experimental aerodynamic research are the viscosity, η, and the thermal conductivity, k. These properties are relatively independent of small changes in pressure and are plotted in figures 7 and 8 as a function of temperature as obtained from reference 11.

The two properties along with the specific heat at constant pressure combine to give the Prandtl number, Pr, an important dimensionless parameter in viscous heat transfer problems, defined as

$$Pr = \frac{\eta C_p}{k} \tag{1.13}$$

This parameter for parahydrogen is shown as a function of temperature at different pressures in figure 9 as obtained from reference 11.

Eucken's relation, derivable through kinetic theory (see, for example, reference 12), gives the Prandtl number as a function of the specific heat ratio, γ, as

$$Pr = \frac{4\gamma}{9\gamma - 5} \tag{1.14}$$

The relationship gives a value of 0.667 for the Prandtl number of an ideal monatomic gas where $\gamma = 1.67$ and a value of 0.737, which is approximately the correct value of 0.725, for the Prandtl number of an ideal diatomic gas where $\gamma = 1.4$.

Comparing Eucken's relation to figure 9 and considering the characteristic rotational temperature influence, there appears to be a major inconsistency. One explanation for the deviation is that Eucken's relation is a reasonably good approximation only for gases at ordinary temperatures. At cryogenic temperatures, the transport properties do not vary in the same manner as they do at room temperatures thereby causing Eucken's relation not to hold at cryogenic temperatures.

Cryogenic temperatures influence the transport properties in such a way as to cause the Prandtl number at one atmosphere and arcund 25 K to be equal to the ideal diatomic gas value of 0.725 instead of the expected value of 0.667, the ideal monatomic gas value. So, under these conditions, the thermal boundary layer profile may be expected to vary from the velocity boundary layer profile for parahydrogen in the same manner as an ideal diatomic gas.

As noted in the introduction, it is necessary to match, as nearly as possible, the Reynolds number between flight conditions and the conditions maintained during aerodynamic testing in the wind tunnel. With the ever increasing flight Reynolds numbers, much work has been devoted to increasing the test Reynolds number by decreasing the testing temperature, by increasing the testing pressure, and by using different gases (see, for example, reference 13). Figure 10 illustrates the benefits, from the viewpoint of increased Reynolds number per meter, of using cryogenic hydrogen compared to nitrogen or air assuming an isentropic expansion from the total conditions. For example, at a Mach number of 0.1, the Reynolds number per meter for hydrogen at the total conditions of one atmosphere and 25 K is about fifteen times that of air at standard conditions and approximately three times that of nitrogen at the total conditions of one atmosphere and 100 K.

The Reynolds number per meter for hydrogen and nitrogen are compared at a free stream Mach number of 1.0 and a total pressure of one atmosphere at various total temperatures in figure 11. The figure illustrates the large benefits that may be obtained by using hydrogen instead of nitrogen from a Reynolds number standpoint. The benefits are a direct result of the lower total temperatures which can be used before the onset of condensation occurs.

Thus, the maximum obtainable Reynolds number per meter is directly dependent upon the saturation limits as imposed by the maximum local Mach number generated on the model being tested. This is illustrated for hydrogen in figure 12 where the Reynolds number per meter is shown

as a function of total temperature for various total pressures with the theoretical saturation boundary superimposed as a function of the maximum local Mach number, M_L. The figure shows that if the maximum local Mach number is 1.4 a factor of 17.5 increase in Reynolds number may be obtained at a pressure of five atmospheres by operating at cryogenic temperatures rather than ambient temperatures. This represents a Reynolds number which is forty-five times that of air at standard conditions.

CHAPTER II

ISENTROPIC FLOW OF PARAHYDROGEN

II.1 Introduction.

A useful approximation to portions of flows in aerodynamic research is the isentropic flow of an ideal diatomic gas. Consequently, any candidate test gas should have isentropic flow ratios similar to an ideal diatomic gas. The purpose of this chapter is to present the real gas isentropic flow solution and results for parahydrogen.

II.2 Isentropic Flow Solution.

By definition an isentropic process occurs under the condition of constant entropy, and the solution may be calculated from the stagnation conditions. An analytical solution may be formulated from the simple equation of state for an ideal gas. The equation of state for a real gas is more complex than the state equation of an ideal gas and an analytical solution for the real gas is not as easily determined.

As noted in Chapter I the equation of state for parahydrogen used in the isentropic flow solution was developed by the National Bureau of Standards. The computer program for the equation of state was modified for the flow solution into a subprogram form (identified as subprogram THERMO) where the inputs are the temperature and pressure, and the outputs are the thermodynamic and related properties.

In addition to the main program, a subprogram (identified as ISENT) was also developed that makes use of THERMO. ISENT calculates the pressure and other thermodynamic properties for a given temperature and entropy by using a modified interval halving technique,

and it is this subprogram that the main isentropic flow solution program centers around.

The main program iterates on the Mach number and employs an interval halving technique, modified for the isentropic flow solution, to calculate the isentropic expansion of parahydrogen at various total temperatures and total pressures. Generalized flow charts describing the main program and subprogram ISENT are presented in figure 13 and the steps involved in the solution are discussed in detailed in reference 14.

II.3 Isentropic Expansion Coefficient.

The pressure and density relationship for an isentropic expansion of an ideal gas is described by the exponential equation

$$p \propto \rho^{\gamma} \tag{2.1}$$

where γ is the ratio of specific heats and is a constant for an ideal gas. As noted earlier in figure 6, the specific heat ratio for the real gas parahydrogen is not constant but with decreasing temperature deviates considerably from the ideal diatomic gas value of 1.4. Because the specific heat ratio varies with temperature, equation 2.1, with γ equal to a constant, would not be expected to be valid for the isentropic flow solution of parahydrogen.

In reference 15, Woolley and Benedict indicate that equation 2.1 may hold true for an isentropic expansion of a real gas except that the exponent would no longer be equal to the specific heat ratio. They define the exponent as the isentropic expansion coefficient, ξ, which may be calculated from the formula

$$\xi = \frac{\gamma Z}{Z - P\left(\frac{\partial Z}{\partial P}\right)_T} \tag{2.2}$$

and indicate that equation 2.1 may be used for an isentropic expansion of a real gas provided that ξ is used instead of γ.

In this thesis the isentropic expansion coefficient was determined from the expression

$$\frac{P_{i-1}}{P_i} = \left(\frac{\rho_{i-1}}{\rho_i}\right)^{\xi} \tag{2.3}$$

where the states $i-1$ and i represent an increment along an isentrope which is equivalent to a variation of 0.05 in Mach number. The variation of the isentropic expansion coefficient with total temperature at a total pressure of one atmosphere is illustrated in figure 14 for expansions of parahydrogen to a Mach number of 2.0. This figure illustrates that the isentropic expansion coefficient is approximately constant outside the characteristic rotational temperature influence range and equivalent to the specific heat ratio for an ideal monatomic and an ideal diatomic gas below and above the influence range respectively. These values agree with those predicted by Woolley and Benedict when the rotational degrees of freedom are either unexcited or fully excited.

II.4 Isentropic Flow Ratios.

As noted in section II.2, since, by definition, an ideal diatomic gas is both thermally and calorically perfect, the isentropic flow ratios may be easily solved for by using the simple ideal gas equation

of state. These fundamental equations are found to be

$$\frac{P}{P_t} = \left[1 + 0.5(\gamma - 1)M^2\right]^{\frac{-\gamma}{\gamma-1}} \tag{2.3}$$

$$\frac{T}{T_t} = \left[1 + 0.5(\gamma - 1)M^2\right]^{-1} \tag{2.4}$$

$$\frac{\rho}{\rho_t} = \left[1 + 0.5(\gamma - 1)M^2\right]^{\frac{-1}{\gamma-1}} \tag{2.5}$$

$$\frac{A}{A^*} = \frac{1}{M}\left(\frac{\gamma+1}{2}\right)^{\frac{\gamma+1}{2(1-\gamma)}}\left[1 + 0.5(\gamma - 1)M^2\right]^{\frac{\gamma+1}{2(\gamma-1)}} \tag{2.6}$$

and are a function of Mach number, M, and the specific heat ratio, γ, only.

As previously noted, any candidate wind tunnel test gas should have behavior similar to air which, under flight conditions, acts for all practical purposes like an ideal diatomic gas. For this reason, the isentropic flow ratios for parahydrogen will be compared with the ideal diatomic gas ratios determined from equations 2.3 to 2.6 with the specific heat ratio, γ, equal to 1.4.

The deviation of the isentropic flow ratios from the gas values are presented in graphical form. The plots were obtained from the tabulated values generated by the computer program discussed in reference 14.

The deviation of the pressure ratio for an isentropic expansion of parahydrogen to Mach 1.0 from the ideal diatomic gas value is illustrated in figure 15. The figure shows that the deviation is

mainly dependent upon the total temperature variation while the effect of the total pressure on the deviation is comparatively small. Once again the real gas behavior of parahydrogen, this time in terms of the isentropic expansion pressure ratio, may be explained by the influence of the relatively high value of the characteristic rotational temperature since the greatest deviations occur within and below the characteristic rotational temperature influence range, defined in section I.3 as 75 K to 200 K.

The effect of Mach number on the deviation of the isentropic pressure ratio is shown in figure 16. The deviation is shown to be insignificant for low values of Mach number, which is expected because the flow may be assumed to be incompressible under these conditions. It is interesting to note that the maximum deviation of the isentropic pressure ratio for parahydrogen occurs at approximately the same Mach number as that determined for nitrogen by Adcock in reference 16. This occurance surely must be coincidental because Adcock shows that for nitrogen this deviation is in the positive sense and the maximum value increases with both Mach number and pressure whereas for parahydrogen the deviation is in the negative sense and the maximum value increases with pressure but decreases with Mach number. Figure 16 also verifies the fact that the deviation with respect to the total pressure variation is comparatively small.

Figure 17 shows how the temperature ratio for an isentropic expansion of parahydrogen to Mach 1.0 deviates from the ideal diatomic gas value. Like the pressure ratio, the deviation in temperature ratio is seen to be only slightly dependent upon the variation in total

pressure and to be basically dependent upon the total temperature. The isentropic temperature ratio as a function of total temperature curve is identical in shape to the isentropic pressure ratio versus total temperature curve. The influence of the characteristic rotational temperature is again the dominant factor responsible for the deviation.

The Mach number effect on the isentropic temperature ratio deviation is illustrated in figure 18. Similar to the isentropic pressure ratio, the deviation of the temperature ratio is insignificant in the incompressible range of low Mach number values. This figure also verifies that the deviation with respect to the total pressure is negligible when compared with the deviation caused by the total temperature variation.

An illustration of the isentropic density ratio deviation for an expansion of parahydrogen to Mach 1.0 is given in figure 19. This figure shows that the density ratio deviates in the same manner as the isentropic pressure and temperature ratios. That is, the isentropic density ratio varies mainly with respect to the total temperature and only comparatively slightly with respect to total pressure. The characteristic rotational temperature influence is once again the dominant factor controlling the deviation.

The deviation of the isentropic density ratio is shown to be generally less than the deviation of the pressure and temperature ratio. The deviation may be explained by realizing that pressure, density, and temperature are all interelated. As previously noted,

the isentropic pressure ratio deviation and the isentropic temperature ratio deviation have curves which are similar in shape, so that when the density ratio deviation is calculated, the deviations of temperature ratio and pressure ratio have a tendency to cancel each other, thereby keeping the density ratio deviation closer to unity.

Figure 20 gives the effect of Mach number on the deviation of the isentropic density ratio. In the incompressible range of low Mach numbers the real gas effects are once again shown to be insignificant. Figure 20 also verifies that the deviation with respect to the total pressure variation is comparatively insignificant when considering the deviation caused by the total temperature variation.

The real gas effects on the isentropic stream-tube area ratio for parahydrogen are illustrated in figures 21 and 22. Since A is equivalent to A^* when the Mach number is equal to 1.0, the deviation from the ideal diatomic gas value is zero at sonic conditions and small in the transonic region, as shown in figure 21. The deviation is shown to be more dependent on total temperature than on total pressures and is smaller in the incompressible range than in the supersonic range. The deviation with respect to total temperature, illustrated in figure 22, is again dominated by the characteristic rotational temperature influence.

II.5 Conclusions.

1. The isentropic expansion coefficient for parahydrogen cannot be assumed to be constant but is governed by the characteristic rotational temperature influence range.

2. The characteristic rotational temperature is also found to be the dominant factor controlling the deviations of the isentropic flow parameters.
3. The deviations of the isentropic flow parameters are primarily a function of the total temperature, with the influence of the total pressure being small in comparison.
4. At low Mach numbers, where the assumption of incompressibility is valid, the isentropic flow deviations are negligible.

CHAPTER III

PRANDTL-MEYER EXPANSION FLOW OF PARAHYDROGEN

III.1 Introduction.

One type of isentropic flow which requires further discussion is the supersonic isentropic flow that occurs in the turning of a flow around a corner. This type of flow is known as a Prandtl-Meyer flow. The relation between the flow inclination and change in Mach number in an isentropic turn is given by the Prandtl-Meyer function. By knowing the flow inclination all of the isentropic flow ratios may be obtained at the resulting Mach number through the use of the Prandtl-Meyer function. The purpose of this chapter is to present the Prandtl-Meyer flow solution and the dependency of Mach number on the Prandtl-Meyer function for flow in parahydrogen as compared to the results for an ideal diatomic gas.

III.2 Prandtl-Meyer Expansion Flow Solution.

Consider the semi-infinite flow field above a convex wall as shown in figure 23 where the subscripts a and b are used to identify the upstream and downstream conditions of the expansion wave. Here a uniform parallel supersonic flow of Mach M_a is expanded to a higher speed, M_b, by an increase in the local flow angle, $\theta_b - \theta_a$. As in all Prandtl-Meyer flows, the Mach lines, which are inclined relative to the local flow direction at the Mach angle, μ, given by

$$\tan \mu = (M^2 - 1)^{-1/2} \tag{3.1}$$

form as straight lines from the wall. In addition, the flow parameters are constant along these lines. Therefore, the problem of determining the flow above the wall transforms into the determination of the velocity and the thermodynamic state as a function of the initial conditions and the change in the local flow direction imposed by the wall.

The governing differential equation for Prandtl-Meyer flow can be determined from the geometry of a differential velocity change across a Mach line, considered as a weak, discrete expansion wave, as shown in figure 24. Here the tangential components of the velocities on both sides of the Mach line are equal, that is,

$$u_t = (u + \delta u)_t \tag{3.2}$$

From the law of sines

$$\frac{u + \delta u}{u} = \frac{\sin\left(\frac{\pi}{2} + \mu\right)}{\sin\left(\frac{\pi}{2} - \mu - \delta\theta\right)} \tag{3.3}$$

or, using trigonometry

$$1 + \frac{\delta u}{u} = \frac{\cos(\mu)}{\cos(\mu)\cos(\delta\theta) - \sin(\mu)\sin(\delta\theta)} \tag{3.4}$$

So, for small $\delta\theta$

$$1 + \frac{du}{u} = \frac{\cos(\mu)}{\cos(\mu) - \sin(\mu)d\theta} \tag{3.5}$$

This equation reduces to

$$1 + \frac{du}{u} = \frac{1}{1 - \tan(\mu)d\theta} \tag{3.6}$$

or, neglecting higher order terms

$$1 + \frac{du}{u} = 1 + \tan(\mu)d\theta \tag{3.7}$$

Combining equation 3.7 with equation 3.1, the well-known differential equation for Prandtl-Meyer flow is obtained

$$d\theta = \sqrt{M^2 - 1}\ \frac{du}{u} \tag{3.8}$$

To obtain a solution, two additional equations are required, the adiabatic energy equation,

$$H_T = H_a + \frac{1}{2} u_a^2 = H_b + \frac{1}{2} u_b^2 \tag{3.9}$$

and the thermodynamic equation of state, given here in terms of the speed of sound, c, for an isentropic process,

$$c = c(H,S) = c(H,S_a) \tag{3.10}$$

With the initial conditions given, equations 3.8, 3.9, and 3.10 can be solved for any three of the four variables, θ, u, c, H, in terms of the fourth.

For an ideal gas, equation 3.10 can be written in a simple form and the equations can easily be solved. For a real gas, the equation

of state is more complex than the ideal gas state equation and such a simple solution to the system of equations is not as easily determined.

A computer program was written to solve the set of equations for parahydrogen. The main part of the program follows the generalized flow chart given in figure 25 and the steps involved are discussed in reference 17.

III.3 Prandtl-Meyer Expansion Flow Results.

As previously stated, the system of equations for an ideal gas may easily be solved for, resulting in the well-known equation for the Prandtl-Meyer function for an ideal diatomic gas

$$\theta_i' = 2.4495 \tan^{-1}\left(0.40825\sqrt{M_i'^2 - 1}\right) - \tan^{-1}\sqrt{M_i'^2 - 1} \qquad (3.11)$$

The Prandtl-Meyer expansion flow results for parahydrogen will be compared with the ideal diatomic gas values since, as mentioned earlier, any candidate wind tunnel test gas must behave like air which, under flight conditions, acts like an ideal diatomic gas.

The deviations from the ideal diatomic gas values for the Prandtl-Meyer expansion flow in parahydrogen are presented in graphical form. The results, shown in figure 26, were obtained from the tabulated values, given in reference 17, generated by the computer program mentioned in the previous section.

Figure 26 shows the Mach number deviation as a function of total temperature for Prandtl-Meyer expansions from Mach 1.0 through angles of five and twenty-five degrees at total pressures of one and ten atmospheres.

As was the case for the isentropic flow ratios, the deviation is mostly dependent upon the total temperature variation while the deviation with respect to the variation in total pressure is comparatively small. Once again the influence of the characteristic rotational temperature appears to be the dominant factor affecting the Mach number deviation, just as it is in the deviations of the isentropic ratios. The Mach number deviation also appears to increase with increasing Prandtl-Meyer function, θ. This is explained by the facts that the Mach number increases with θ and, from Chapter II, that the isentropic deviations increase with increasing Mach number.

III.4 Conclusions.

1. The characteristic rotational temperature is the dominant factor influencing the Mach number deviation for the Prandtl-Meyer expansion in parahydrogen.
2. The Mach number deviation is small with respect to total pressure variations when compared to the influence of total temperature.
3. The Mach number deviation generally increases with increasing values of the Prandtl-Meyer function.

CHAPTER IV

NORMAL SHOCK WAVES IN PARAHYDROGEN

IV.1 Introduction.

Shock waves are usually present around models tested at transonic and supersonic speeds and the investigator would like the jump conditions across the shock wave to have a behavior similar to air. So, any candidate test gas should have normal shock ratios similar to an ideal diatomic gas. The purpose of this chapter is to present the normal shock flow solution and results for parahydrogen.

IV.2 Normal Shock Wave Solution.

Consider a standing normal shock wave as shown in figure 27. If the subscripts a and b are used to identify the upstream and downstream conditions of the shock wave, the conservation equations of mass, momentum, and energy are

$$\rho_a M_a c_a = \rho_b M_b c_b \tag{4.1}$$

$$P_a + \rho_a M_a^2 c_a^2 = P_b + \rho_b M_b^2 c_b^2 \tag{4.2}$$

$$H_{t,a} = H_{t,b} \tag{4.3}$$

Equation 4.3 may be written in terms of the static enthalpy as

$$H_a + \frac{1}{2} M_a^2 c_a^2 = H_b + \frac{1}{2} M_b^2 c_b^2 \tag{4.4}$$

Using equation 4.1, equations 4.2 and 4.4 may be written as

$$P_b = P_a + \rho_a M_a^2 c_a^2 (1 - \rho_a/\rho_b) \tag{4.5}$$

$$H_b = H_a + \frac{1}{2} M_a^2 c_a^2 \left[1 - (\rho_a/\rho_b)^2\right] \tag{4.6}$$

If the conditions upstream of the shock are known, equations 4.5 and 4.6 constitute two equations for the three unknowns P_b, H_b, ρ_b. The system of equations can be completed by assuming the gas to be in thermodynamic equilibrium on each side of the shock wave, which will supply the equation of state

$$\rho = \rho(P,H) \tag{4.7}$$

The requirement given by the second law of thermodynamics, that the entropy downstream of the shock wave, S_b, be greater than the entropy upstream of the shock wave, S_a, assures the uniqueness of the solution.

For an ideal gas, equation 4.7 may be written as

$$\rho = P[\gamma/(\gamma - 1)]/H \tag{4.8}$$

where γ is the specific heat ratio. The system of equations may then easily be solved for analytically.

In the case of a real gas the equation of state is more complex than the state equation of an ideal gas, and an analytical solution of the system of equations cannot be determined algebraically.

A computer program was written to solve the normal shock wave system of equations for parahydrogen. The equations were solved by iterating on the upstream Mach number and employing a modified interval-halving method to converge on the downstream static enthalpy and density. To determine the conditions on either side of the shock wave, the program used the assumption of local thermodynamic equilibrium and employed subprograms THERMO and ISENT, which were discussed in Chapter II.

A generalized flow chart for the main part of the computer program is given in figure 28 and the steps involved are discussed in reference 18. One step that should be mentioned here is step 10 where the static temperature downstream of the shock is initially assumed. For this assumption the ideal diatomic gas equation was utilized, that is

$$T_{a,i} = T_{t,a}(1 + 0.2M_{a,i}^2)^{-1} - \left|T_{t,a}(1 + 0.2M_{a,i-1}^2)^{-1} - T_{a,i-1}\right| \tag{4.9}$$

where the expression enclosed between the absolute value signs represents the deviation from the ideal diatomic gas value for the previous iteration. The above method provided rapid convergence throughout the domain studied.

IV.3 Normal Shock Wave Results.

The normal shock wave ratios for an ideal gas may, as previously noted, be solved for analytically and are given as

$$\frac{P_b}{P_a} = \frac{2\gamma M_a^2 - (\gamma - 1)}{\gamma + 1} \tag{4.9}$$

$$\frac{T_b}{T_a} = \frac{\left[2\gamma M_a^2 - (\gamma - 1)\right]\left[(\gamma - 1)M_a^2 + 2\right]}{(\gamma + 1)^2 M_a^2} \tag{4.10}$$

$$\frac{\rho_b}{\rho_a} = \frac{(\gamma + 1)M_a^2}{(\gamma - 1)M_a^2 + 2} \tag{4.11}$$

$$\frac{M_b}{M_a} = \frac{1}{M_a}\left[\frac{(\gamma - 1)M_a^2 + 2}{2\gamma M_a^2 - (\gamma - 1)}\right]^{1/2} \tag{4.12}$$

$$\frac{P_{t,b}}{P_{t,a}} = \frac{\rho_{t,b}}{\rho_{t,a}} = \left[\frac{(\gamma + 1)M_a^2}{(\gamma - 1)M_a^2 + 2}\right]^{\frac{\gamma}{\gamma-1}}\left[\frac{\gamma + 1}{2\gamma M_a^2 - (\gamma - 1)}\right]^{\frac{1}{\gamma-1}} \tag{4.13}$$

$$\frac{T_{t,b}}{T_{t,a}} = 1 \tag{4.14}$$

The fundamental equations are found to be functions of the upstream Mach number, M_a, and the specific heat ratio, γ, only.

As mentioned earlier, any candidate wind tunnel test gas should behave similar to an ideal diatomic gas. For this reason, the normal shock wave ratios for parahydrogen will be compared with the ideal diatomic gas ratios determined from equation 4.9 to 4.14 with the specific heat ratio, γ, equal to 1.4.

The deviations of the normal shock wave ratios for parahydrogen from the ideal diatomic gas values are presented in graphical form. The plots were obtained from the tabulated values given in reference 18 which were generated by the computer program discussed in section IV.2.

The deviations of the static ratios P_b/P_a, T_b/T_a, and ρ_b/ρ_a, across a normal shock wave in parahydrogen from the ideal diatomic gas values at various upstream total pressures and for an upstream Mach number of 2.0 are illustrated in figures 29 to 31. The figures show that the nonideal gas behavior of parahydrogen is mainly dependent upon the upstream total temperature variation, while the deviations with respect to the upstream total pressure are comparatively small. The greatest influence on the deviations is the previously mentioned high value of the characteristic rotational temperature of hydrogen.

Figures 32 through 34 show how the deviations of the static ratios across a normal shock wave in parahydrogen vary with respect to the upstream Mach number, M_a, at various upstream total temperatures and for an upstream total pressure of one atmosphere. The figures show that the deviations generally increase with increasing upstream Mach number. They also show that the deviations, as a function of total temperature, have the same shape at the various upstream Mach numbers, and appear to be greatly influenced by the relatively high value of the characteristic rotational temperature.

The real gas effects on the Mach number downstream of a normal shock in parahydrogen are illustrated in figure 35 for an upstream Mach number of 2.0. The deviation from the ideal diatomic gas value is shown to be only slightly dependent upon the upstream total pressure when compared to the dependence upon the upstream total temperature. Once again the dependency is explained by the characteristic rotational temperature range of influence.

Figures 36 through 38 give the effect of the upstream total pressure on the deviations of the total ratios $P_{t,b}/P_{t,a}$, $T_{t,b}/T_{t,a}$, $\rho_{t,b}/\rho_{t,a}$, from the ideal diatomic gas values for an upstream Mach number of 2.0. The figures show that the total pressure ratio and the total density ratio deviations are mainly dependent upon the upstream total temperature variation and are only comparatively slightly influenced by the variation in the upstream total pressure. The deviations are shown to be predominantly influenced by the characteristic rotational temperature.

On the other hand, the deviation of the total temperature ratio from that of an ideal diatomic gas does not appear to be influenced by the characteristic rotational temperature. The greatest deviations of the total temperature is on the same order of magnitude as the total pressure and density deviations.

Figures 39 through 41 illustrate how the deviations of the total ratios across a normal shock wave in parahydrogen vary with respect to upstream Mach number, M_a, at various upstream total temperatures and for an upstream total pressure of one atmosphere. The figures show that the deviations generally increase with increasing upstream Mach number. Comparing figure 40 with figure 37, the deviation from the ideal diatomic gas value of the total temperature ratio is shown to be only slightly dependent upon the upstream Mach number when compared to the dependency of the upstream total temperature.

IV.4 Conclusions.

1. The characteristic rotational temperature is the dominant factor controlling the deviations of the static ratios

across a normal shock wave in parahydrogen from the ideal diatomic gas values.

2. The deviations of the normal shock wave static ratios increase with increasing upstream Mach number.
3. The deviations of the static ratios are small with respect to the total pressure variations when compared to the influence of the total temperature.
4. The characteristic rotational temperature is also the dominant factor controlling the deviations of the total pressure and total density ratios across a normal shock wave in parahydrogen from the values for an ideal diatomic gas, while the total temperature ratio deviation is not influenced by the characteristic rotational temperature.
5. The deviations of the total pressure and total density ratios are small with respect to the total pressure variations when compared to the influence of the total temperature, while the inverse is true for the total temperature ratio.
6. The deviations of the stagnation ratios across normal shock waves increase with increasing upstream Mach number.

CHAPTER V

NOZZLE FLOW OF PARAHYDROGEN

V.1 Introduction.

The previous chapters have described how hydrogen differs from an ideal diatomic gas for various flow situations. Also, the dramatic increase in Reynolds number attainable through the use of cryogenic hydrogen instead of air or cryogenic nitrogen was shown in Chapter II, along with the conclusion that cryogenic hydrogen will behave like an ideal diatomic gas in the incompressible flow regime.

This chapter considers inviscid one-dimensional cryogenic parahydrogen flow, both isentropic and with a normal shock, through the diverging section of a supersonic nozzle. Through this analysis the differences between cryogenic hydrogen and an ideal diatomic gas will be studied in specific compressible flow situations.

V.2 Isentropic Flow.

The dimensions for the diverging section of a Mach 2.0 nozzle were obtained from reference 19. The values were then fitted with an equation of the form

$$\frac{A}{A^*} = \sum_{k=0}^{6} y_k \left(\frac{x}{L}\right)^k \tag{5.1}$$

where

L total length of the diverging section of the nozzle

x distance downstream from the nozzle throat

A area at distance x

A* area at the nozzle throat

and the values of y_k are as follows:

$$y_0 = 1.0$$

$$y_1 = 0.0169041$$

$$y_2 = 6.873320$$

$$y_3 = -18.3097$$

$$y_4 = 23.9338$$

$$y_5 = -16.5135$$

$$y_6 = 4.67734$$

The area distribution, along with the resulting one-dimensional isentropic flow ratios for an ideal diatomic gas, is presented in figure 42.

The computer program discussed in reference 14 was modified to obtain the one-dimensional, inviscid, isentropic flow of parahydrogen through the diverging section of the Mach 2.0 nozzle given by equation 5.1. Since the purpose of this study is to investigate the behavior of hydrogen under cryogenic conditions where the Reynolds number advantage occurs, the isentropic flow ratios were calculated for total conditions of 45 K and one atmosphere. These conditions give a Reynolds number per meter value of about seven times that of air at one atmosphere and 300 K.

The results at the above total conditions are given in figure 43 in terms of the deviations from the ideal diatomic gas values. As expected from the results of Chapter II, the deviations increase with increasing x/L and show a rather large deviation in the isentropic ratios even at the throat. The figure leads to the conclusion that although substantial increases in Reynolds numbers may be obtained with

cryogenic hydrogen, hydrogen is unacceptable as a test gas if it is essential to model an ideal diatomic gas under supersonic isentropic flow situations.

V.3 Nozzle Flow with a Normal Shock

The isentropic nozzle flow solution discussed in the preceding section was altered to study the nonideal gas behavior of parahydrogen associated with a one-dimensional normal shock wave. This was done by using the real gas normal shock wave relations derived in Chapter IV and assuming isentropic flow upstream and downstream of the shock. As in the previous section, to take advantage of hydrogen's high Reynolds number capability at cryogenic temperatures, the Mach number distribution and nozzle flow ratios were calculated for upstream total conditions of 45 K and one atmosphere.

The parahydrogen and ideal diatomic gas results for shocks occurring at Mach 1.3 and 1.8 are shown in figures 44 and 45, respectively. As expected from the results of Chapter II, the deviation in the shock wave location between parahydrogen and an ideal diatomic gas increases with increasing shock Mach number. This is predictable from the fact that in the supersonic range, the deviation for parahydrogen from the ideal diatomic gas value of the isentropic stream-tube area ratio, A^*/A, increases with increasing Mach number (as shown in figure 22). The results indicate that the shock wave location on an airfoil being tested at supersonic speeds in cryogenic parahydrogen would probably be in error by an unacceptable amount, when compared to the shock wave location in air, thereby possibly nullifying any

advantage of testing at the increased Reynolds number which may be obtained by using cryogenic parahydrogen.

The results of figures 44 and 45 are in agreement with the results of Chapter II, and demonstrate that the deviations in the Mach number and nozzle flow ratios are generally smaller downstream of the shock wave than they are upstream of the shock wave. The results support the conclusion reached in the Chapter II that the isentropic flow ratios for cryogenic parahydrogen at low subsonic Mach numbers do not deviate substantially from the ideal diatomic gas values.

V.4 Conclusions.

1. Cryogenic hydrogen is unacceptable as a test gas if it is essential to model an ideal diatomic gas under supersonic isentropic flow situations.
2. Cryogenic hydrogen is unacceptable as a test gas if it is essential to model an ideal diatomic gas under supersonic flow situations where a shock occurs.

CHAPTER VI

FLOW ABOUT A DIAMOND-SHAPED AIRFOIL

VI.1 Introduction.

Chapter V concluded that, when compared to an ideal diatomic gas, cryogenic parahydrogen is unacceptable as a supersonic wind tunnel test gas. The purpose of this chapter is to verify this conclusion and, like the nozzle flow study, to gain insight into the flow characteristics of cryogenic parahydrogen in the transonic Mach number region. This is done by using the shock-expansion theory to study the inviscid flow about a diamond-shaped airfoil.

VI.2 The Oblique Shock Wave.

One of the basic concepts involved in the shock-expansion theory is the oblique shock wave, the geometry of which is given in figure 46. The oblique shock wave may be treated in the same manner as a normal shock wave taking into consideration the additional velocity component, v, tangent to the shock wave.

The continuity equation across an oblique shock may be given in terms of the normal velocity components as

$$\frac{u_2}{u_1} = \frac{\rho_1}{\rho_2} \tag{6.1}$$

where u is the velocity component normal to the shock wave and ρ is the density.

From the oblique shock wave geometry given in figure 46 the following may be written

$$\tan(\beta - \delta) = \frac{u_2}{v} \tag{6.2}$$

and

$$\tan \beta = \frac{u_1}{v} \tag{6.3}$$

Using the trigonometric identity

$$\tan(\beta - \delta) = \frac{\tan\beta - \tan\delta}{1 + \tan\beta \tan\delta} \tag{6.4}$$

equations 6.2 and 6.3 may be combined to yield

$$\frac{u_2}{u_1} = \frac{1 - \frac{v}{u_1}\tan\delta}{1 + \frac{u_1}{v}\tan\delta} \tag{6.5}$$

But, the tangential component of the velocity, v, may be written as

$$v = \sqrt{w_1^2 - u_1^2} \tag{6.6}$$

so that

$$\frac{v}{u_1} = \sqrt{\left(\frac{w_1}{u_1}\right)^2 - 1} \tag{6.7}$$

Introducing the speed of sound, c, the above may be written as

$$\frac{v}{u_1} = \sqrt{M_1^2 \left(\frac{c_1}{u_1}\right)^2 - 1} \tag{6.8}$$

where M_1 is the upstream Mach number and the ratio u_1/c_1 is referred to as the equivalent normal shock Mach number. Substituting equation 6.8 into equation 6.5 gives the following result based only on the geometric considerations of an oblique shock wave

$$\frac{u_2}{u_1} = \frac{1 - \sqrt{M_1^2\left(\frac{c_1}{u_1}\right)^2 - 1}\,\tan\delta}{1 + \frac{\tan\delta}{\sqrt{M_1^2\left(\frac{c_1}{u_1}\right)^2 - 1}}} \tag{6.9}$$

From the above equation and the equation of continuity, 6.1, the solution for the oblique shock wave may be determined at a specified value of δ.

VI.3 The Shock-Expansion Theory.

The oblique shock wave along with the isentropic expansion wave are the two fundamental components used to analyze many two-dimensional flow problems by uniting the appropriate combination of the two solutions. The shock-expansion theory may be used to analyze the flow over two-dimensional airfoils.

Consider, for example, the symmetrical diamond-section airfoil in figure 47. A shock forms at the leading edge compressing the flow to pressures P_2 and P_4 above and below the airfoil. Centered expansion waves located at the shoulders expand the flow to pressures P_3 and P_5. Finally, the trailing edge shock recompresses the flow to (nearly) the free-stream pressure value.

A supersonic wave drag is induced on the airfoil due to the over-pressure on the forward faces and the underpressure on the rearward faces. This type of supersonic drag exists even in the idealized,

nonviscous fluid and is fundamentally different from the frictional drag and separation drag associated with the viscous boundary layer. For unit span, the supersonic wave drag associated with the diamond-section airfoil is given by

$$D = [(P_2 + P_4) - (P_3 + P_5)]t \qquad (6.10)$$

where t is the maximum thickness of the airfoil.

VI.4 Flow Solution.

Now consider the symmetric diamond-section airfoil in figure 47 with a chord length, ℓ, of three meters flying at an altitude of 8000 meters and a Mach number, M_1, of 1.3. At this altitude, reference 20 gives the following conditions

static pressure: 0.352 atm

kinematic viscosity: 2.904×10^{-5} m^2/sec

speed of sound: 308.07 m/sec

static density: 0.526 kg/m^3

From the above values, the Reynolds umber based on the chord length is 41.4×10^6. To match the Reynolds number in a cryogenic hydrogen wind tunnel, with a total pressure of one atmosphere and a total temperature of 50 K a chord length of 0.4576 meters is required, which could easily be accommodated in a wind tunnel.

The lift and drag coefficients associated with the diamond-section airfoil given in figure 47 may be determined using the shock-expansion theory. For the ideal diatomic gas the values are easily determined

using the equations given in chapters II, III, and IV following the calculation procedure outlined in reference 21.

Because of the complex equation of state for a real gas, an analytical solution for hydrogen is not as easily determined. The results obtained in chapters II, III, and IV may be used along with the shock-expansion theory to calculate the lift and drag coefficients. Using the normal shock wave solution tables, given in reference 18, along with equations 6.1 and 6.9, the Mach number normal to the shock wave upstream of the shock wave may be determined for various deflection angles, δ. Figure 48 gives the solution for the free-stream conditions of one atmosphere and 50 K, and for deflection angles, δ, of two and four degrees, and an upstream Mach number, M_1, of 1.3.

The lift and drag coefficients were calculated for various free-stream Mach numbers, M_1, airfoil half angles, ϕ, and angle of attack, α, and are presented in table I.

VI.5 Comparison of Results.

The errors in the lift and drag coefficients do not vary in any consistent manner. Occasionally the errors are less than one percent, but, in general, the errors are large enough to make hydrogen unacceptable as a cryogenic wind tunnel test gas if an ideal diatomic gas is to be simulated.

VI.6 Conclusions.

The results from the diamond-shaped airfoil study confirm the conclusions reached in the nozzle flow study. That is, considering

that high local Mach number regions may occur in transonic and supersonic flow situations, and recognizing the possibility of large errors in the determination of the lift and drag coefficients, cryogenic hydrogen is unacceptable as a transonic and supersonic wind tunnel test gas if an ideal gas is to be simulated.

CHAPTER VII

SELECTED WIND TUNNEL DESIGN CONSIDERATIONS

VII.1 Introduction.

The purpose of this chapter is to discuss selected design aspects which must be considered if a cryogenic wind tunnel is to be built or if an existing wind tunnel is to be modified to use cryogenic parahydrogen as the test gas. No attempt is made to cover all of the design considerations associated with a cryogenic wind tunnel. Only those aspects peculiar to the use of hydrogen will be examined. These include: drive power requirements, cooling requirements, material compatability, and safety.

VII.2 Drive Power Requirements.

This section consists of a theoretical analysis of the power required for isentropic compressions of cryogenic parahydrogen to determine how the real gas effects influence the drive power requirements of a closed circuit wind tunnel. The analysis covers a temperature range of 25 K to 300 K, a pressure range of one to five atmospheres, and a fan pressure ratio range of 1.019 to 1.200. The values cover the range of variables likely to be encountered in a fan-driven cryogenic wind tunnel with hydrogen as the test gas. The results are compared to air at total conditions of one atmosphere and 300 K.

In reference 22, Adcock and Ogburn present power calculations for the isentropic compressions of cryogenic nitrogen, and their analytical wind tunnel model, presented in figure 49, shall be examined for the hydrogen case.

The assumption is made that the only losses that occur are between the tunnel throat and fan. The simplifying assumption is a direct result of wind tunnel data which show that most of the tunnel losses do occur in this portion of the tunnel because of the higher flow velocities. As a consequence of the simplification, the total conditions are the same at the fan outlet and the tunnel throat.

To remove the heat conducted through the walls of the tunnel and the heat added to the stream by the fan, the assumption is made that a cooling system is placed upstream of the fan. A further assumption is made that the cooling is accomplished by injecting liquid hydrogen directly into the tunnel circuit thereby cooling the circuit through evaporation. The location of the cooler is upstream of the fan rather than downstream to allow a more thorough mixing of the evaporating hydrogen with the main stream. In the case of nitrogen, Adcock and Ogburn have shown that the additional mass flow due to the liquid nitrogen being injected for cooling is at most two percent of the mass flow. Their studies indicated that while the absolute power levels were increased by about two percent because of the additional mass being compressed, the ratio of the power required to compress nitrogen to that required to compress an ideal diatomic gas was insignificantly affected. Since they were primarily interested in this ratio, the assumption was made that cooling occured without mass addition. The same assumption will also be made here, realizing that the power calculations do not include the additional power required to compress the mass flow of the coolant.

Based on the fan pressure ratios necessary to achieve a given test section Mach number in several existing tunnels, the fan pressure

ratios presented in table II have been assumed for this analytical study.

Based on experience with existing tunnels, the fan pressure ratio needed to achieve a given test section Mach number is assumed to be invariant with stagnation temperature and pressure. In accordance with the conclusions made so far with respect to the usefullness of hydrogen as a test gas, the low subsonic Mach number region will be studied in greater detail than the higher Mach number region.

The tunnel mass flow calculations are carried out at the throat conditions. For subsonic velocities the assumption is made that the throat and test section Mach numbers are identical. For supersonic speeds, the effective flow area in the test section must be greater than that of the throat. In practice, this larger effective area is created either by diverging the walls of the test section or by allowing some of the test gas entering the test section to flow through slotted or porous test section walls into a plenum chamber surrounding the test section. In the latter case, the mass may be removed from the plenum chamber by auxiliary suction or it may be allowed to reenter the tunnel circuit at the diffuser entrance. For this analysis it will be assumed that all the mass that passes through the tunnel throat will also pass through the fan.

The test gas of a closed circuit fan driven wind tunnel is forced to flow around the tunnel circuit by the energy imparted by the fan. Assuming that the steady flow compression that occurs at the fan is an isentropic process, the power per unit area imparted to the test gas is given by

$$Pwr = \dot{m} \left(H_{t,2} - H_{t,1}\right)_s \tag{7.1}$$

where

$\dot{m}$ = mass flow rate per unit area of the test gas

and

$\left(H_{t,2} - H_{t,1}\right)_s$ = enthalpy difference, at constant entropy, across the fan.

The mass flow rate per unit area may be determined by

$$\dot{m} = \rho M c \tag{7.2}$$

and for an isentropic process of an ideal gas, this may be expressed as a function of the stagnation conditions and Mach number

$$\dot{m} = P_t M \sqrt{\frac{\gamma}{RT_t}} \left(1 + \frac{\gamma-1}{2} M^2\right)^{\frac{\gamma+1}{2(1-\gamma)}} \tag{7.3}$$

Also, for an ideal gas the enthalpy difference may be expressed as

$$\left(H_{t,2} - H_{t,1}\right)_s = C_p T_{t,1} \left[\left(\frac{P_{t,2}}{P_{t,1}}\right)^{\frac{\gamma-1}{\gamma}} - 1\right] \tag{7.4}$$

where $(P_{t,2}/P_{t,1})$ is commonly referred to as the fan pressure ratio. Equations 7.3 and 7.4 may then be substituted into 7.1 to give the power requirements for an ideal gas.

In the case of a real gas such a closed form solution cannot be as easily determined. But, by using the isentropic flow computer

program discussed in chapter II, and specifying the fan pressure ratio, the throat Mach number, and the total conditions at the throat, the power requirements for a wind tunnel using parahydrogen as the test gas may be calculated using the previously discussed analytical model.

Figure 50 gives the power requirements for a hydrogen wind tunnel relative to the power requirements for an ambient air wind tunnel as a function of fan outlet total temperature, $T_{t,2}$. Each fan outlet total pressure line, $P_{t,2}$, corresponds to every test section Mach number at which the power requirements were calculated. The maximum deviation was approximately one-half of one percent between a Mach number of 1.2 and a Mach number of 0.1. This result suggests that the power requirement ratio is relatively independent of Mach number, a fact which shall be applied later.

Table III shows how the test section size, the tunnel pressure, and the tunnel power requirement is affected by changing the test gas. The table illustrates the advantage of hydrogen compared to nitrogen or air. At a given Mach number and Reynolds number the drive power requirement for hydrogen is less than the power requirement for nitrogen or air. The advantage of hydrogen is a direct result of the saturation boundary allowing operation at a greatly reduced total temperature.

Since the advantage of parahydrogen lies in its high Reynolds number capability, the power requirements for a certain Reynolds number advantage will be considered. The power requirement is analyzed best as a ratio of the parahydrogen power requirement to the power required for air near standard conditions. Kilgore, in reference 13, suggests that both the Reynolds number and power are directly proportional to the total pressure. Therefore, if the Reynolds number, divided by the

total pressure, is plotted against the required power, divided by the total pressure, only one curve should arise since the total pressure dependency should cancel out. Figure 51 gives this function for parahydrogen in terms of the Reynolds number advantage (ratio of the Reynolds number for parahydrogen at various total pressures and temperatures to the Reynolds number for air at one atmosphere and 300 K), divided by the total pressure, as a function of the required power ratio (power per unit area for parahydrogen at various total pressures and temperatures divided by the power per unit area for air at one atmosphere and 300 K), divided by the total pressure. The values for air were determined by using the ideal gas equations for an ideal diatomic gas.

The solid line labeled ideal gas in figure 51 evolved from a modification of the closed form solution of the ideal gas equations. The Reynolds number per meter is given by

$$(\text{Re/meter}) = \frac{\rho M c}{\eta} \tag{7.5}$$

By using the isentropic flow equations for an ideal gas this equation may be given by

$$(\text{Re/meter}) = \frac{M P_t}{\eta} \sqrt{\frac{\gamma}{RT}} \left(1 + \frac{\gamma-1}{2} M^2\right)^{-\frac{\gamma}{\gamma-1}} \tag{7.6}$$

The viscosity, η, is usually given by Sutherland's equation, but, as pointed out in reference 7, a more accurate value for parahydrogen is given by Diller's formula (see the appendix). The static temperature, T, is given by

$$T = T_t \left(1 + \frac{\gamma-1}{2} M^2\right)^{-1} \tag{7.7}$$

As noted in chapter I, the specific heat ratio, γ, for parahydrogen is not constant but varies with temperature. For this analysis the specific heat ratio is given as

$$\gamma = \sum_{k=0}^{8} \gamma_k T^k \tag{7.8}$$

where

T = temperature, K

and where the values of γ_k are as follows:

$\gamma_0 = 2.6735$ $\qquad$ $\gamma_1 = -1.8562 \times 10^{-2}$

$\gamma_2 = 6.9001 \times 10^{4}$ $\qquad$ $\gamma_3 = -1.0288 \times 10^{-5}$

$\gamma_4 = 5.3581 \times 10^{-8}$ $\qquad$ $\gamma_5 = -6.6509 \times 10^{-12}$

$\gamma_6 = -8.744 \times 10^{-13}$ $\qquad$ $\gamma_7 = 2.894 \times 10^{-15}$

$\gamma_8 = -2.9464 \times 10^{-18}$

Equation 7.8 approximates the specific heat ratio, C_p/C_v, given in figure 6.

The drive power requirements for parahydrogen were then approximated by using equations 7.1, 7.3, and 7.4 with $\gamma = 1.4$ and the appropriate values for the specific heat at constant pressure, C_p, and the gas constant, R. The curve was calculated for a Mach number equal to one. Calculations were performed at other Mach numbers but these resulted in similar curves demonstrating the relative independence of Mach number.

VII.3 Cooling Requirements.

The amount of liquid hydrogen required for cooling may be divided into two categories: i) the amount initially required to cool the cryogenic tunnel to its operating temperature, and, ii) the amount required to remove the heat being conducted through the tunnel walls and the heat energy added to the stream by the drive fan while the tunnel is running.

The amount of liquid hydrogen required to cool a cryogenic wind tunnel to its operating temperature is dependent upon the cool-down procedure used as well as the physical characteristics of the tunnel.

To calculate the minimum liquid requirement, the simplifying assumptions are made that no heat is conducted through the insulated tunnel walls and that no heat is added by the drive fan to the test gas during the cool-down process. With these assumptions the minimum liquid hydrogen requirement for cool-down occurs when the tunnel is cooled slowly in such a way that the hydrogen gas will leave the tunnel circuit at the same temperature as that of the warmest part of the tunnel structure. Assuming further that all of the liquid hydrogen vaporizes, the maximum amount of liquid hydrogen required for cool-down may be calculated when only the refrigeration available in the latent heat of vaporization is utilized and the hydrogen gas leaves the tunnel at the saturation temperature.

If σ represents the mass of liquid hydrogen required to cool a unit mass of material through a given temperature range, then, following the analysis given in reference 23, $\sigma_{min} = 0.031$ and $\sigma_{max} = 0.14$ for cooling a stainless steel structure from 260 K to 30 K.

Cooling through such a large temperature range would not always occur since under some circumstances the tunnel circuit would be allowed to remain cold between runs. Under these conditions the heat to be removed would be equal to the heat gained by the tunnel structure and test gas by conduction through the insulation. This heat conduction could be kept to an acceptable level by properly designing the insulation.

One possible way of reducing the cost of cooling a cryogenic hydrogen wind tunnel would be to use relatively inexpensive liquid nitrogen to cool the structure to approximately 77 K and to use hydrogen to cool the structure to the lower operating temperature.

The heat to be removed while the tunnel is running consists of the heat conduction through the walls of the tunnel and the heat energy added by the drive fan. The cooling thermal capacity of parahydrogen is equal to the latent heat of vaporization (445.5 joules per gram at the normal boiling point) together with the sensible heat of the gas phase between the saturation temperature and the desired total temperature.

Figure 52 gives the cooling thermal capacity for parahydrogen for a range of final gas conditions. Here the cooling thermal capacity is equal to the latent heat together with the sensible heat of the gas phase between the saturation temperature and the final gas total temperature.

Kilgore, in reference 13, gives the cooling thermal capacity for nitrogen. By comparison, the cooling thermal capacity for parahydrogen is much greater than that of nitrogen, on a mass basis.

At a temperature of 300 K, the cooling capacity of parahydrogen is approximately nine times that of nitrogen and, on a mass basis, the latent heat of vaporization of parahydrogen is more than twice that of nitrogen.

The additional power required for cooling is best illustrated by an example. The mass flow rate of the liquid hydrogen (LH_2) required to remove the heat of compression is equal to the drive fan power added to the stream, Pwr, given by equation 7.1, divided by the cooling capacity, given in figure 52 and Appendix I.

If ε represents the energy required to produce a unit mass of liquid hydrogen, then the power equivalent of liquid hydrogen used to remove the heat of compression is

$$\text{Power}_{LH_2} = \varepsilon \dot{m}_{LH_2} \tag{7.9}$$

where $\dot{m}_{LH_2}$ is the mass flow rate of the liquid hydrogen.—

Table IV compares the results for cryogenic hydrogen, cryogenic nitrogen, and air at standard temperature at a free stream Mach number of 1.0, a Reynolds number of 50×10^6, a total pressure of 2.5 atmospheres and a local saturation Mach number of 1.2. The value of ε for nitrogen was obtained from the work reported by Kilgore in reference 13. The value of ε for hydrogen was then selected to be consistent with the liquefaction work requirements for nitrogen and hydrogen given in reference 24. The results show that although the drive power requirements for cryogenic hydrogen is substantially less than the drive power requirements for cryogenic nitrogen or air at

ambient temperature, the total power requirements for cryogenic hydrogen is considerably greater because of the liquefaction power requirements.

VII.4 Material Compatibility.

Atomic hydrogen is capable of entering steel and many other metals and alloys. When this penetration occurs, any one of several undesirable phenomena may take place which are collectively referred to as hydrogen embrittlement. Hydrogen embrittlement is a delayed-failure phenomenon which is also known as "hydrogen-induced, delayed brittle failure" or "hydrogen-stress cracking" since a loss of ductility as measured in the tensile test is not necessarily associated with the condition.

The presence of hydrogen affects the mechanical behavior of iron and steel principally by: reducing the ductility (embrittlement), lowering the fracture stress, and causing a delayed brittle failure under suitable conditions. If an apparatus is to be used in a hydrogen environment it should be constructed of material that would not be affected by the hydrogen.

As a general rule for the selection of metal alloys to use in a hydrogen environment, the aluminum alloys and the stable austenitic stainless steels, such as SAE 321, have been found to be insensitive to the presence of gaseous hydrogen and, therefore, any system using these materials should be free from degradation due to hydrogen embrittlement. Thus, if these or similar hydrogen compatible materials are used exclusively in a hydrogen wind tunnel, problems caused by exposure to gaseous hydrogen will not occur.

VII.5 Hydrogen Safety.

Perhaps the greatest safety hazard encountered when handling hydrogen is its high combustability. The ordinary burning of a mixture of hydrogen and air can occur within the broad limits of about four percent to seventy-five percent of hydrogen by volume. When combustion occurs rapidly an explosion results. Thus unless suitable precautions are taken, a flammable mixture is possible in a hydrogen wind tunnel during some stage of operation and any source of ignition could then cause serious trouble. Because hydrogen is a highly combustable substance, the wind tunnel designer and technician should be familiar with the combustion of hydrogen. The following discussion serves only as an introduction to this subject and in the event that a hydrogen wind tunnel is constructed, the designer should refer to specific details in other sources, for example, reference 25.

When hydrogen and air are burned the reaction is

$$H_2 + \frac{1}{2} O_2 + 1.89N_2 = 1.89N_2 + H_2O + \text{heat} \qquad (7.10)$$

This is the stoichiometric mixture of thirty percent hydrogen by volume which when burned uses up all of the oxygen in the air. The heat of combustion converts the water to steam and raises the temperature of the resulting mixture. When this occurs in a closed volume, the temperature increases from T_1 to T_2 and the number of moles changes from n_1 to n_2 causing a pressure change of

$$\frac{P_2}{P_1} = \frac{n_2 T_2}{n_1 T_1} \qquad (7.11)$$

The above equation assumes an adiabatic process, uniform temperature distribution throughout the mixture, and negligible dissociation of the combustion products, resulting in a higher calculated pressure than actually occurs.

It is recommended that any wind tunnel designed to use hydrogen as the test gas be constructed so that if the hydrogen is to be discharged into the atmosphere, it could be burned under controlled conditions. The principle is the same as that used in oil refineries where combustable gases are burned rather than allowed to accumulate.

Several safety codes, such as references 26, 27, and 28, exist which could be of help during the design of a hydrogen wind tunnel and auxiliary equipment. Generally, the building in which the wind tunnel is contained should have: 1) a vent system for the apparatus, 2) adequate ventilation, 3) an adequate electrical grounding system, and 4) no pockets near the ceiling which could trap hydrogen.

CHAPTER VIII

CONCLUSIONS

A theoretical analysis to determine the suitability of hydrogen as a cryogenic wind tunnel test gas has been made. The major conclusions to be drawn from the analysis are as follows:

1. A wind tunnel using cryogenic hydrogen, instead of air or cryogenic nitrogen, as the test gas will have a significant increase in test Reynolds number without increasing the aerodynamic loads.
2. The theoretical saturation boundary for parahydrogen is well defined. Therefore, any possible effects caused by the liquefaction of the test gas can easily be avoided provided that the maximum local Mach number on the model is known.
3. The relatively high value of the characteristic rotational temperature causes the behavior of hydrogen, under cryogenic conditions, to differ substantially from the behavior of an ideal diatomic gas when considering the compressible flow regime. Therefore, if it is essential to model an ideal diatomic gas, cryogenic hydrogen is unacceptable as a wind tunnel test gas in compressible flow situations. Consequently, a cryogenic hydrogen wind tunnel would not provide an adequate simulation of transonic and supersonic flow situations in ambient air.

4. At low Mach numbers, where the assumption of incompressibility is valid, the deviations in the isentropic flow parameters for cryogenic parahydrogen from the ideal diatomic gas values are negligible. Thus, in the incompressible flow regime, cryogenic hydrogen is an acceptable test gas. Consequently, a cryogenic hydrogen wind tunnel would provide an adequate simulation of incompressible flow situations in ambient air.
5. A cryogenic hydrogen wind tunnel requires more power to operate than a cryogenic nitrogen wind tunnel. Although a smaller size cryogenic hydrogen wind tunnel may be designed because of the Reynolds number advantage of hydrogen, more power is required to produce liquefied hydrogen than is required to produce liquefied nitrogen. This difference in the liquefaction power requirements results in the above conclusion.
6. In the event that a wind tunnel is constructed which would use hydrogen as a test gas, materials compatible with hydrogen must be used exclusively to avoid possible problems as a result of exposure to gaseous hydrogen.
7. Although hydrogen is a highly combustable gas, safety codes exist which, when followed, minimize the risk involved in handling hydrogen.

LIST OF REFERENCES

1. Heppe, Richard R.; O'Laughlin, B. D.; and Celniker, Leo: New Aeronautical Facilities -- We Need Them Now. Astronaut. & Aeronaut., Vol. 6, no. 3, Mar. 1968, pp. 42-54.

2. Poisson-Quinton, Philippe: From Wind Tunnel to Flight, the Role Of the Laboratory in Aerospace Design. J. Aircraft, vol. 5, no. 3, May-June 1968, pp. 193-214.

3. Adcock, Jerry B.; Kilgore, Robert A.; and Ray, Edward J.: Cryogenic Nitrogen as a Transonic Wind Tunnel Test Gas. AIAA Paper No. 75-143, Jan. 1975.

4. Farkas, Adalbert: Orthohydrogen, Parahydrogen, and Heavy Hydrogen. Cambridge University Press, London, 1935.

5. Sonntag, R. E.; and Van Wylen, G. J.: Fundamentals of Statistical Thermodynamics. John Wiley & Sons, Inc., New York, 1966.

6. Weber, L. A.: Thermodynamic and Related Properties of Parahydrogen From the Triple Point to 300 K at Pressures to 1000 Bar. NASA SP-3088, 1975.

7. McCarty, R. D.; and Weber, L. A.: Thermophysical Properties of Parahydrogen From the Freezing Line to 5000 R for Pressures to 10000 psia. Nat. Bur. Stand. Tech. Note 617, 1972.

8. Roder, H. M.; Weber, L. A.; and Goodwin, R. D.: Thermodynamic and Related Properties of Parahydrogen From the Triple Point to 100 K at Pressures to 340 Atmospheres. Nat. Bur. Stand. Monograph 94, 1965.

9. McCarty, R. D.: A Modified Benedict-Webb-Rubin Equation of State for Parahydrogen. Nat. Bur. Stand. NBSIR 74-357, 1974.

10. Roder, H. M.; McCarty, R. D.; and Hall, W. J.: Computer Programs for Thermodynamic and Transport Properties of Hydrogen (Tabcode-II). Nat. Bur. Stand. Tech. Note 625, 1972.

11. McCarty, R. D.: Hydrogen Technological Survey-Thermophysical Properties. NASA SP-3089.

12. Vincenti, W. G.; and Kruger, C. H.: Introduction to Physical Gas Dynamics. Robert E. Krieger Publishing Company, Huntington, New York, 1975.

13. Kilgore, Robert A.: The Cryogenic Wind Tunnel for High Reynolds Number Testing. Ph.D. Thesis, The University of Southampton, 1974. (Available as NASA TM X-70207.)

14. Haut, R. C.; and Adcock, Jerry B.: Tables of Isentropic Expansions of Parahydrogen and Related Transport Properties for Total Temperatures From 25 K to 300 K and for Total Pressures From 1 atm to 10 atm. NASA TM X-72826, 1976.

15. Woolley, Harold W.; and Benedict, William S.: Generalized Tables of Corrections to Thermodynamic Properties for Nonpolar Gases. NACA TN 3272, 1956.

16. Adcock, Jerry B.: Real-Gas Effects Associated with One-Dimensional Transonic Flow of Cryogenic Nitrogen. NASA TN D-8274, 1976.

17. Haut, R. C.; and Adcock, Jerry B.: Prandtl-Meyer Flow Tables for Parahydrogen at Total Temperatures From 30 K to 290 K and For Nitrogen at Total Temperatures From 100 K to 300 K at Total Pressures From 1 atm to 10 atm. NASA TMX-73932, 1976.

18. Haut, R. C.; and Adcock, Jerry B.: Steady Normal Shock Wave Solution Tables of Parahydrogen for Total Temperatures From 30 K to 290 K and for Total Pressures from 1 atm to 10 atm. NASA TMX-73899, 1976.

19. Computer program developed and run by Mr. R. Cuffel, Jet Propulsion Laboratory (No publication available).

20. U.S. Standard Atmosphere, 1962. Prepared under sponsorship of the National Aeronautics and Space Administration, the United States Air Force, and the United States Weather Bureau.

21. Liepmann, H. W.; and Roshko, A.: Elements of Gasdynamics. John Wiley & Sons, Inc., New York; 1957.

22. Adcock, Jerry B. and Ogburn, Marilyn E.: Power Calculations for Isentropic Compressions of Cryogenic Nitrogen. NASA TM X-73903, 1976.

23. Jacobs, R. B.: Liquid Requirements for Cool-Down of Cryogenic Equipment. Advances in Cryogenic Engineering, vol. 8, Plenum Press, 1963.

24. Haselden, G. G.: Cryogenic Fundamentals. Academic Press, London, 1971.

25. Hernandez, H. P.: Designing for Safety in Hydrogen Bubble Chambers Advances in Cryogenic Engineering, vol. 2, Plenum Press, 1956.

26. National Fire Protection Agency: National Fire Codes, vol. 4, 1975, pages 50A-1 through 50B-16.

27. Hernandez, H. P.: A Review of Liquid-Hydrogen Safety for Research Equipment. Advances in Cryogenic Engineering, vol. 12, Plenum Press, 1966.

28. Hord, J.: Is Hydrogen Safe? Nat. Bur. Stand. Tech. Note 690, 1976.

APPENDICES

APPENDIX A

Figures

FIGURE PAGE

FIGURE PAGE

FIGURE PAGE

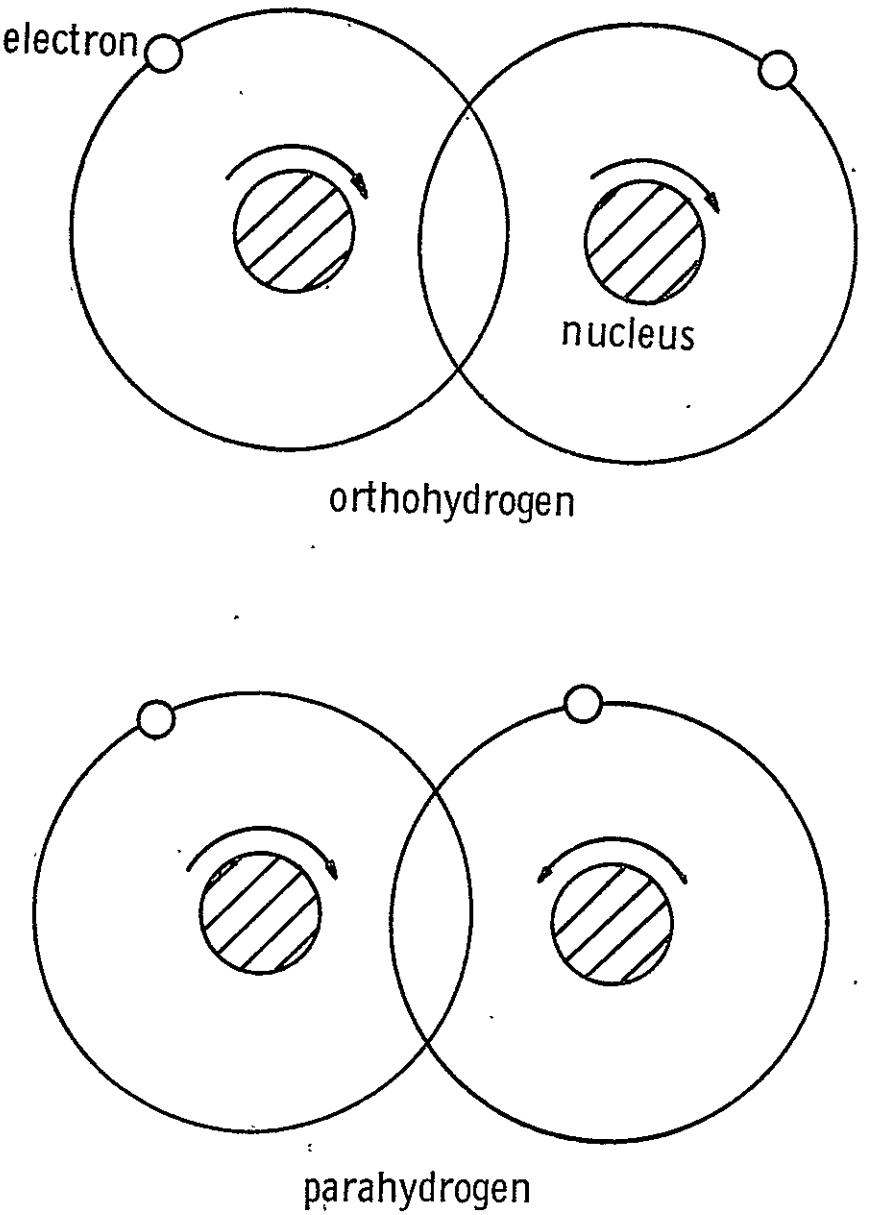

Figure 1. Ortho- and parahydrogen.

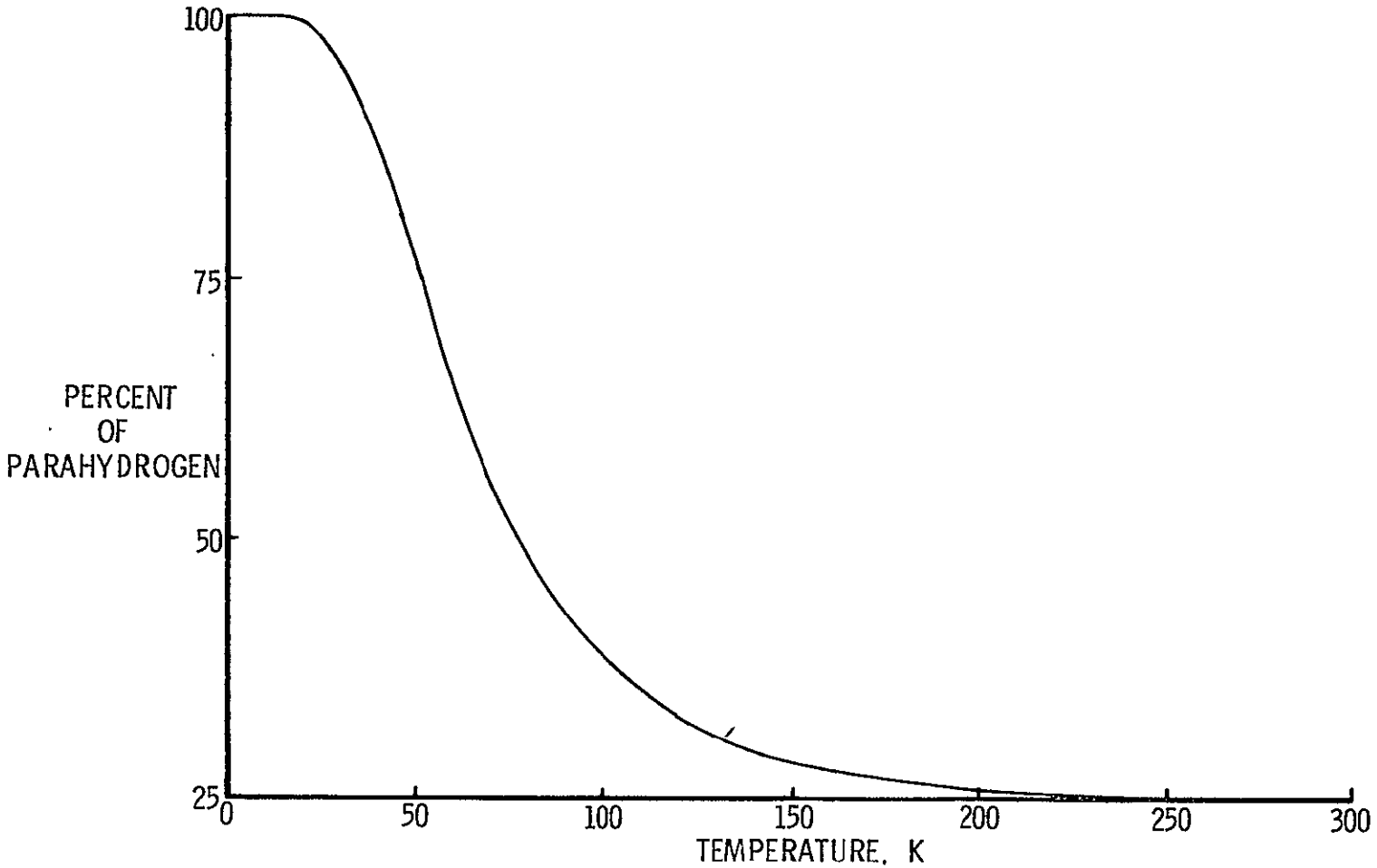

Figure 2. Composition of equilibrium hydrogen.

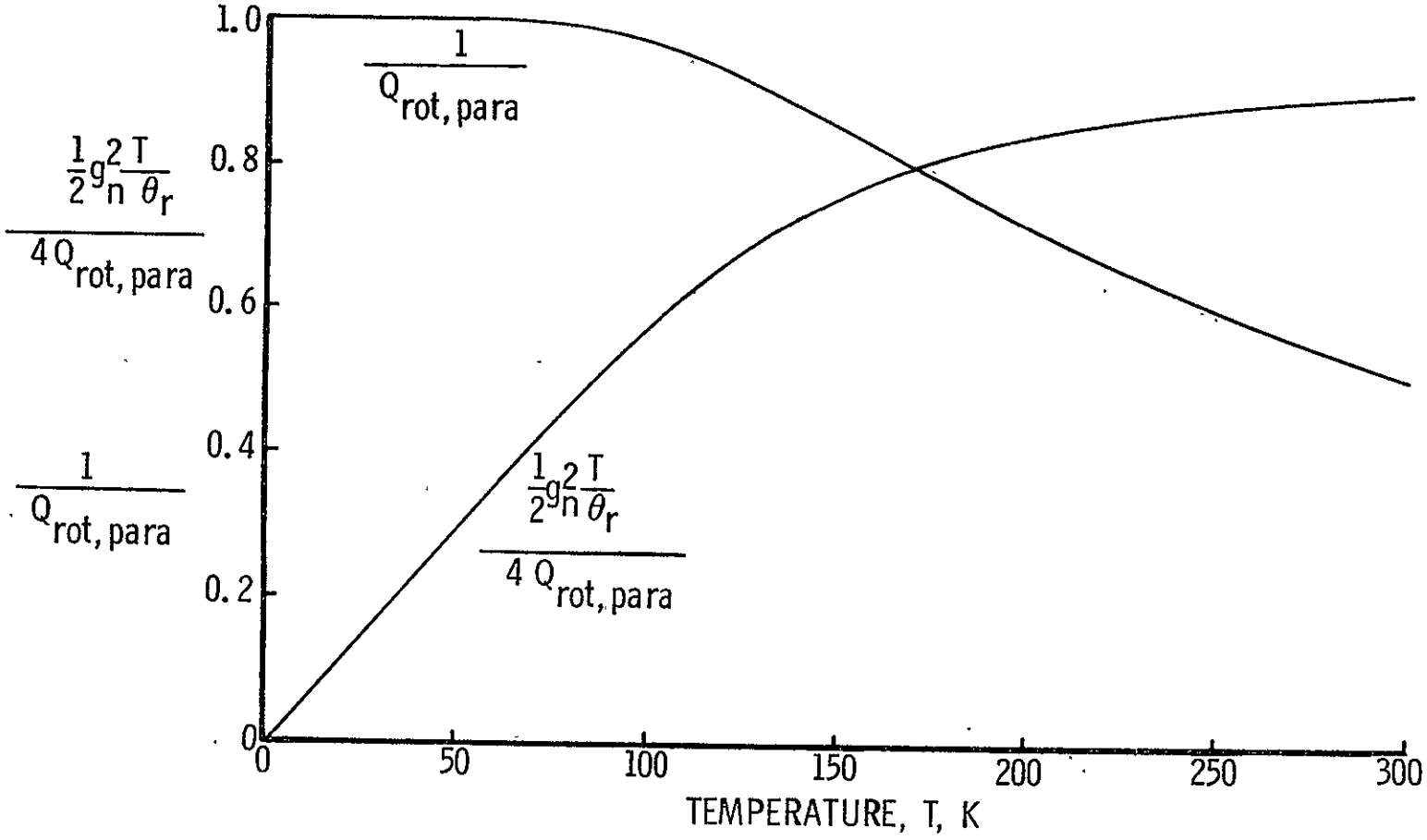

Figure 3. Characteristic rotational temperature influence range as illustrated by the rotational partition function.

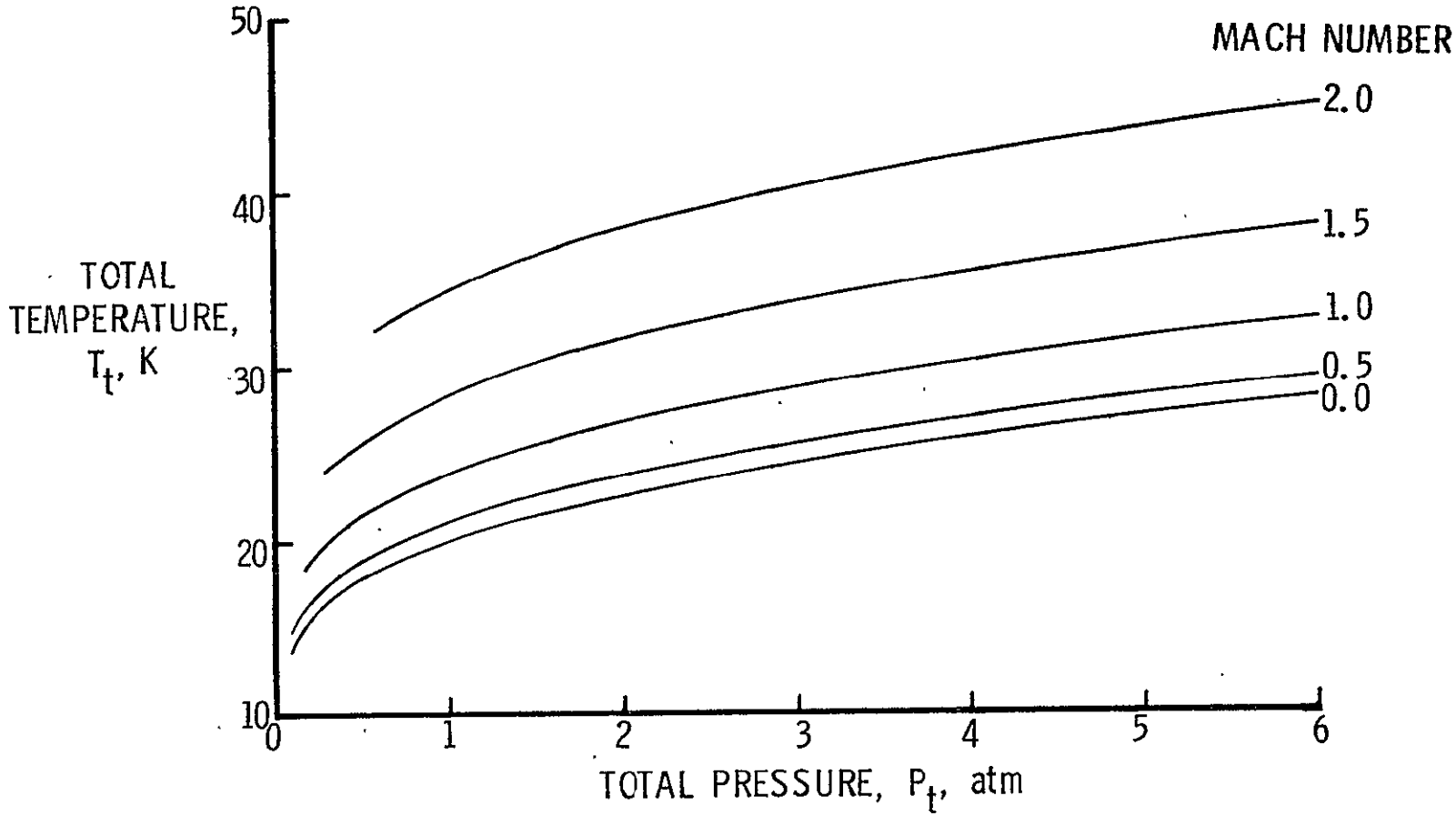

Figure 4. Theoretical saturation boundary of parahydrogen for different maximum local Mach numbers.

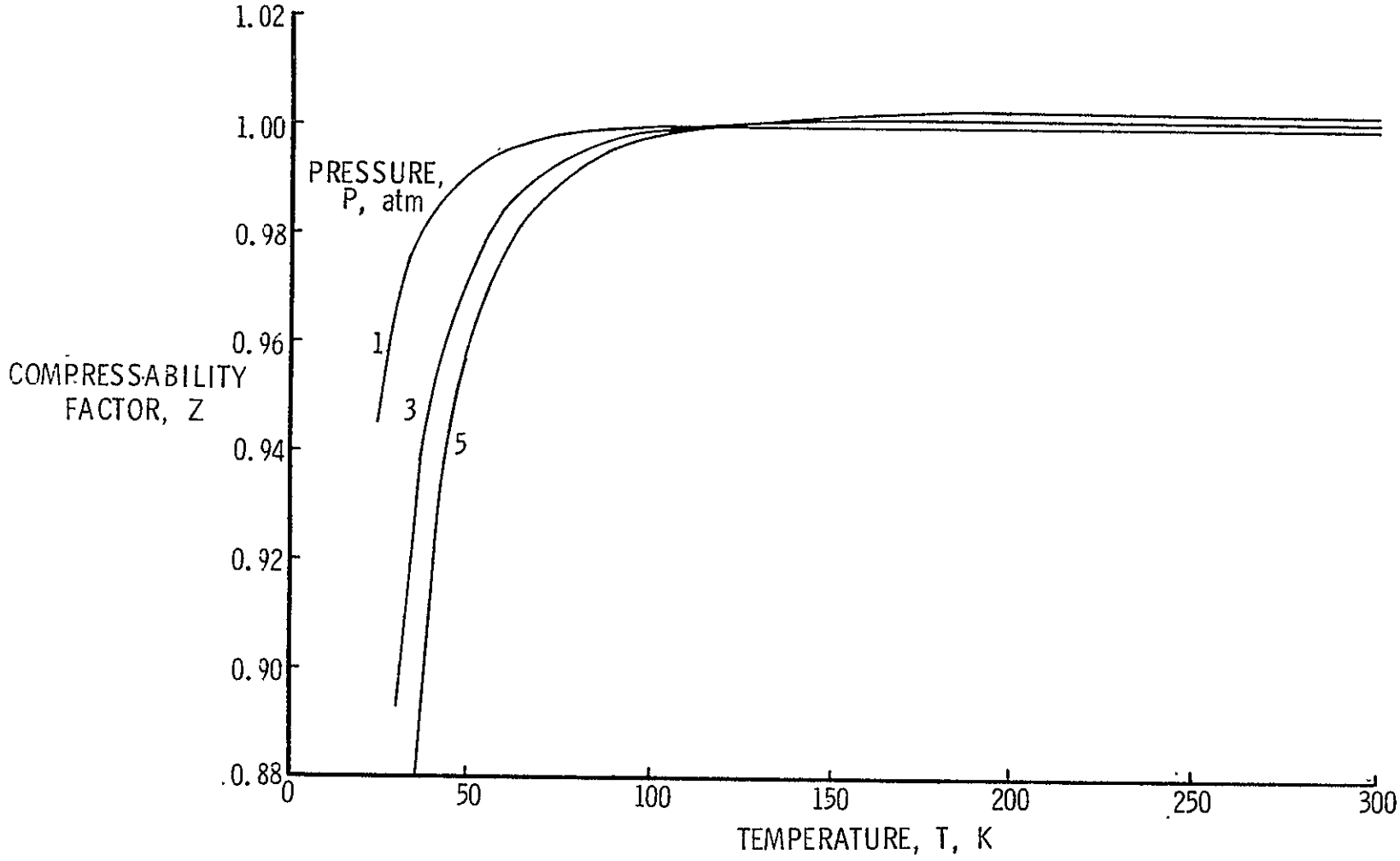

Figure 5. Compressibility factor, Z, for parahydrogen.

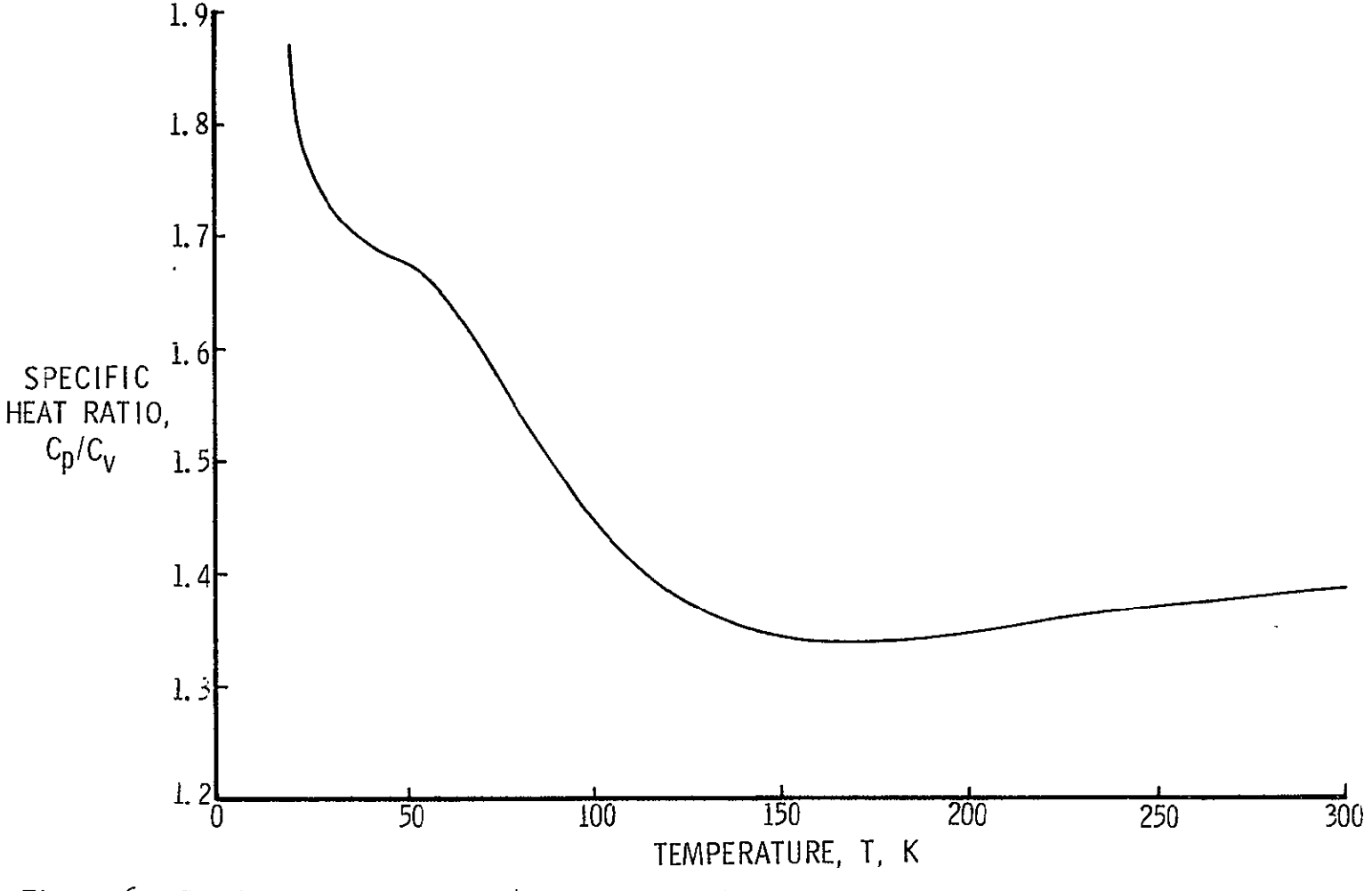

Figure 6. Specific heat ratio, C_p/C_v, for parahydrogen at a pressure of one atmosphere.

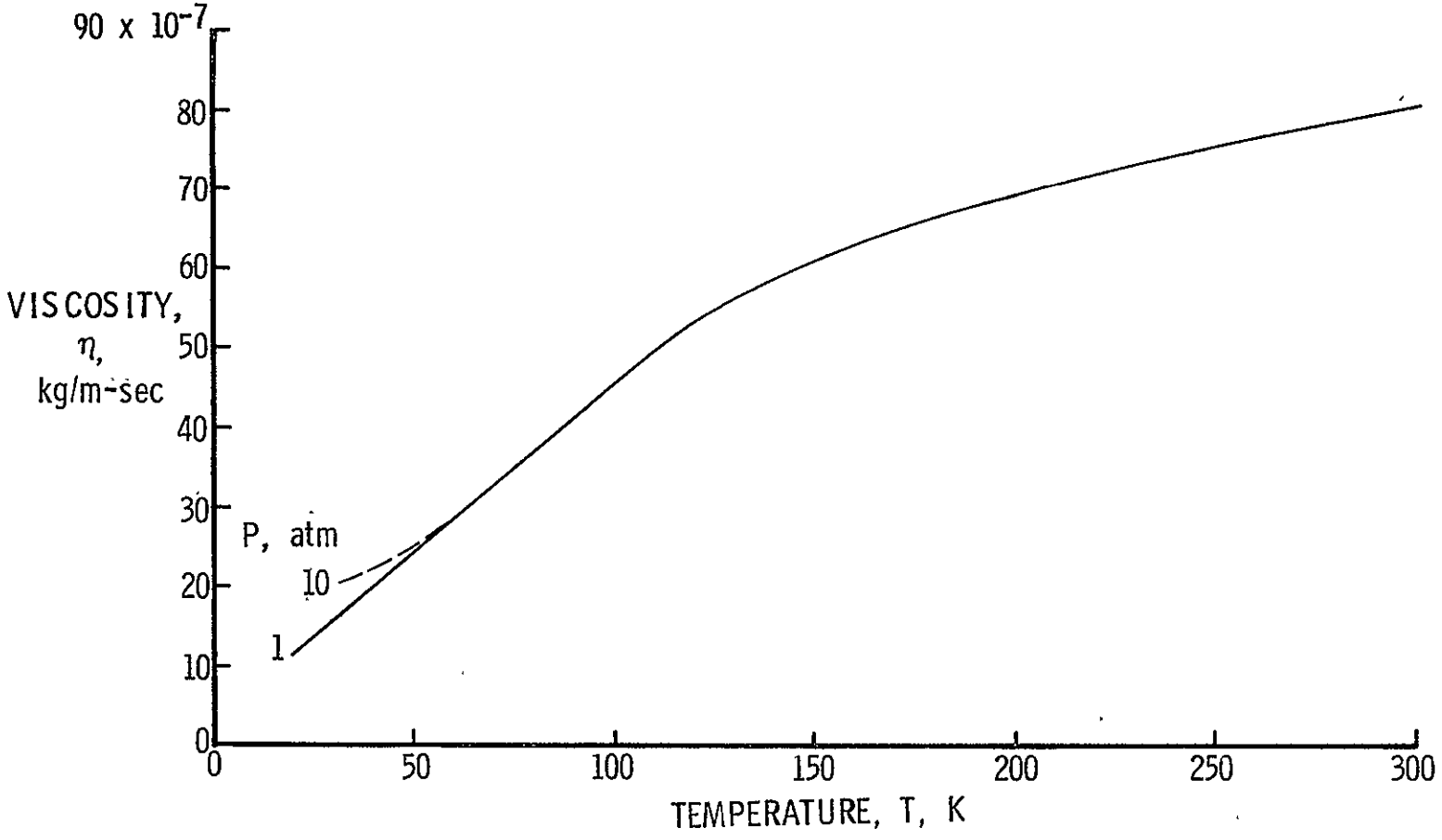

Figure 7. Viscosity, η, for parahydrogen.

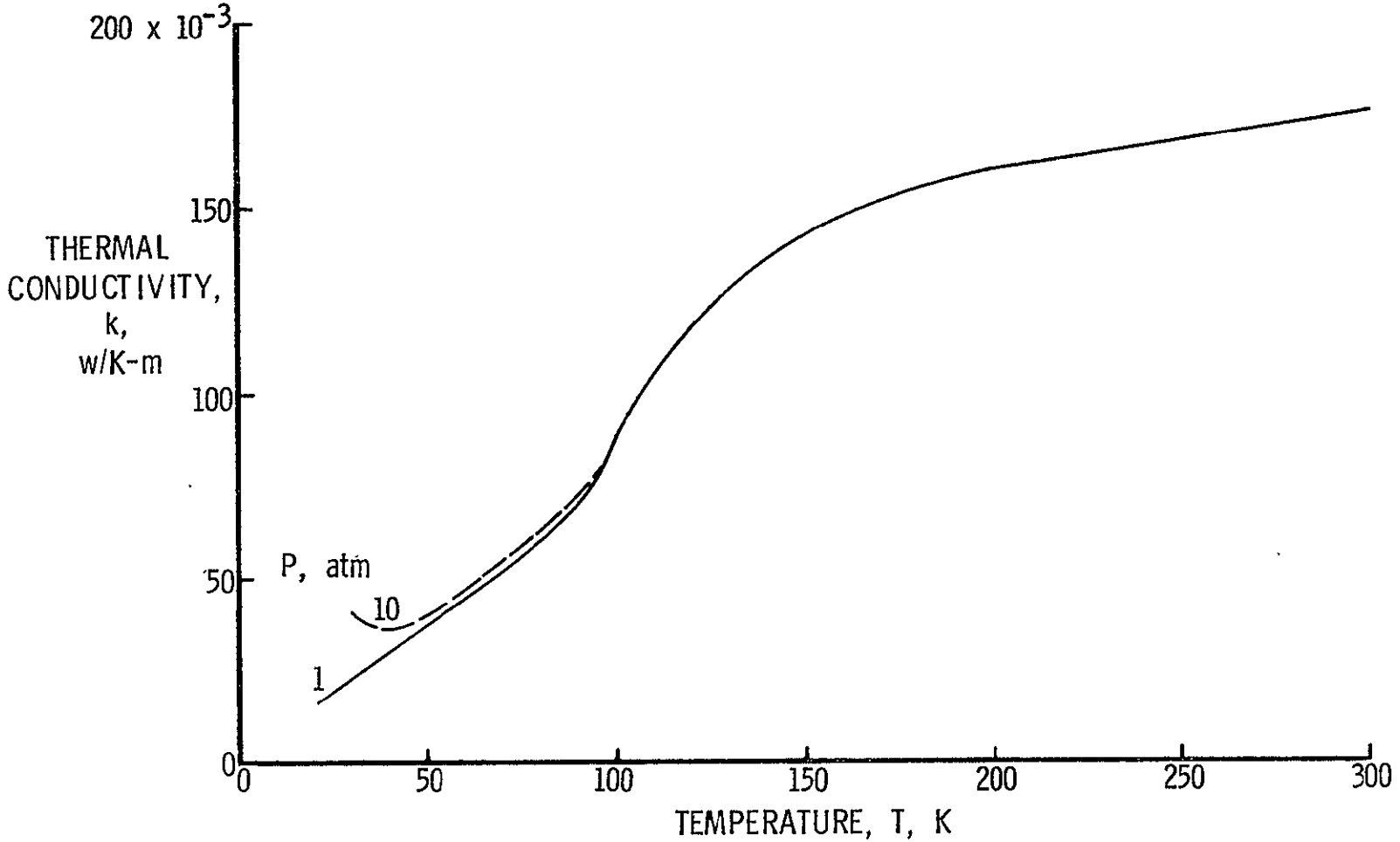

Figure 8. Thermal conductivity, k, for parahydrogen.

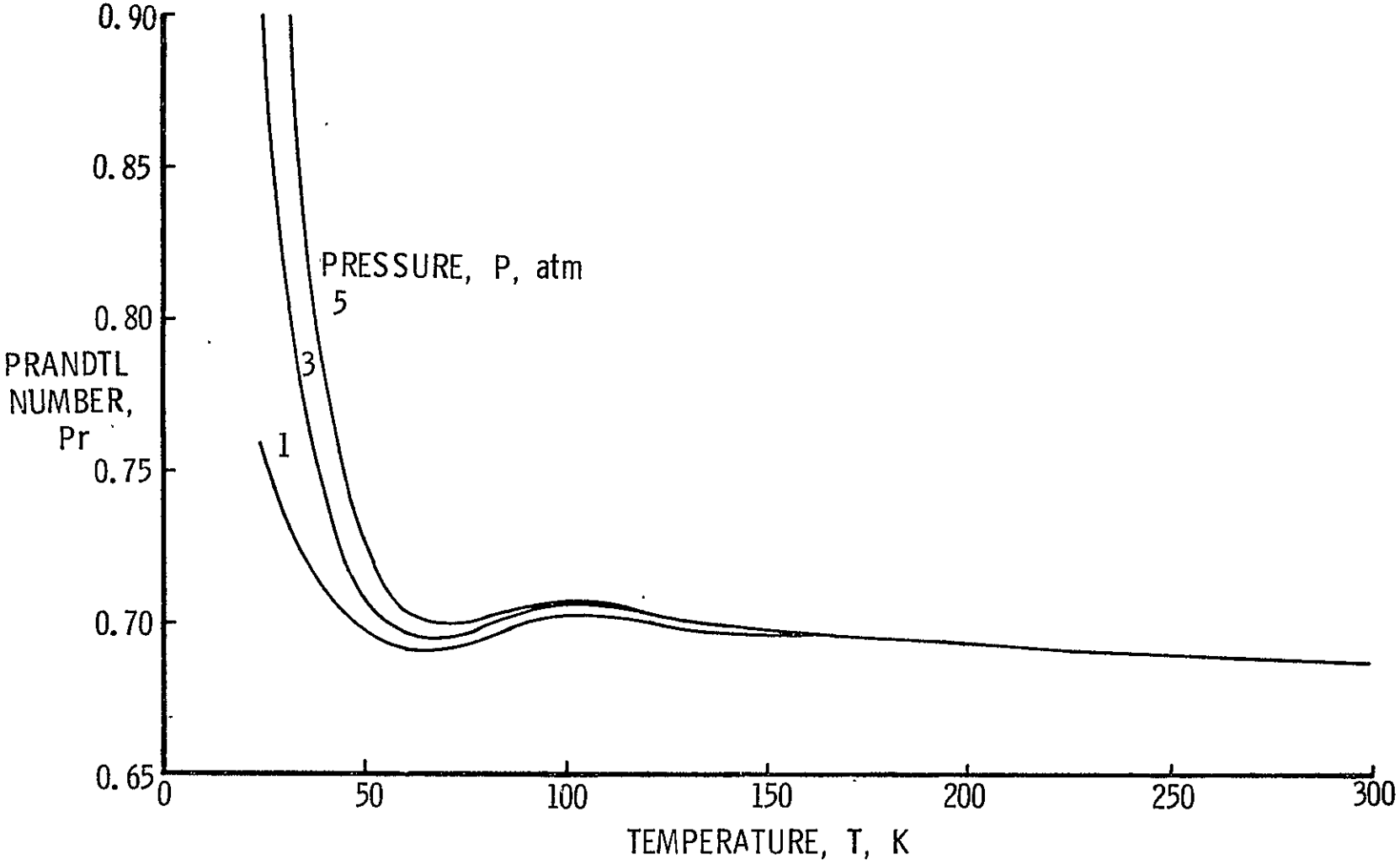

Figure 9. Prandtl number, Pr, for parahydrogen.

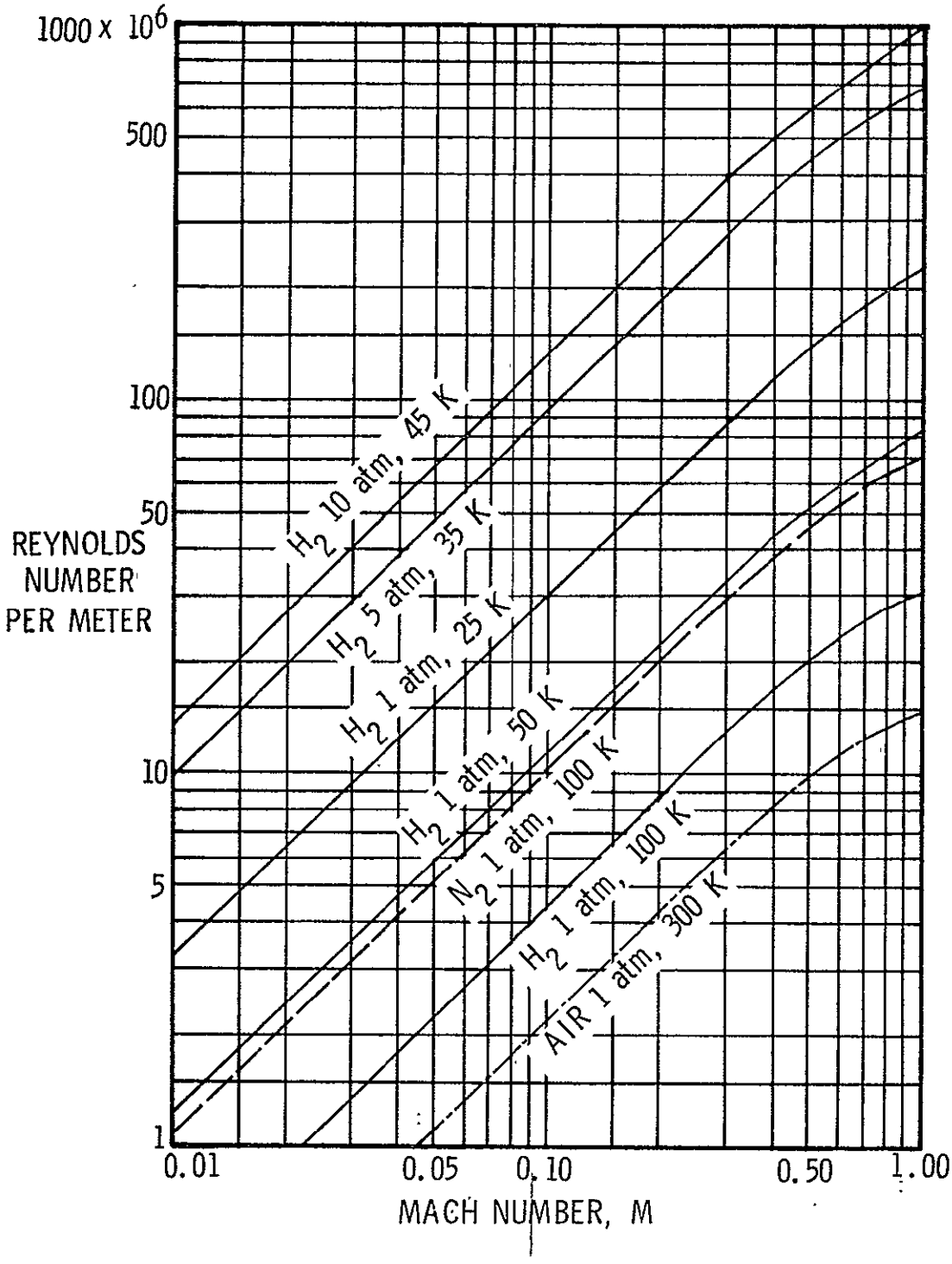

Figure 10. Reynolds number per meter for air, nitrogen, and hydrogen at various total conditions.

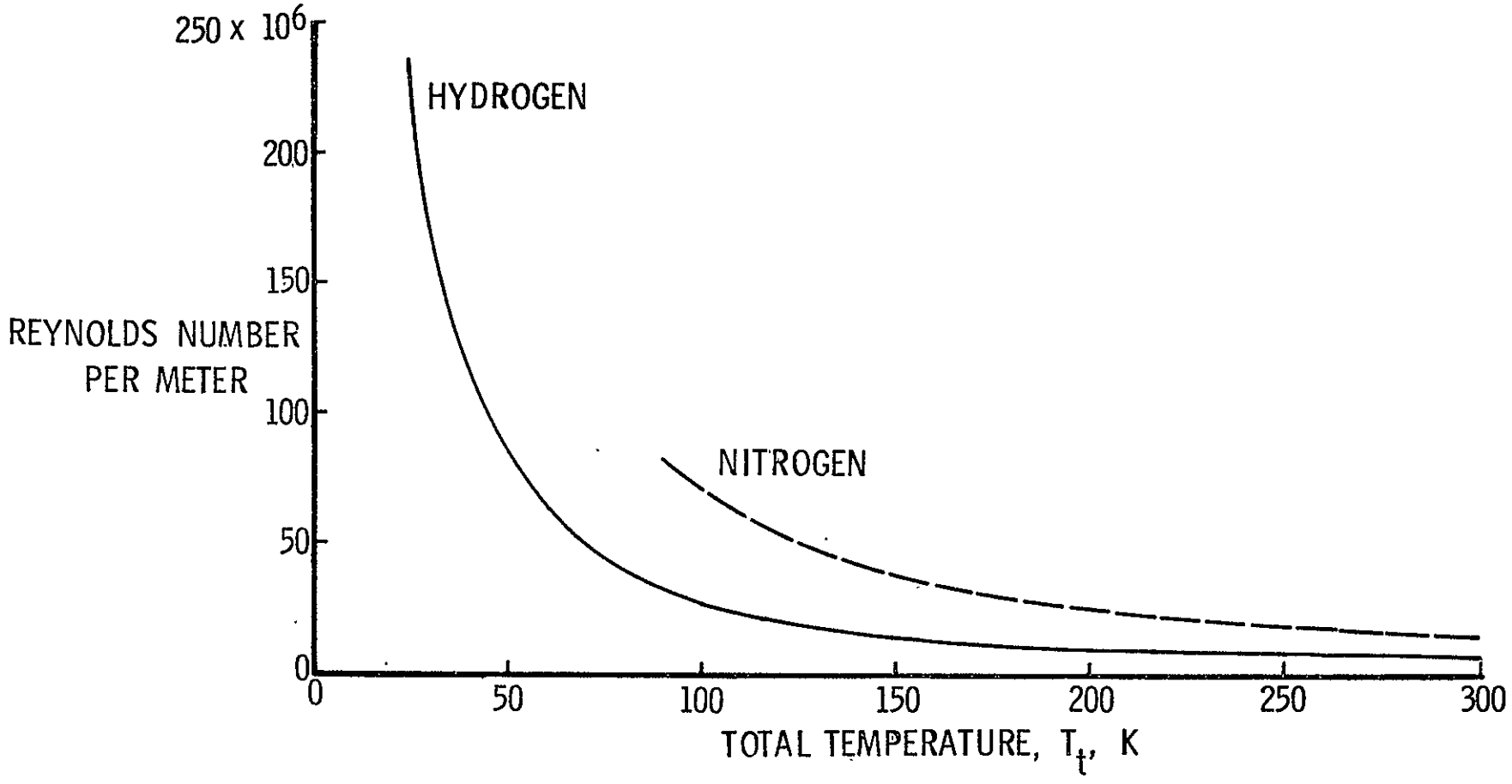

Figure 11. Reynolds number per meter comparison between hydrogen and nitrogen at a free stream Mach number of 1.0 and a total pressure of one atmosphere.

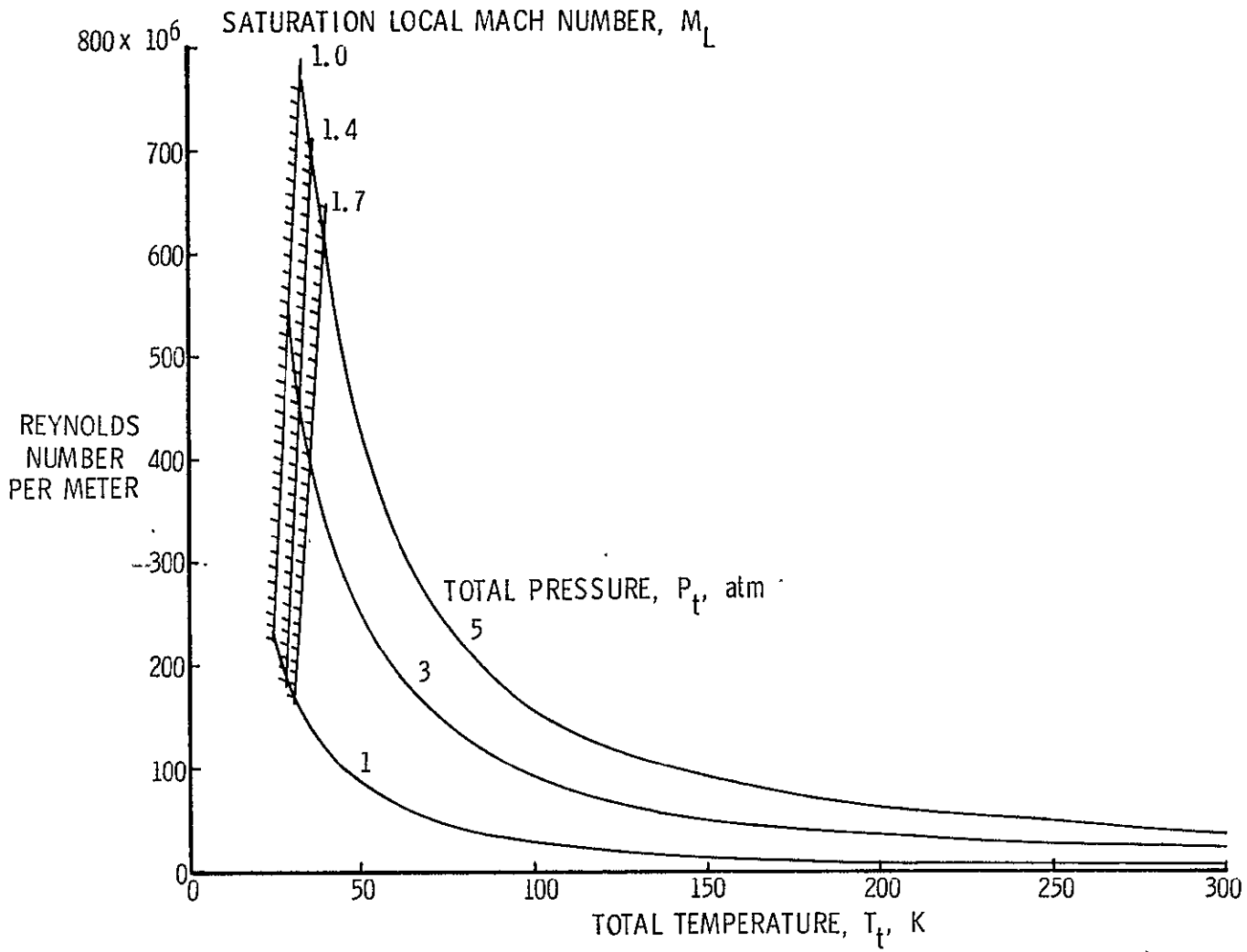

Figure 12. Reynolds number restrictions due to theoretical saturation boundaries at a free stream Mach number of 1.0.

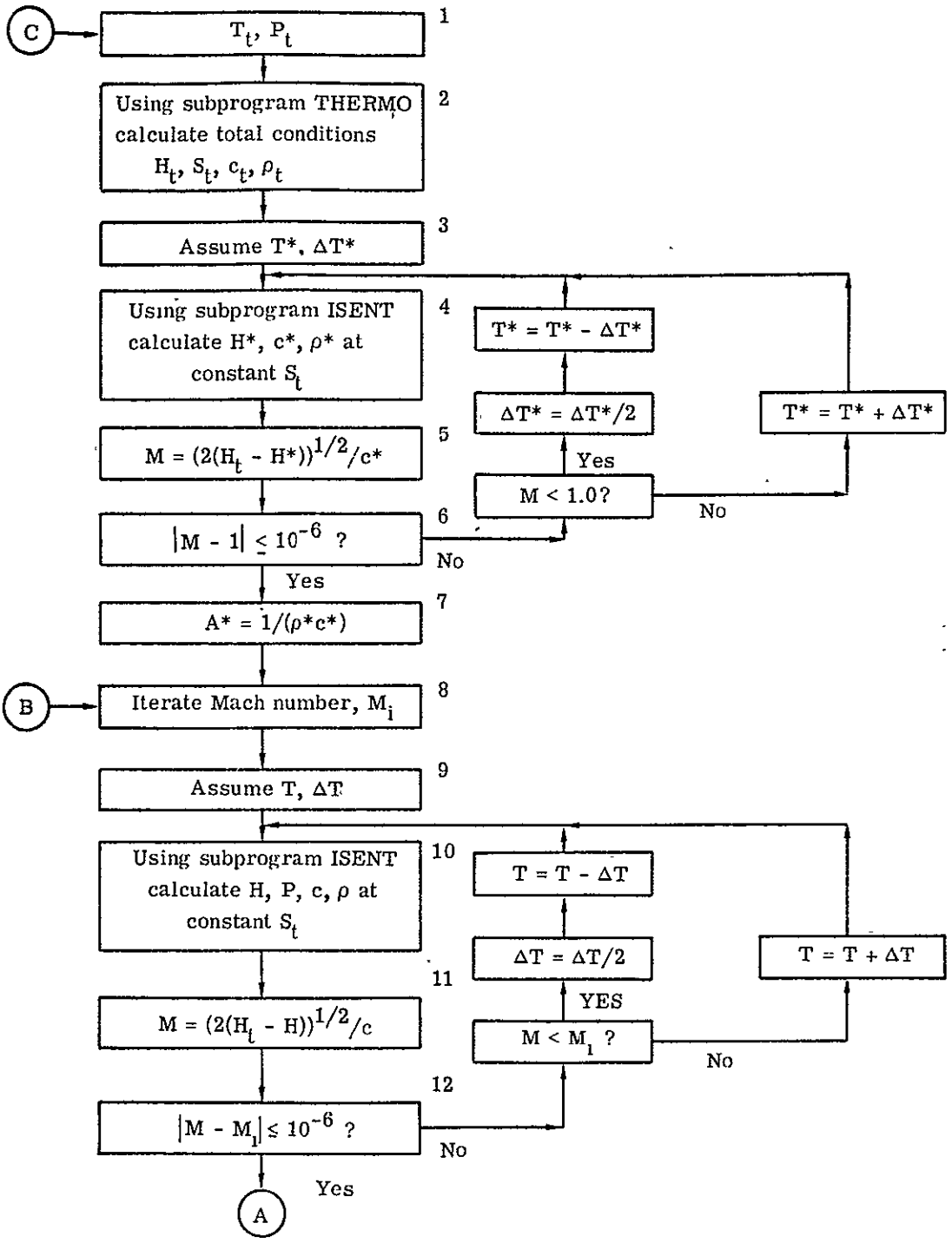

Figure 13. Computer program flow charts for the isentropic flow solution.

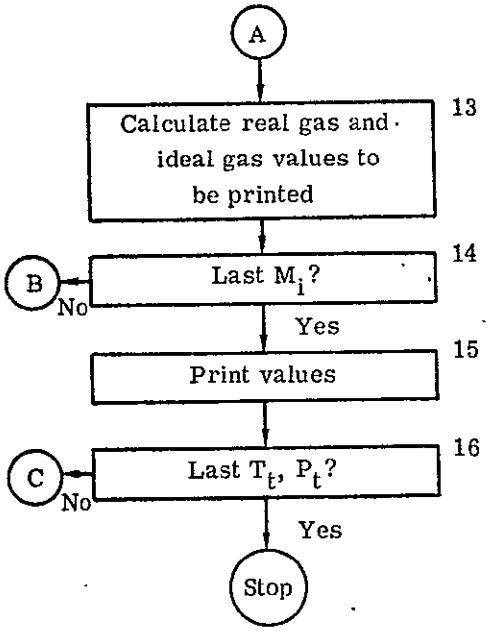

Subprogram ISENT

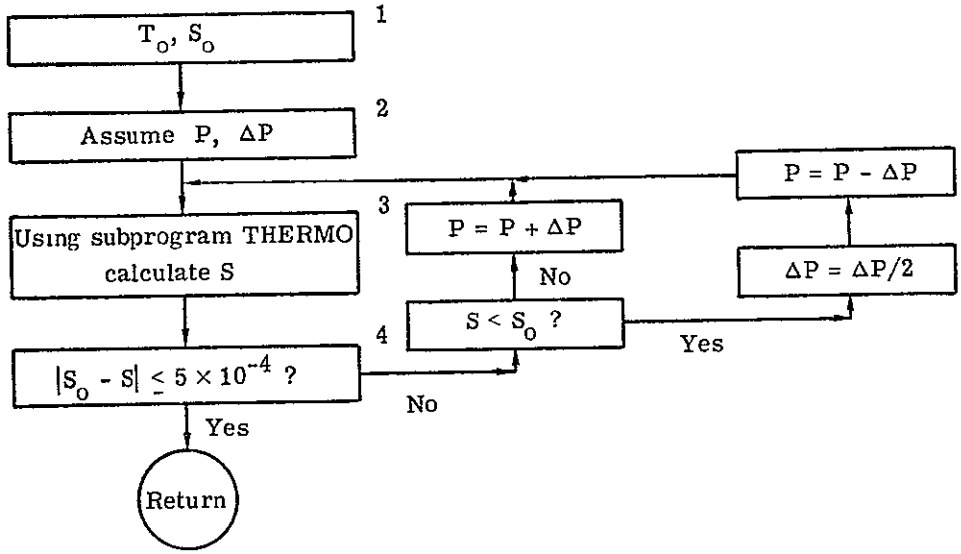

Figure 13. Concluded.

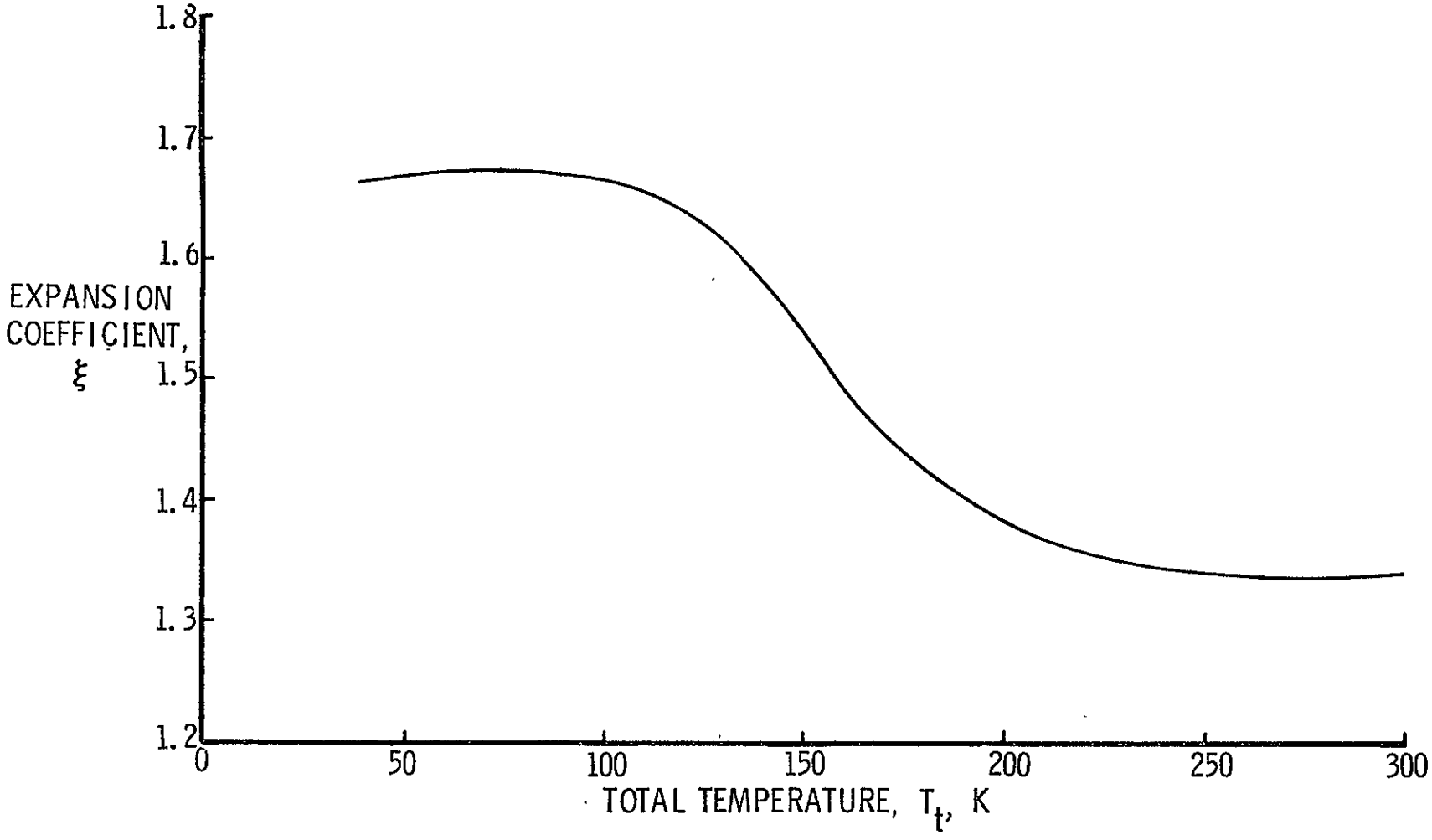

Figure 14. Isentropic expansion coefficient, ξ, for expansions of parahydrogen to a Mach number of 2.0 at a total pressure of one atmosphere.

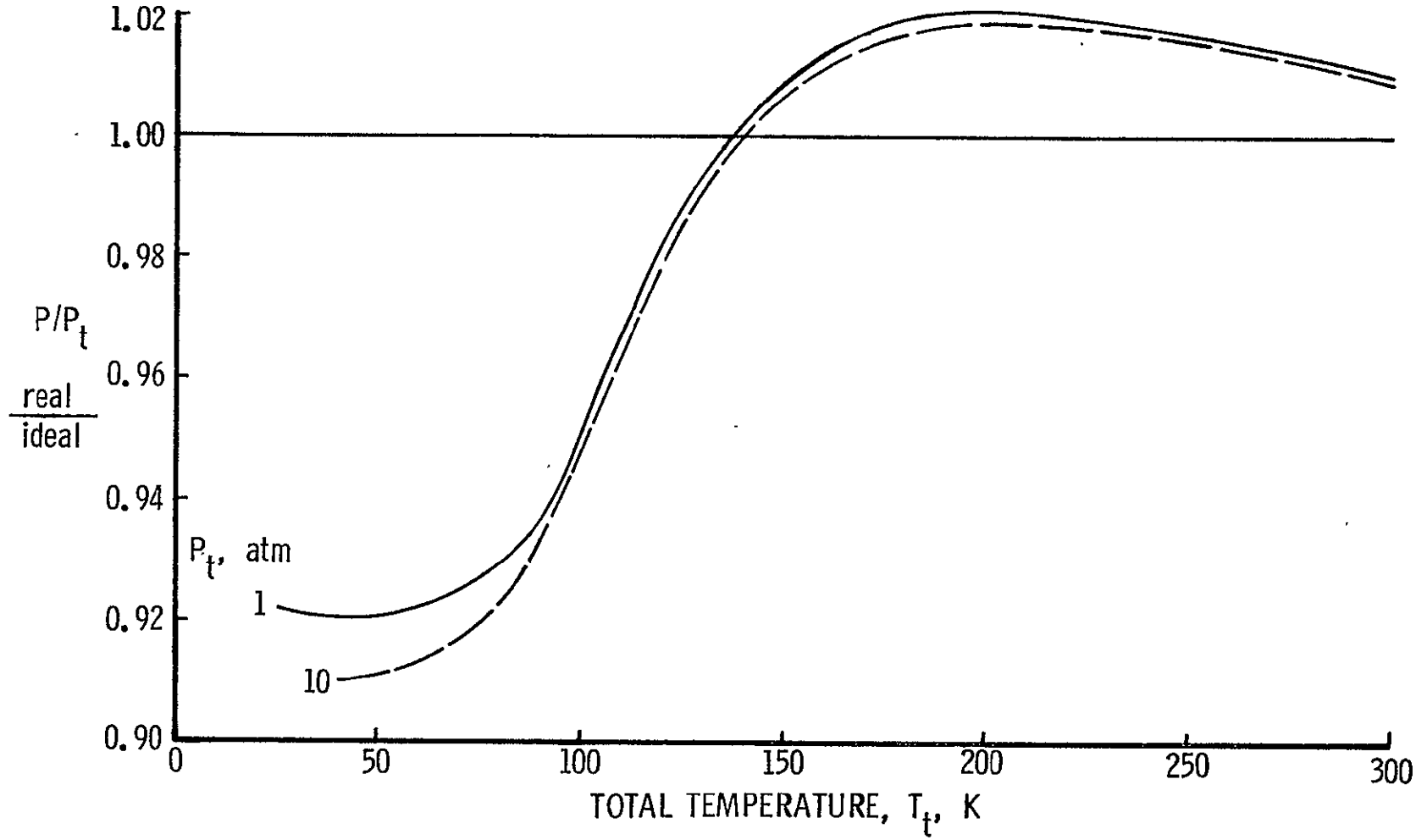

Figure 15. Pressure ratios for the isentropic expansion of parahydrogen to a Mach number of 1.0 relative to the ideal diatomic gas value.

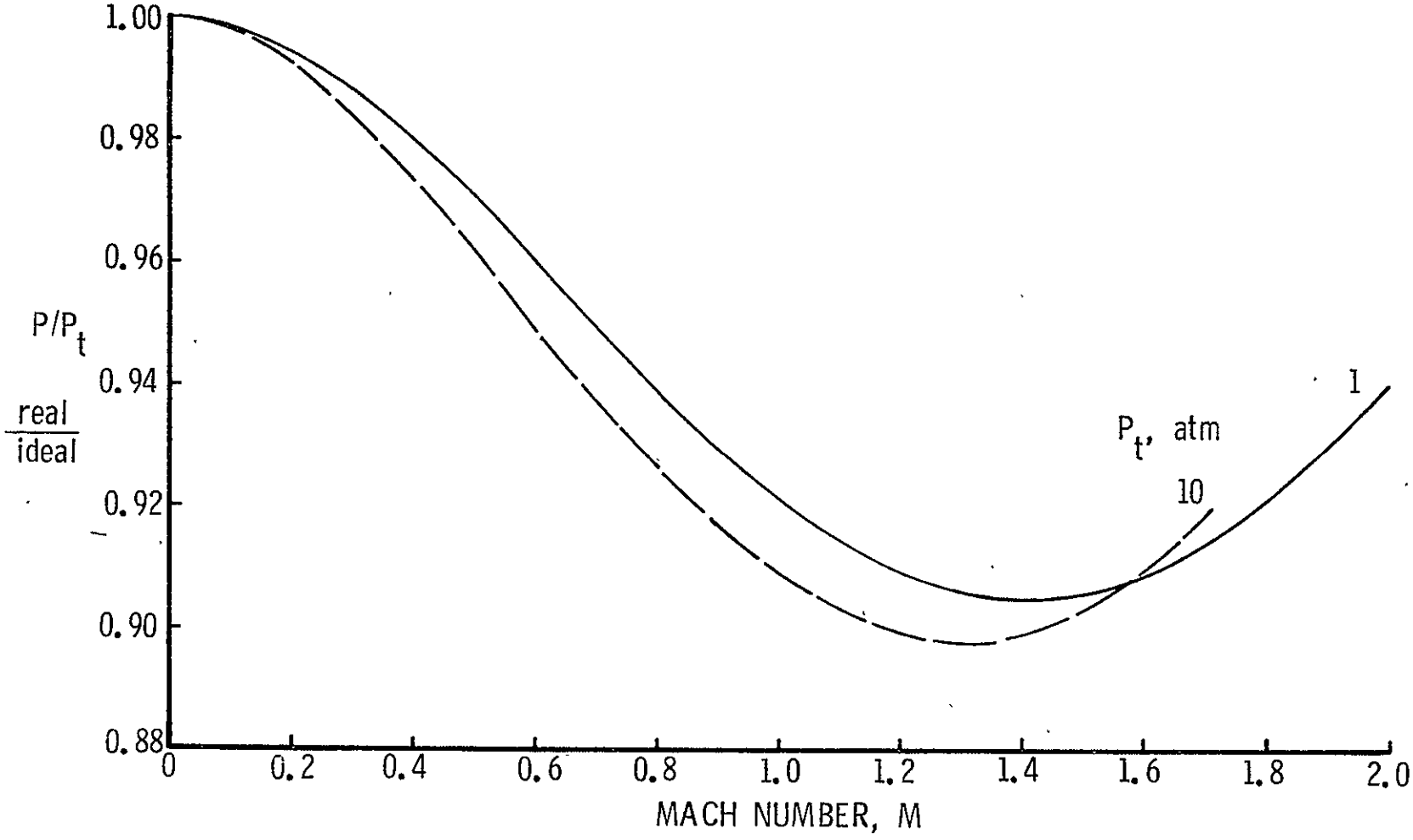

Figure 16. Pressure ratios for the isentropic expansion of parahydrogen to various Mach numbers at a total temperature of 40 K, relative to the ideal diatomic gas value.

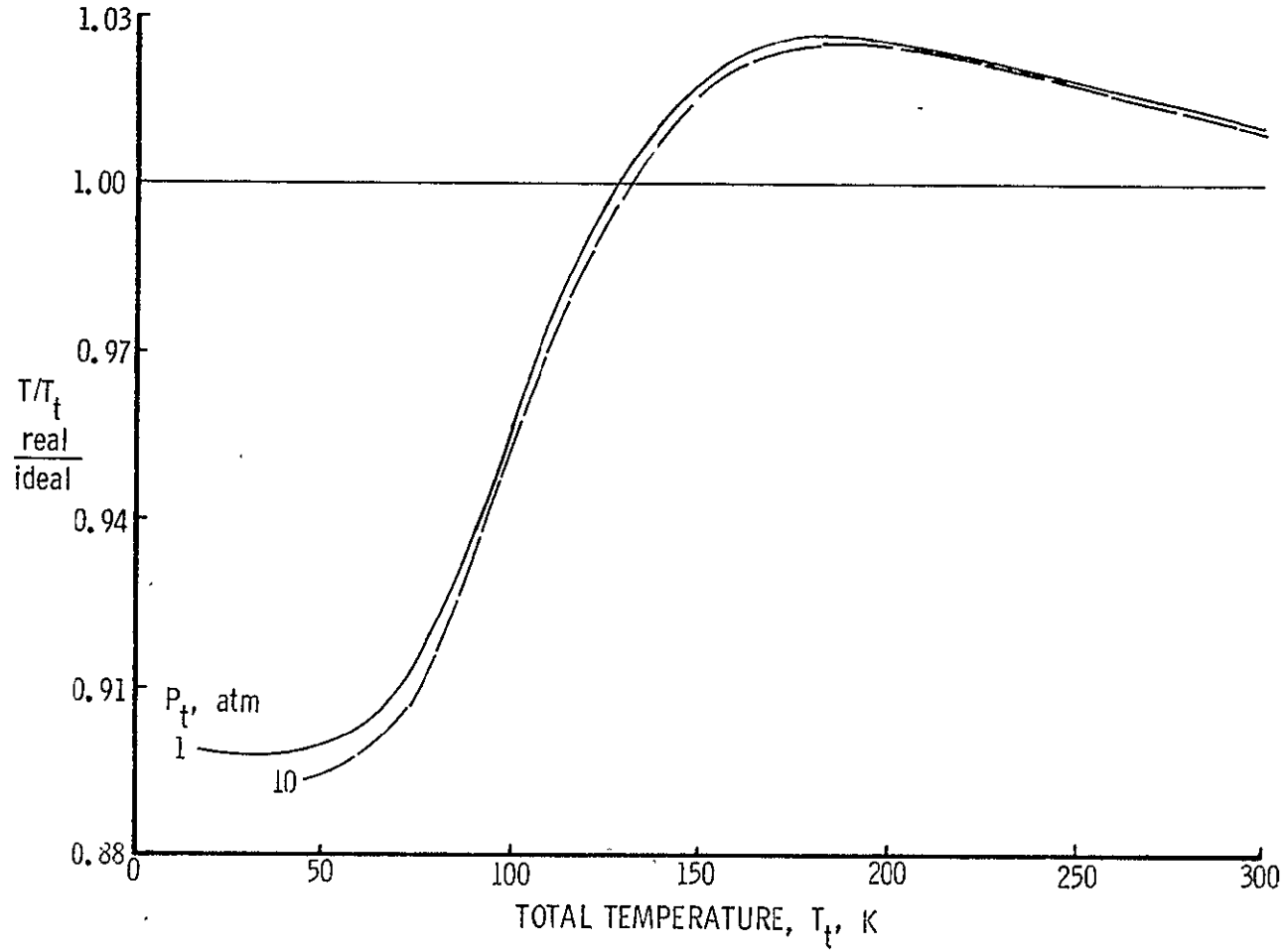

Figure 17. Temperature ratios for the isentropic expansion of parahydrogen to a Mach number of 1.0 relative to the ideal diatomic gas value.

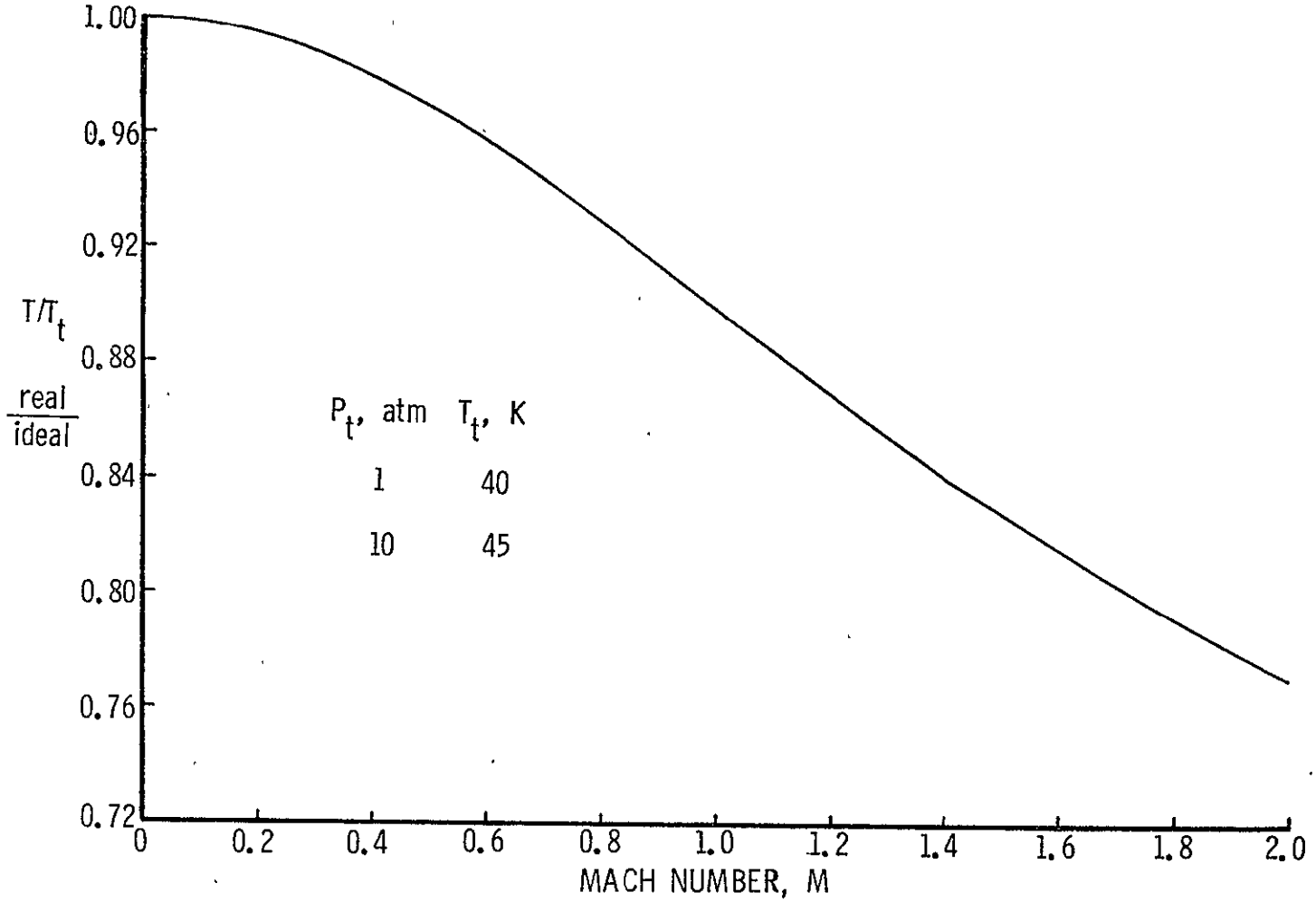

Figure 18. Temperature ratios for the isentropic expansion of parahydrogen to various Mach numbers, relative to the ideal diatomic gas value.

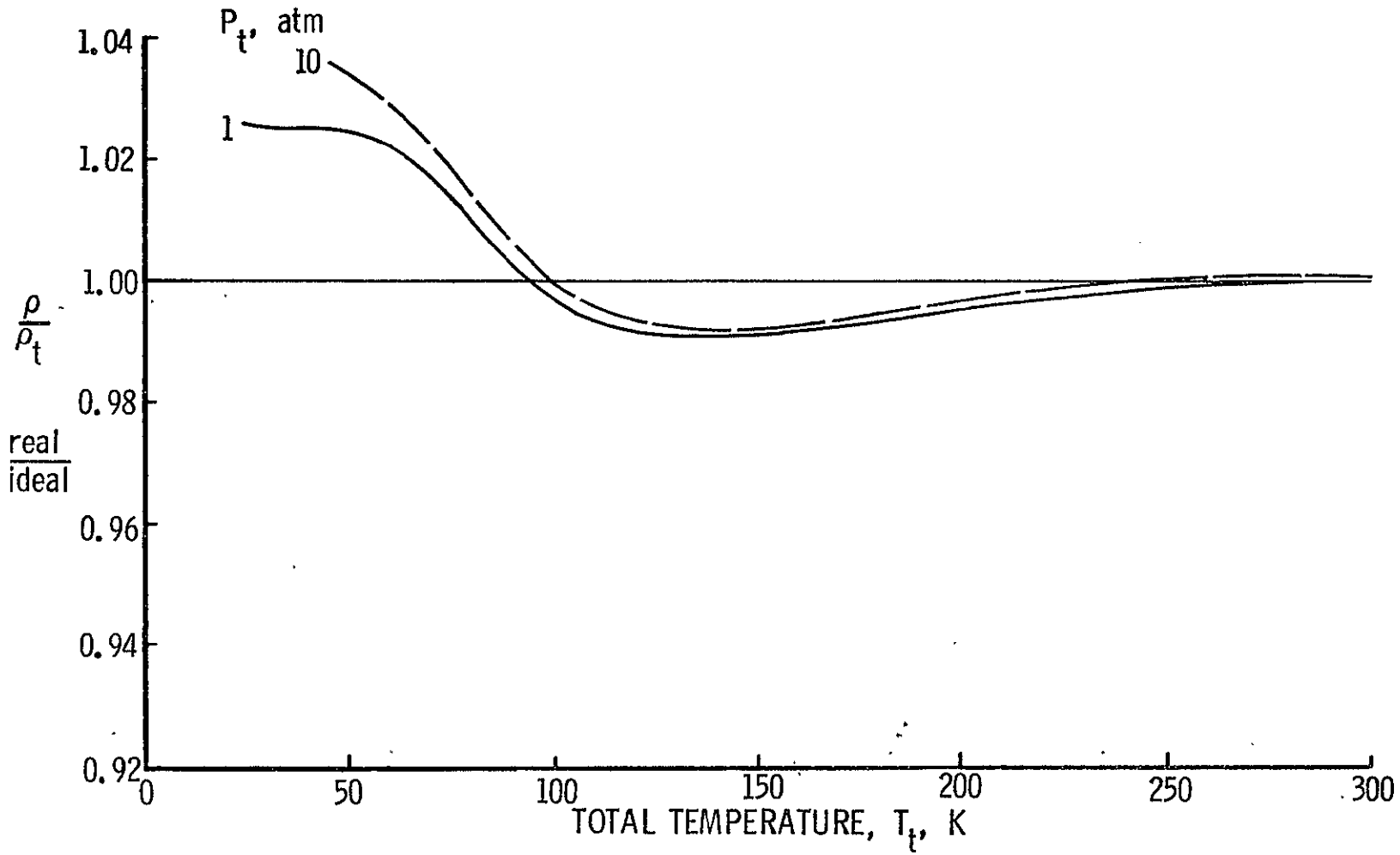

Figure 19. Density ratios for the isentropic expansion of parahydrogen to a Mach number of 1.0 relative to the ideal diatomic gas value.

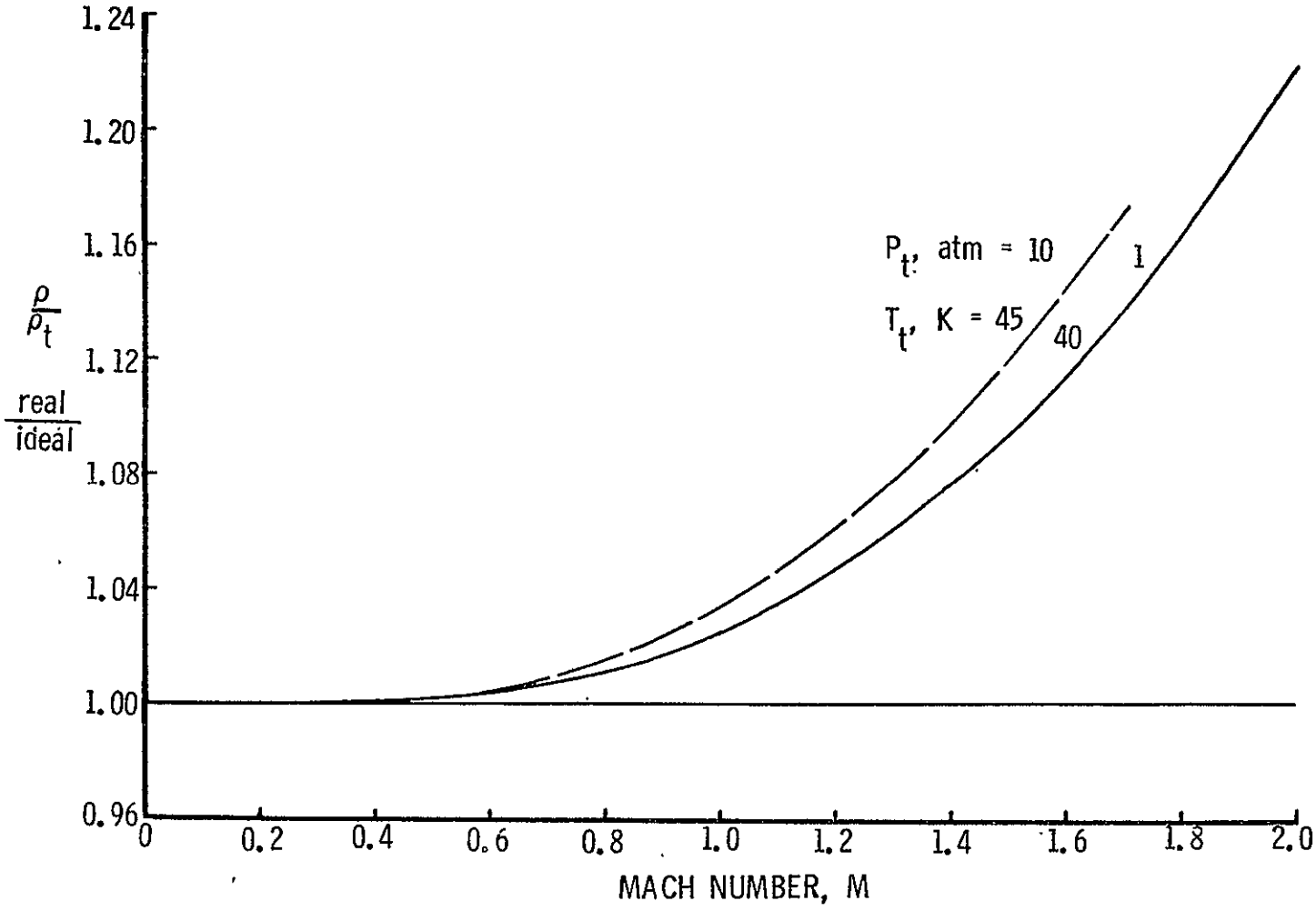

Figure 20. Density ratios for the isentropic expansion of parahydrogen to various Mach numbers, relative to the ideal diatomic gas value.

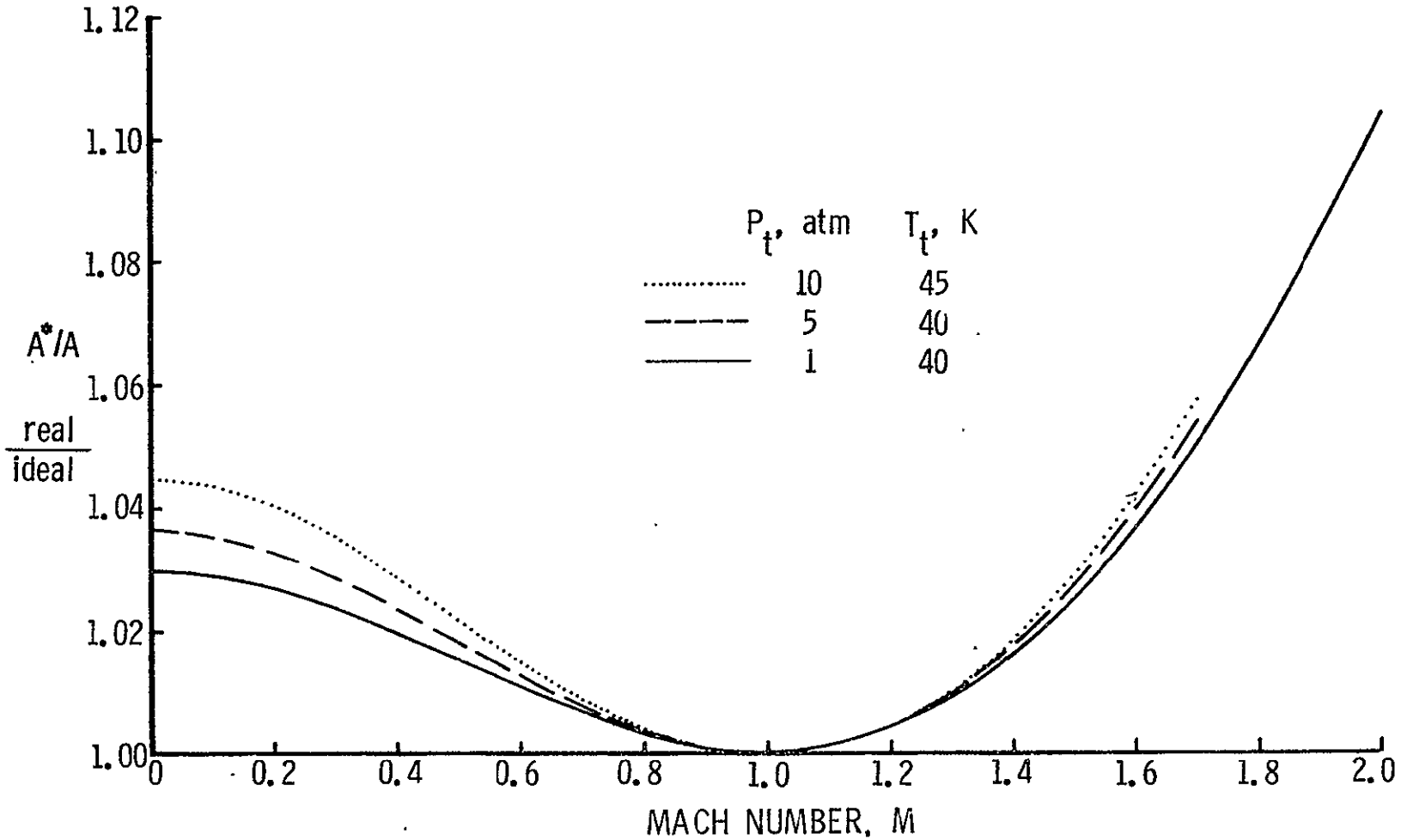

Figure 21. Isentropic stream-tube area ratios for the isentropic expansion of parahydrogen to various Mach numbers relative to the ideal diatomic gas value.

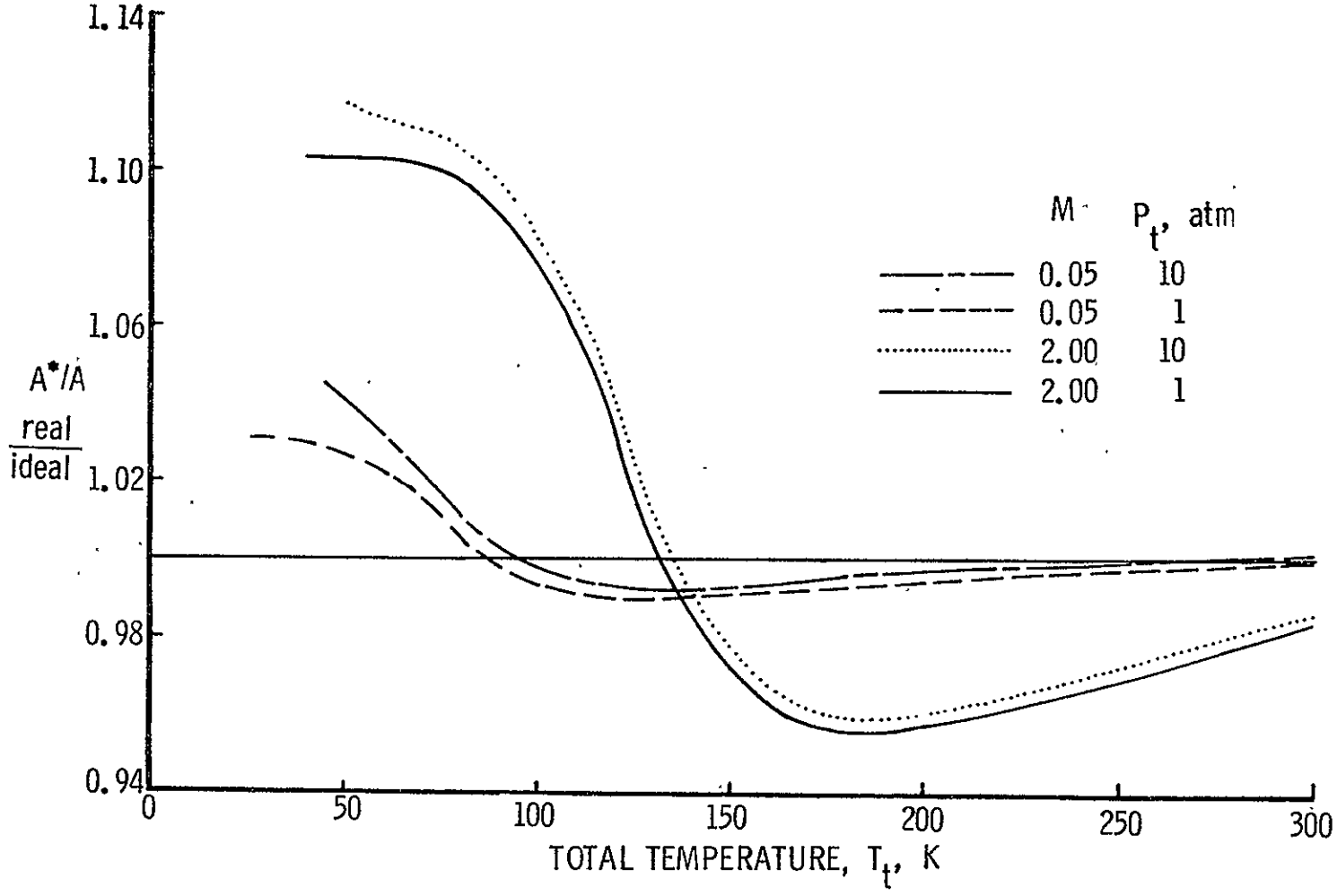

Figure 22. Isentropic stream-tube area ratio for parahydrogen relative to the ideal diatomic gas value.

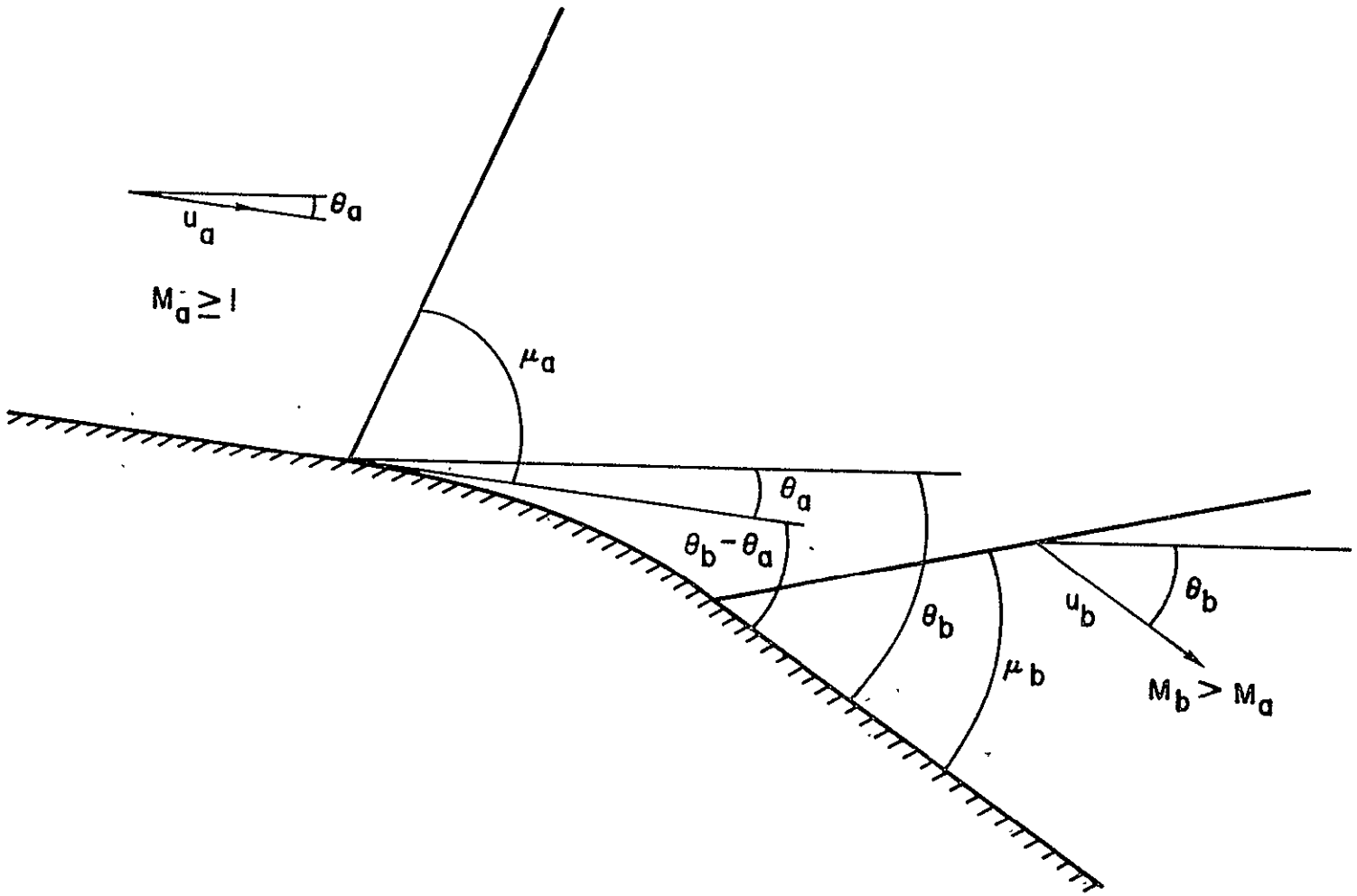

Figure 23. Prandtl-Meyer flow over a convex wall.

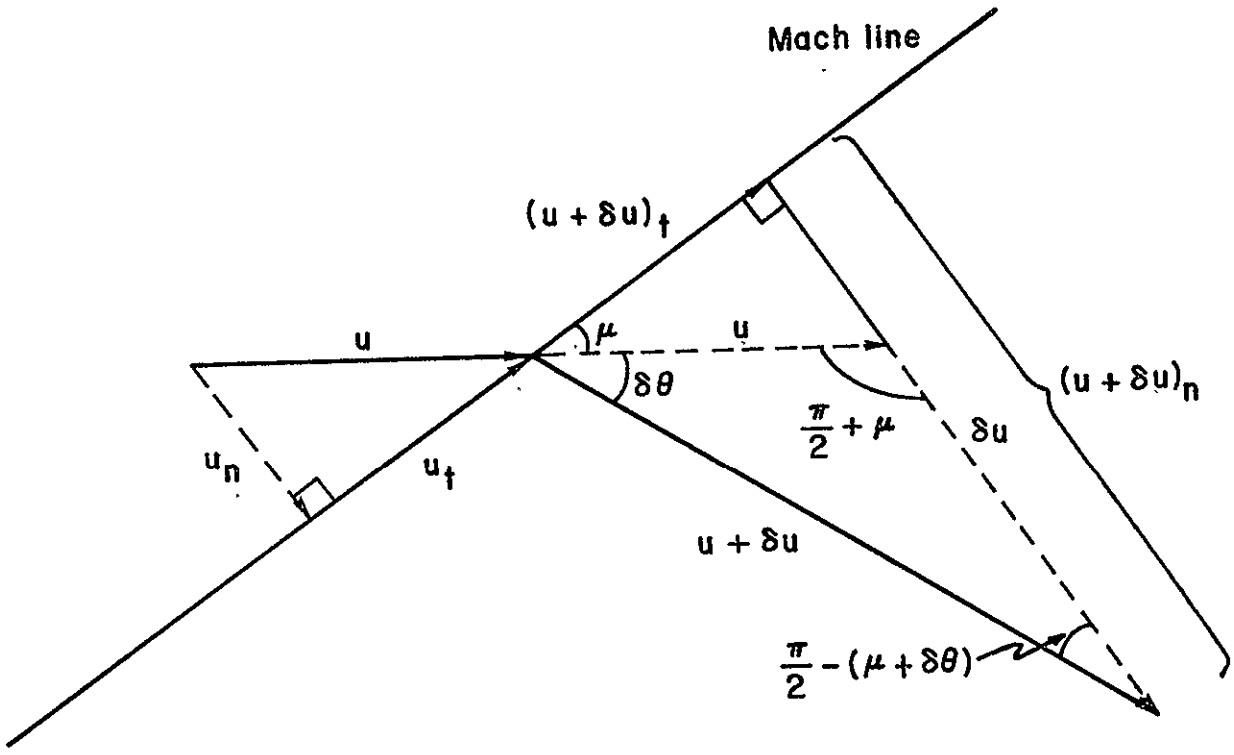

Figure 24. Velocity change across a weak expansion wave (Mach line).

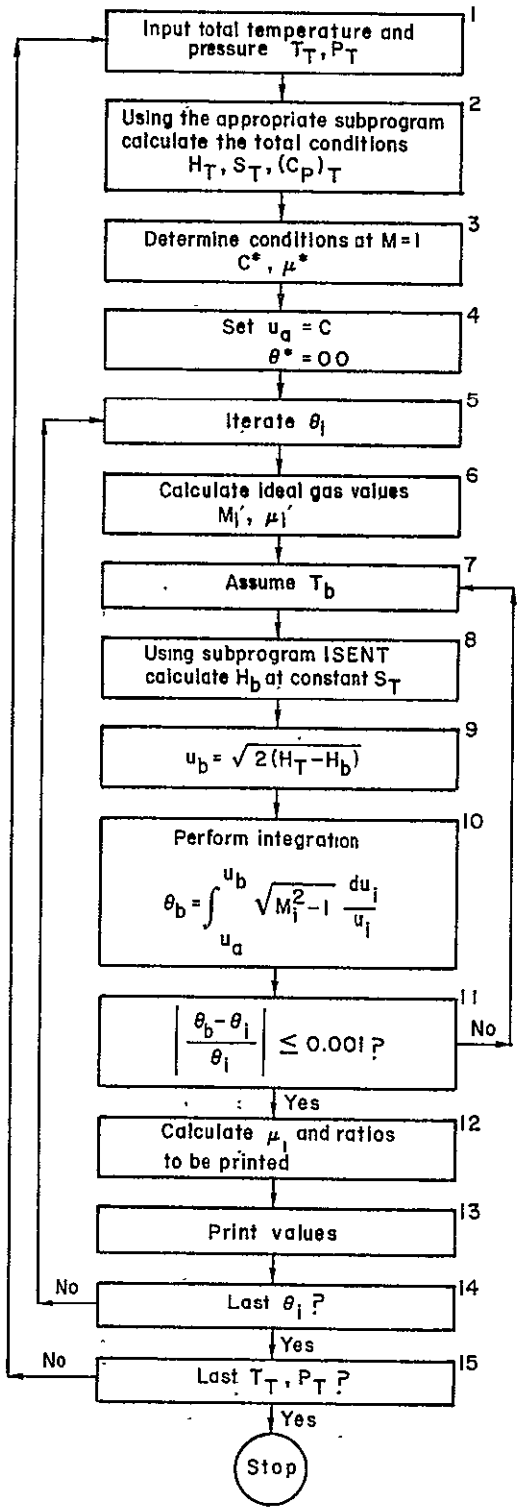

Figure 25. Computer program flow chart for the Prandtl-Meyer flow solution.

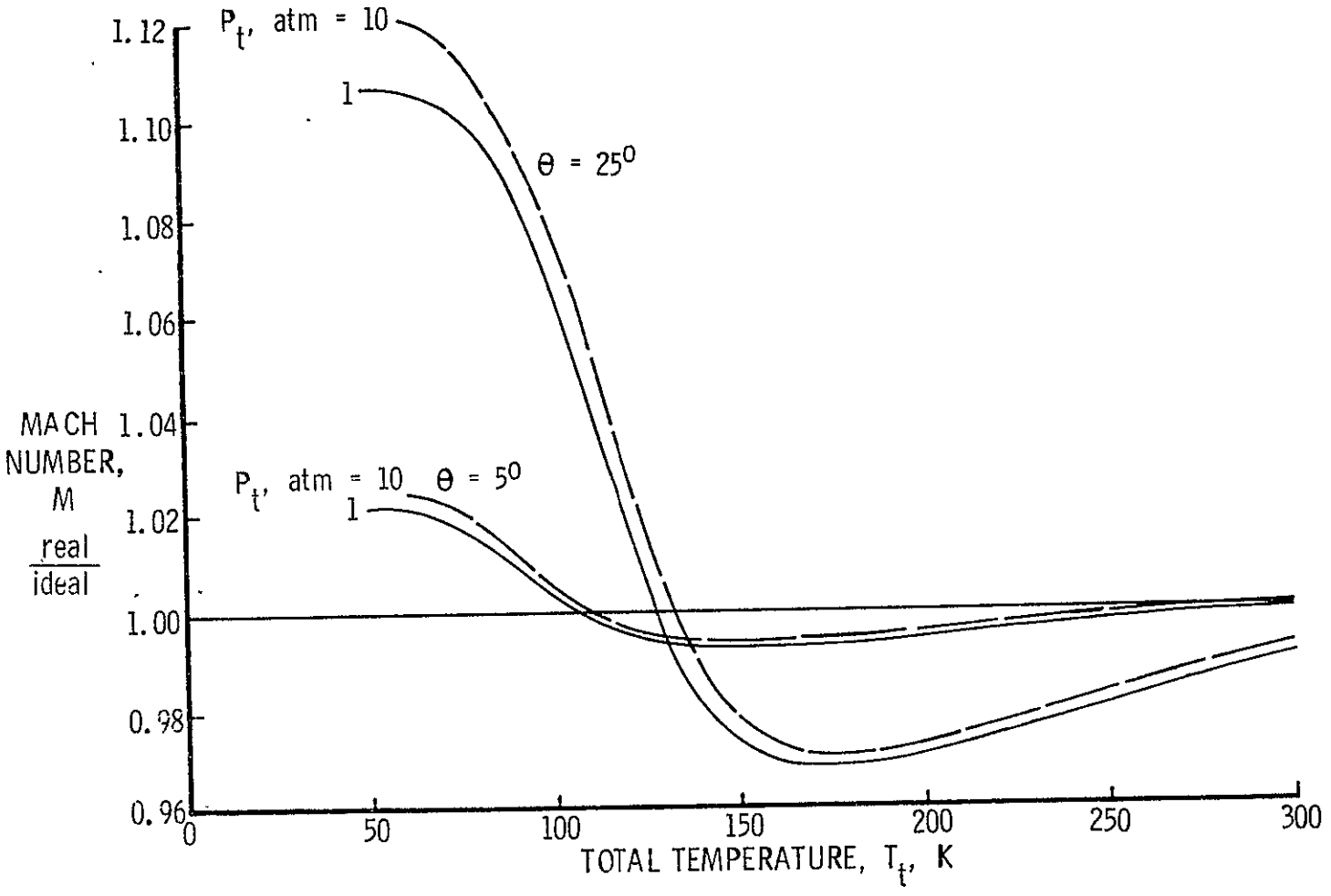

Figure 26. Mach number deviation as a function of total temperature for Prandtl-Meyer expansions from a Mach number of 1.0 through angles of 5 and 25 degrees in parahydrogen.

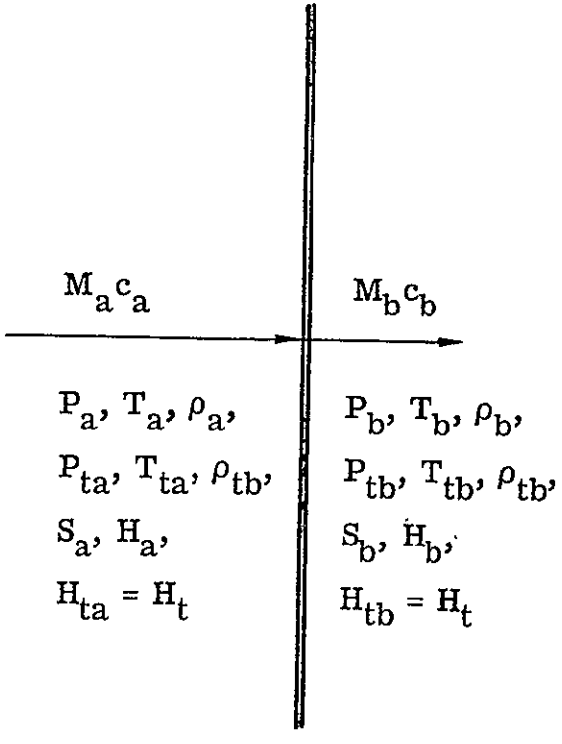

Figure 27. Standing normal shock wave.

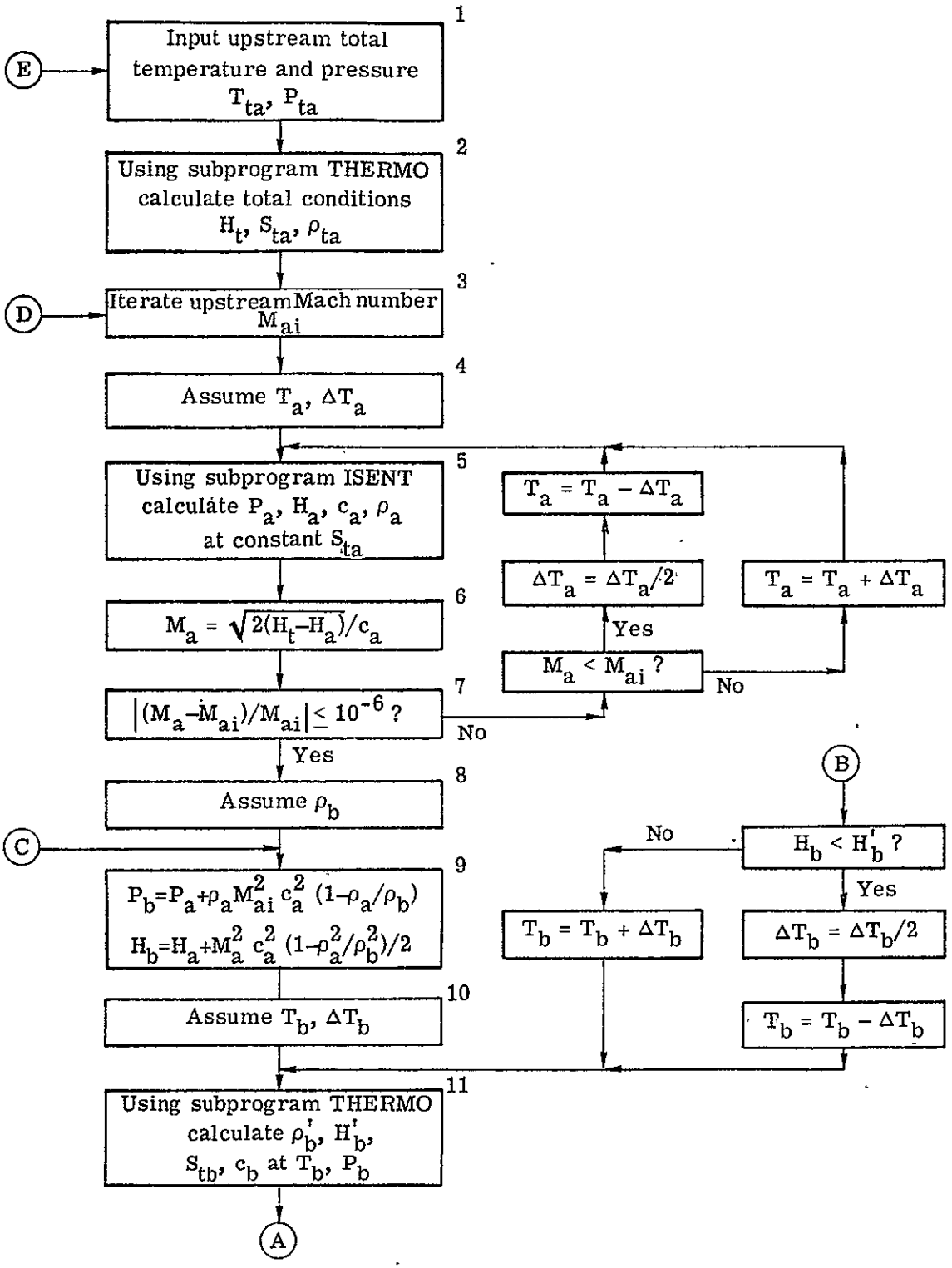

Figure 28. Computer program flow chart for the normal shock wave solution.

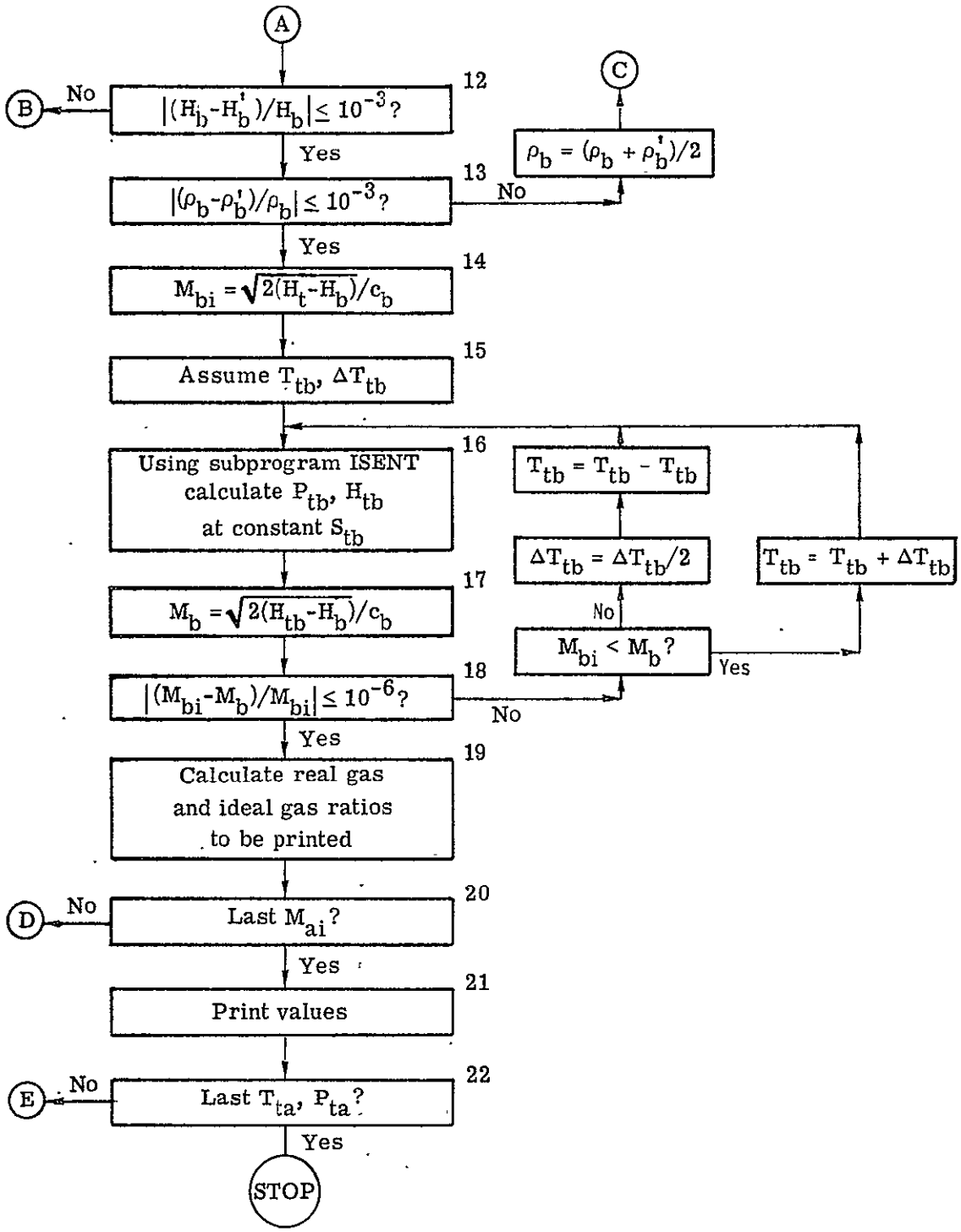

Figure 28. Concluded.

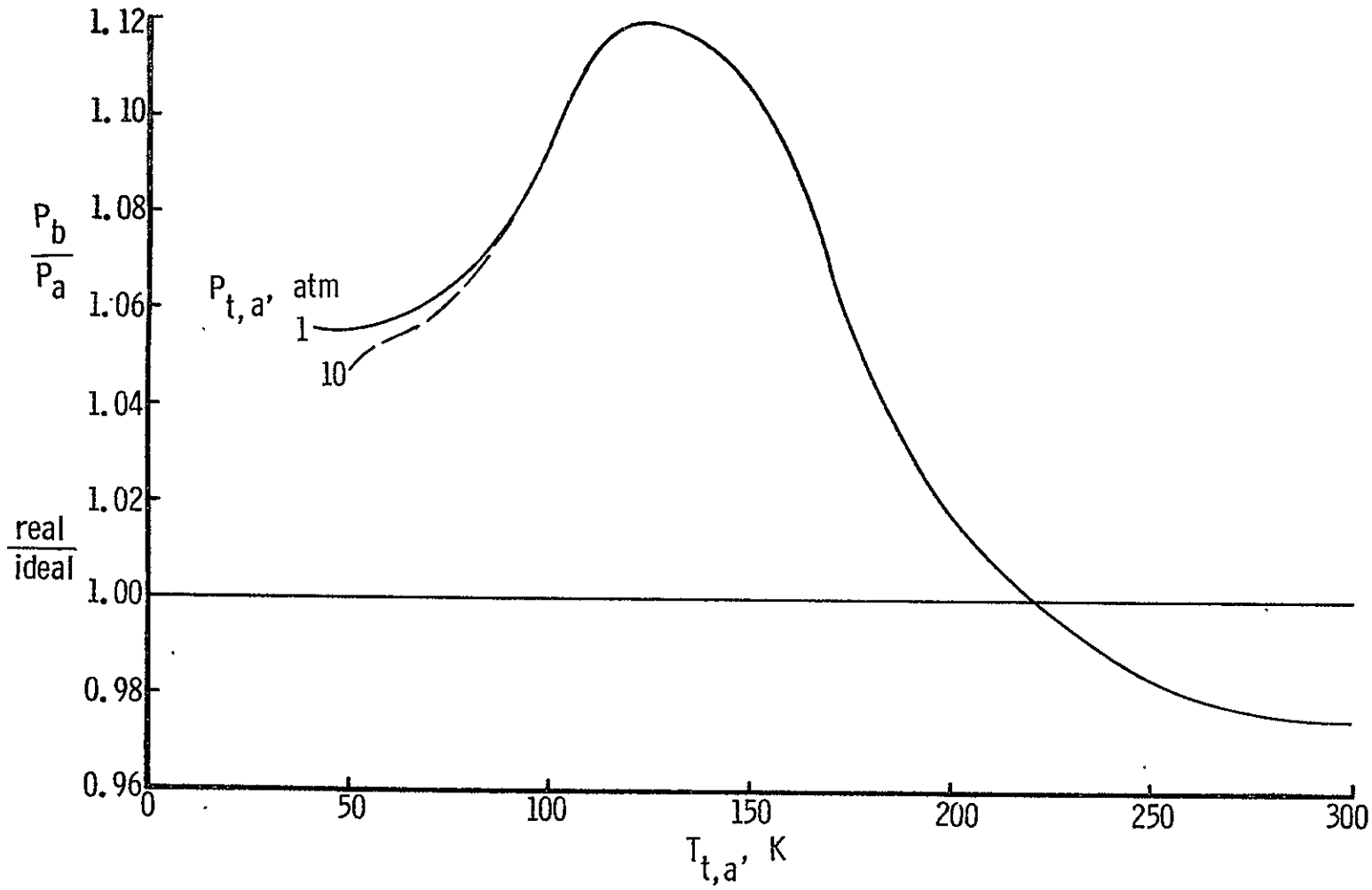

Figure 29. Static pressure ratio across a normal shock wave in parahydrogen relative to an ideal diatomic gas for an upstream Mach number of 2.0.

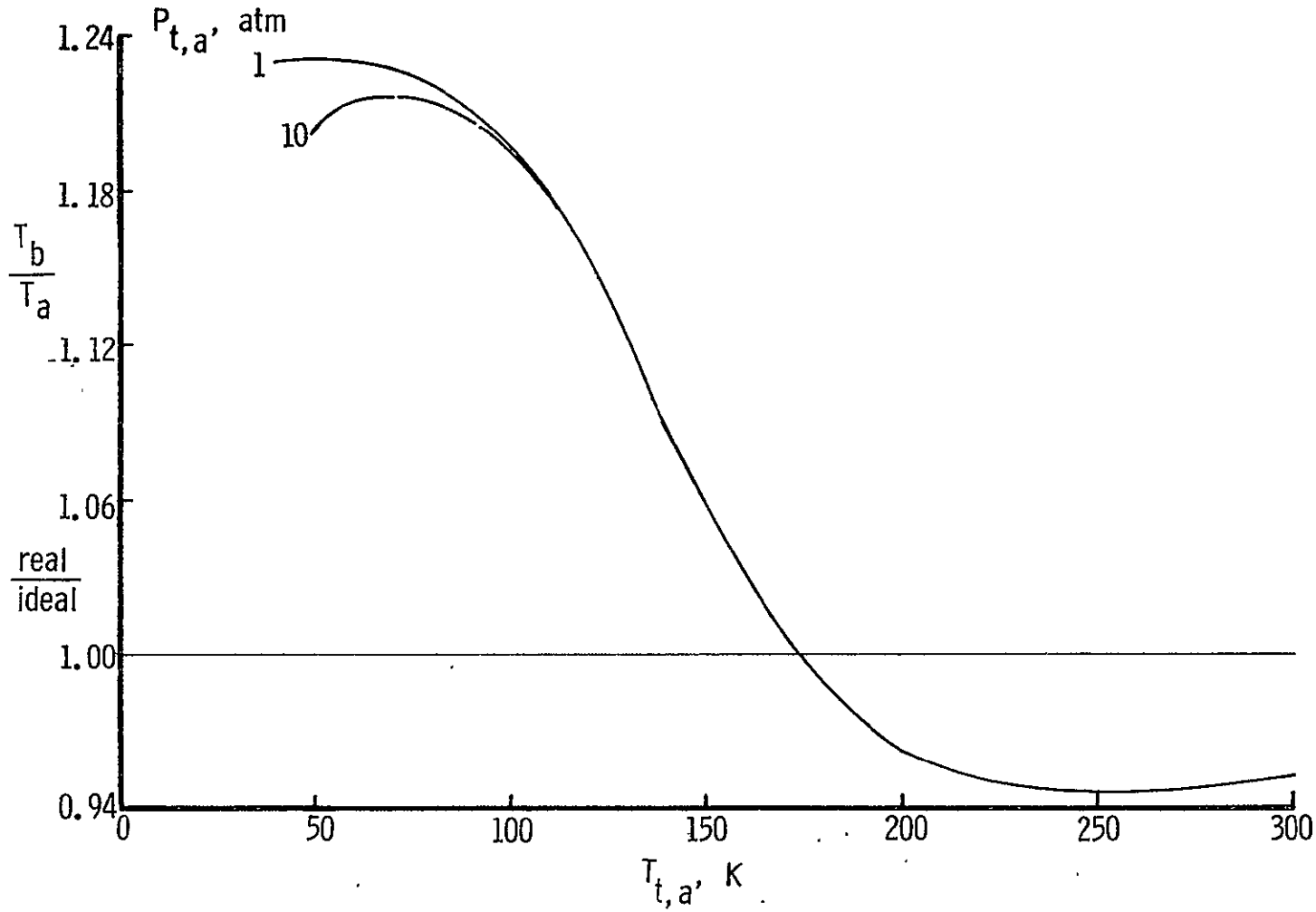

Figure 30. Static temperature ratio across a normal shock wave in parahydrogen relative to an ideal diatomic gas for an upstream Mach number of 2.0.

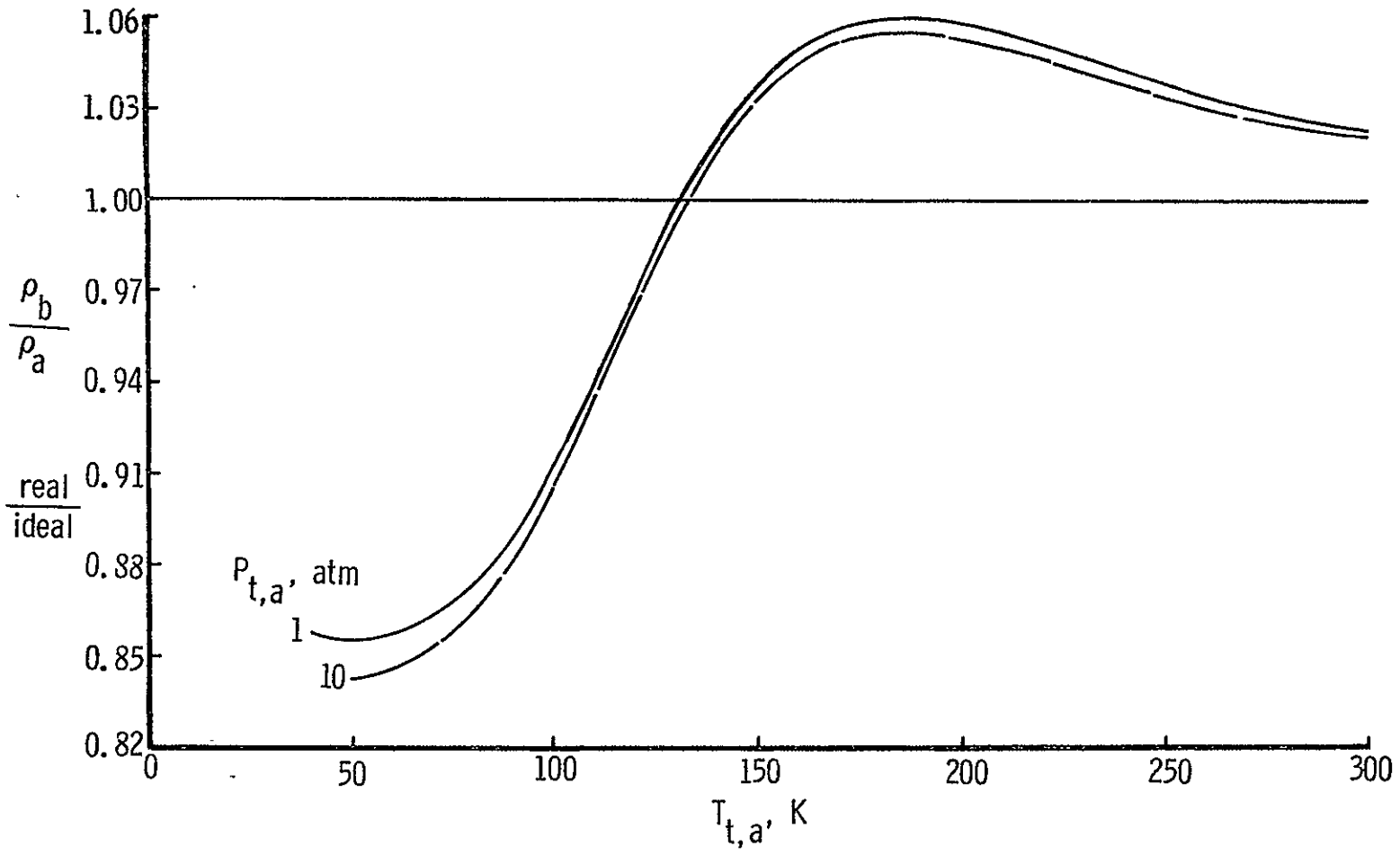

Figure 31. Static density ratio across a normal shock wave in parahydrogen relative to an ideal diatomic gas for an upstream Mach number of 2.0.

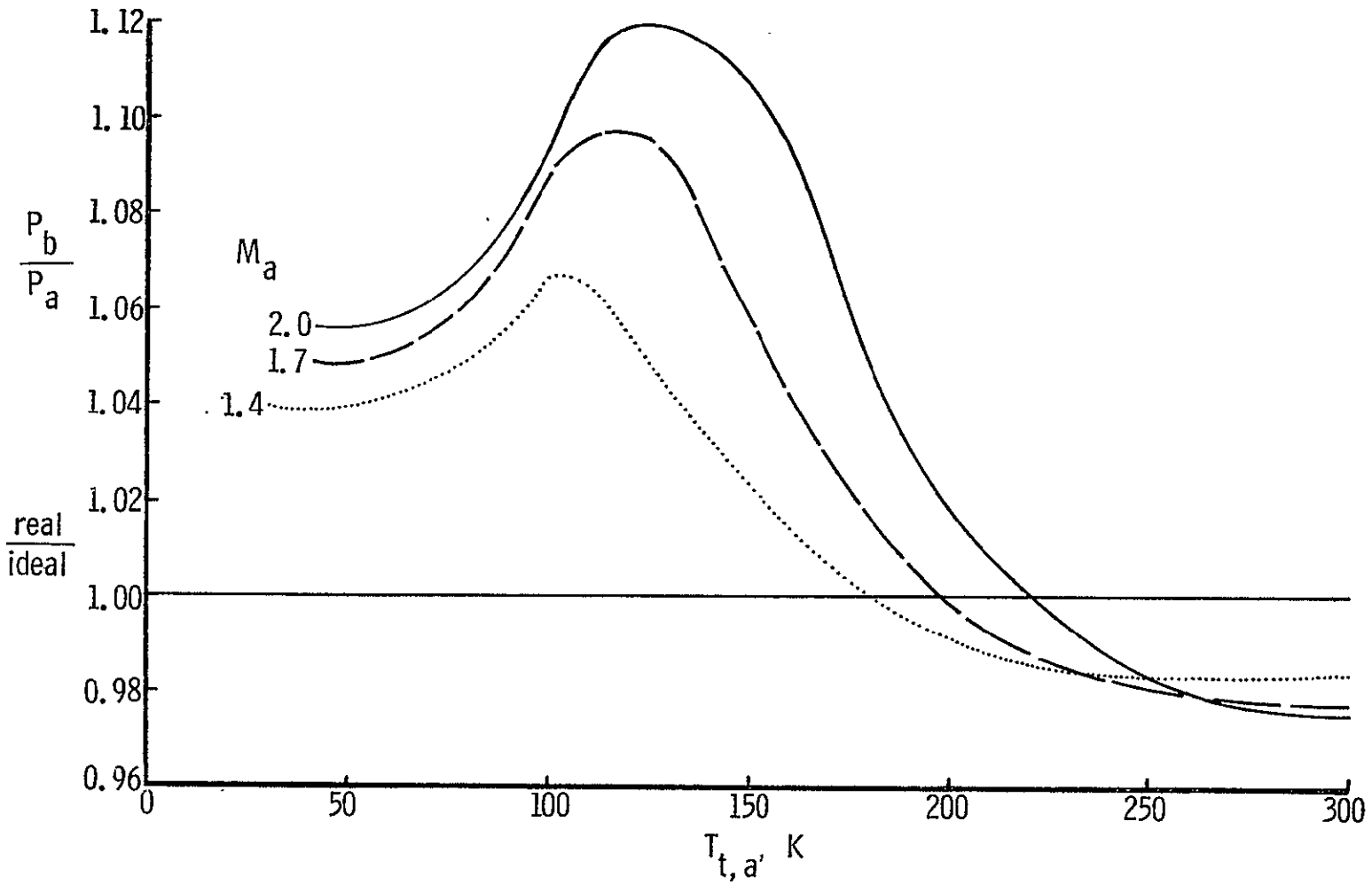

Figure 32. Static pressure ratio across a normal shock wave in parahydrogen relative to an ideal diatomic gas for an upstream total pressure of one atmosphere.

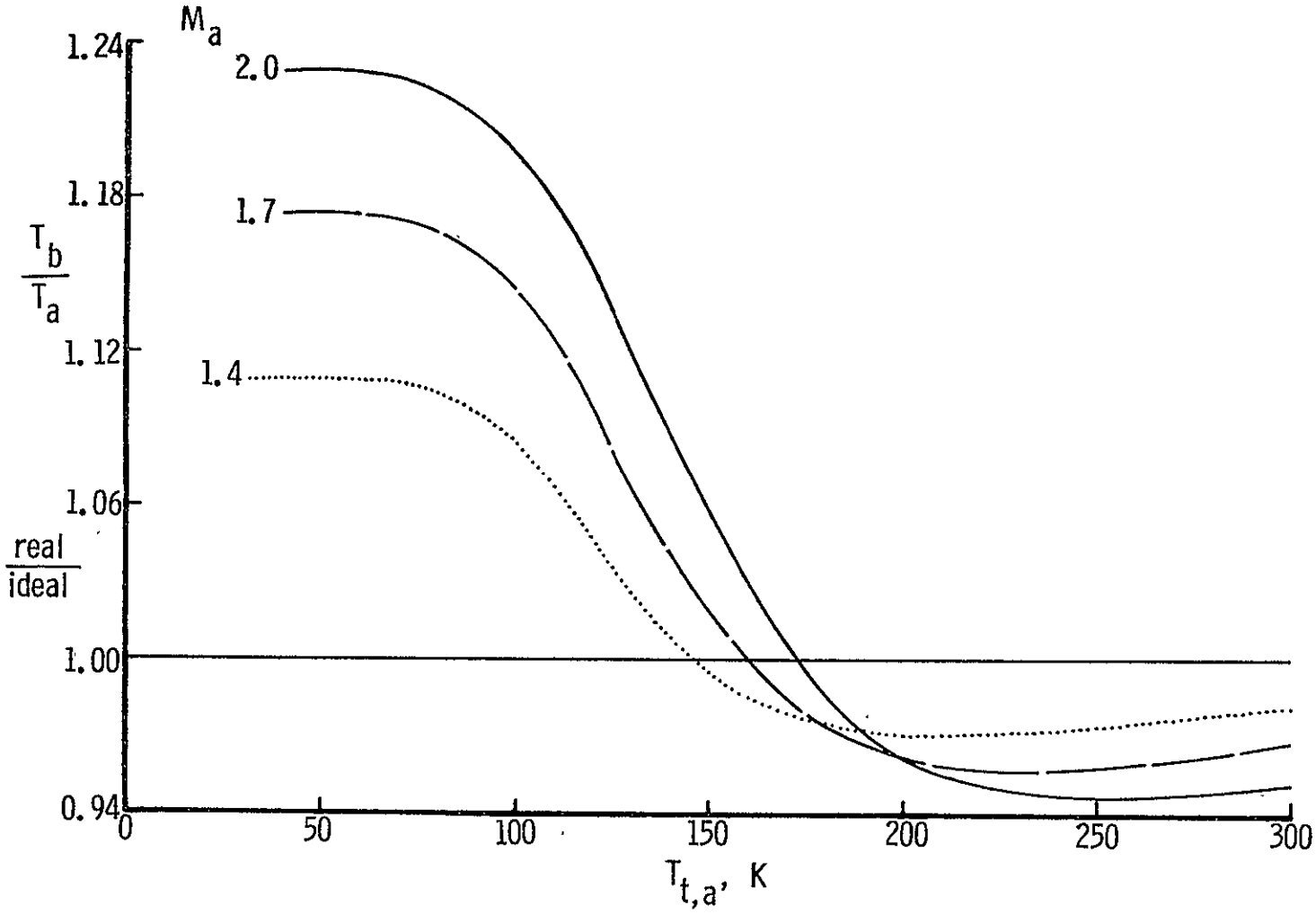

Figure 33. Static temperature ratio across a normal shock wave in parahydrogen relative to an ideal diatomic gas for an upstream total pressure of one atmosphere.

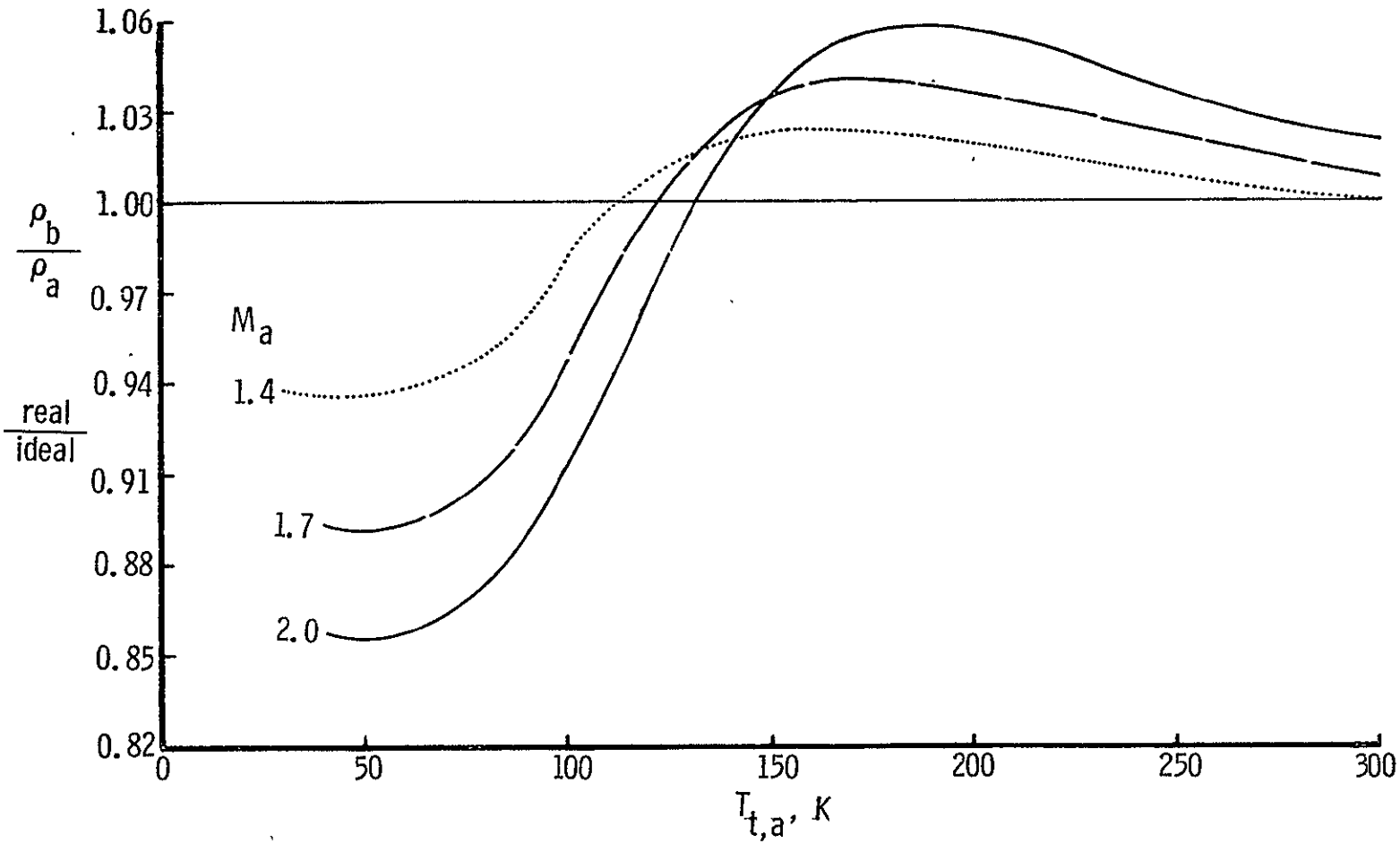

Figure 34. Static density ratio across a normal shock wave in parahydrogen relative to an ideal diatomic gas for an upstream total pressure of one atmosphere.

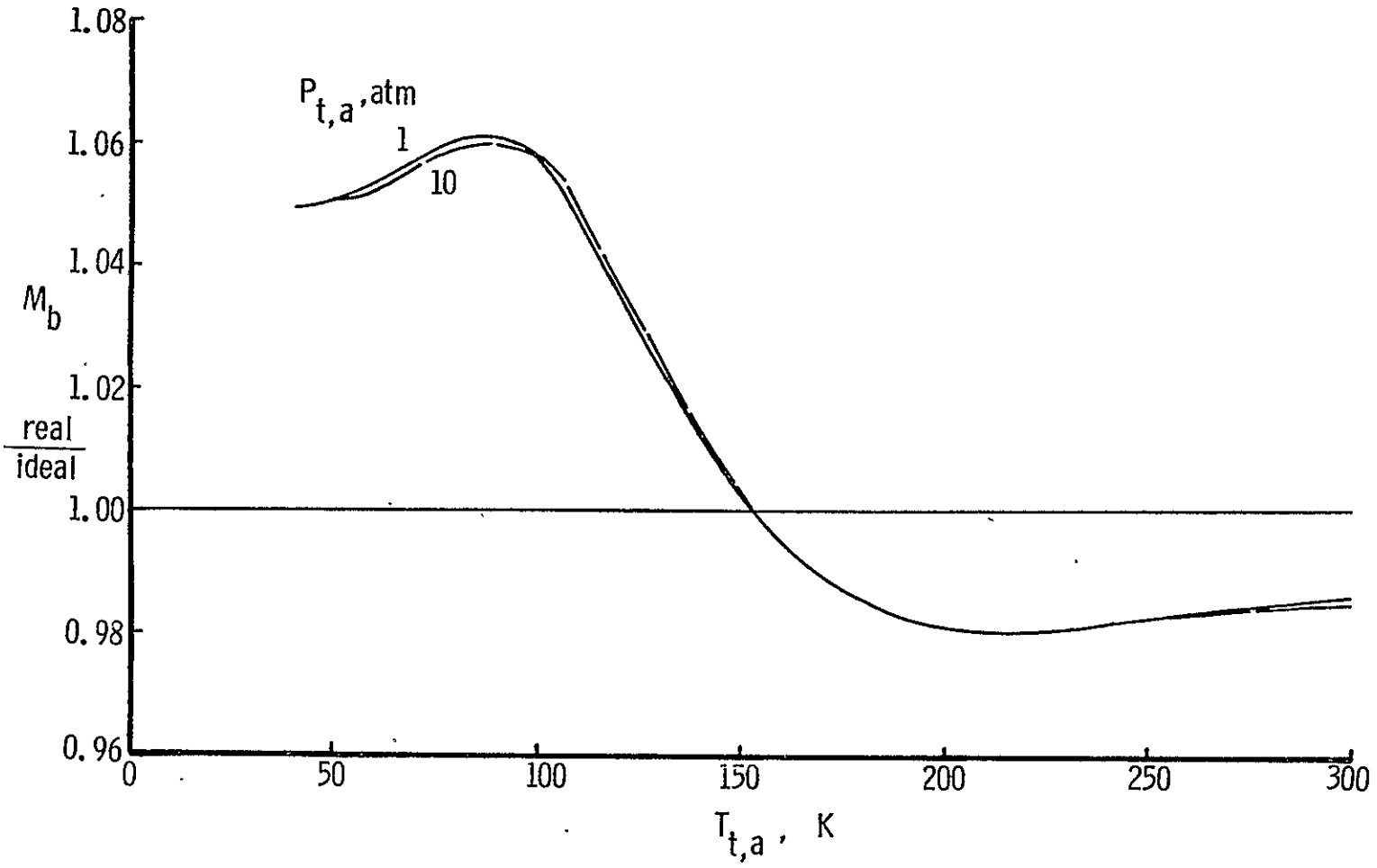

Figure 35. Mach number downstream of a normal shock wave in parahydrogen relative to an ideal diatomic gas for an upstream Mach number of 2.0.

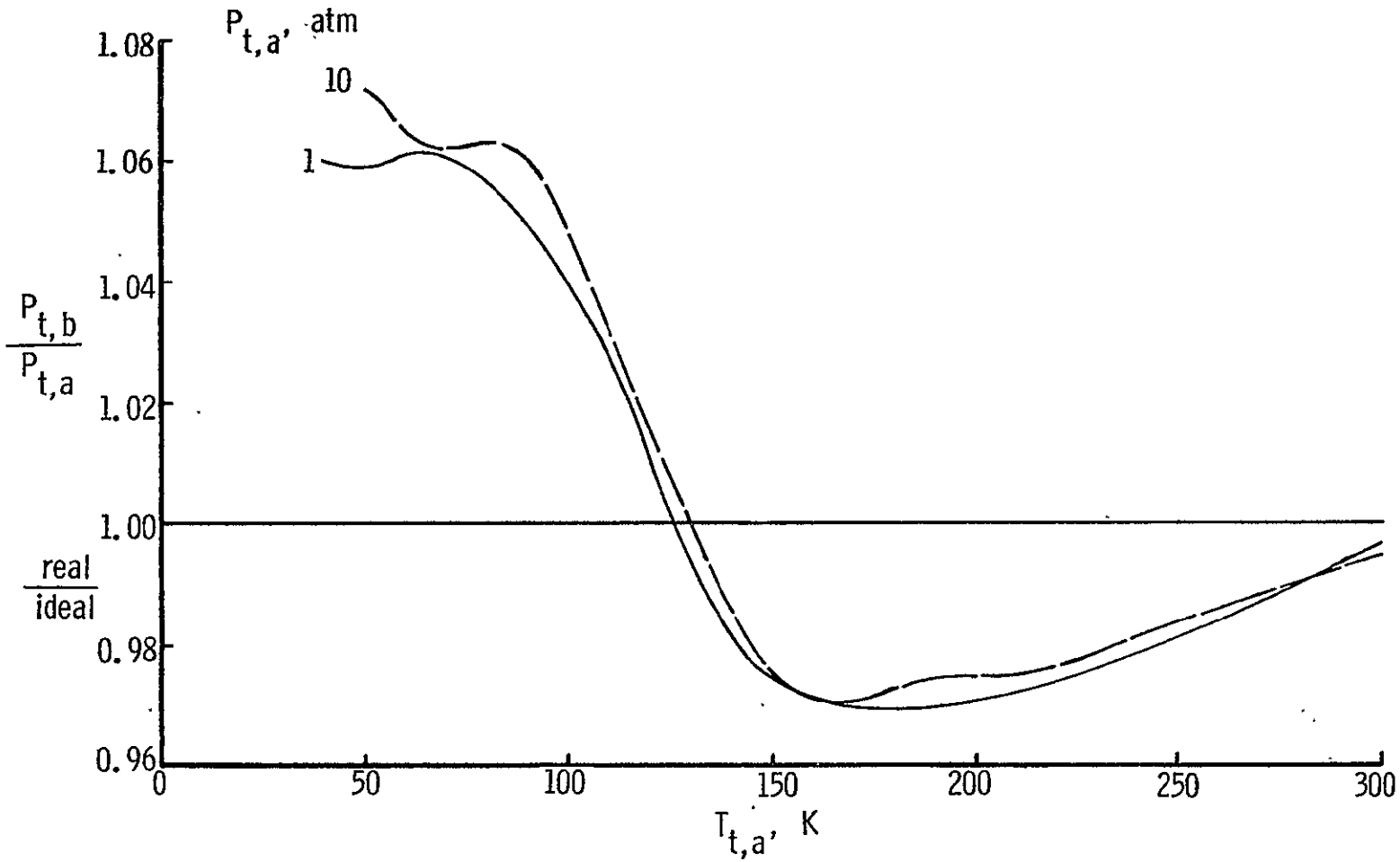

Figure 36. Total pressure ratio across a normal shock wave in parahydrogen relative to an ideal diatomic gas for an upstream Mach number of 2.0.

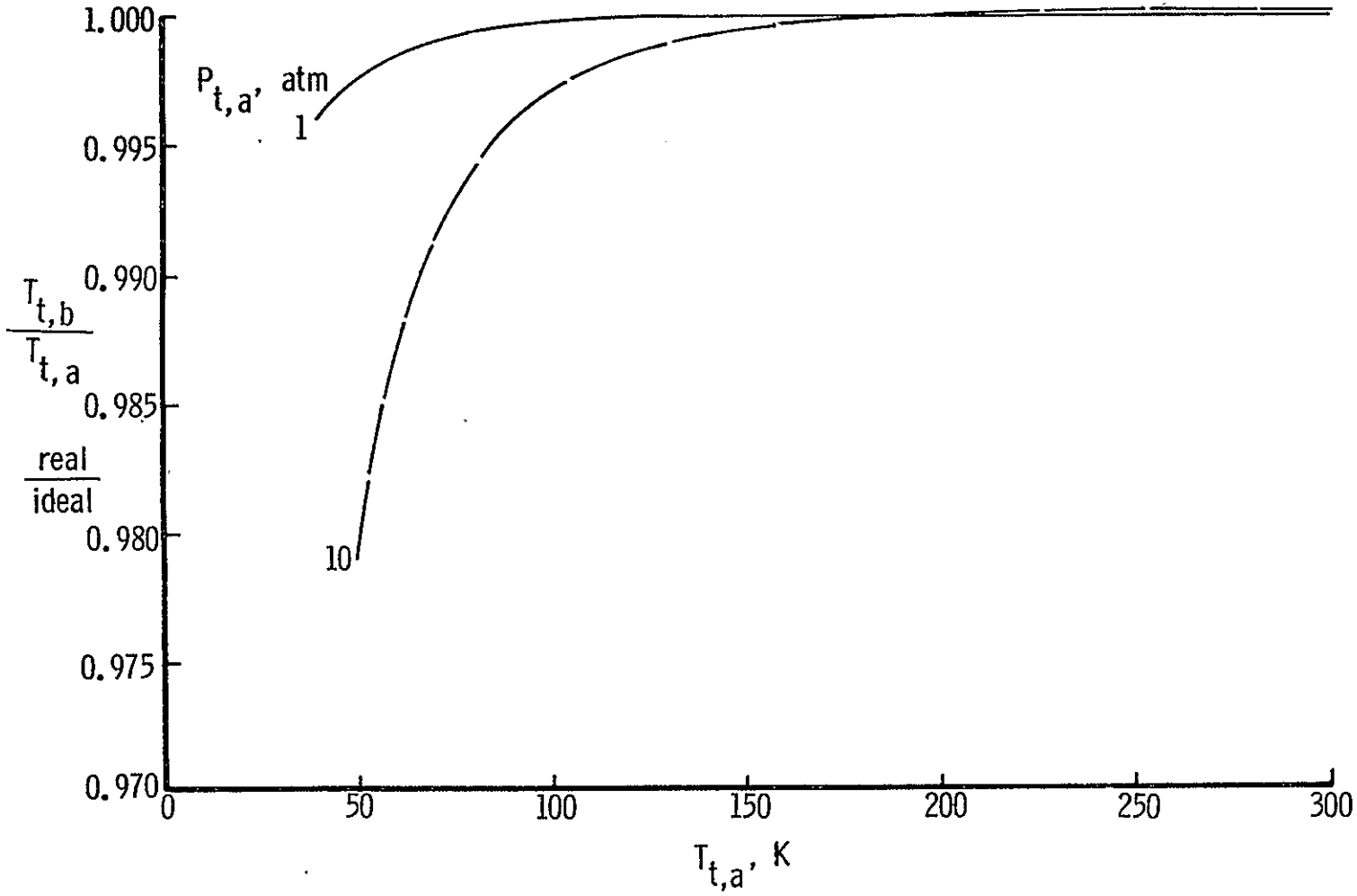

Figure 37. Total temperature ratio across a normal shock wave in parahydrogen relative to an ideal diatomic gas for an upstream Mach number of 2.0.

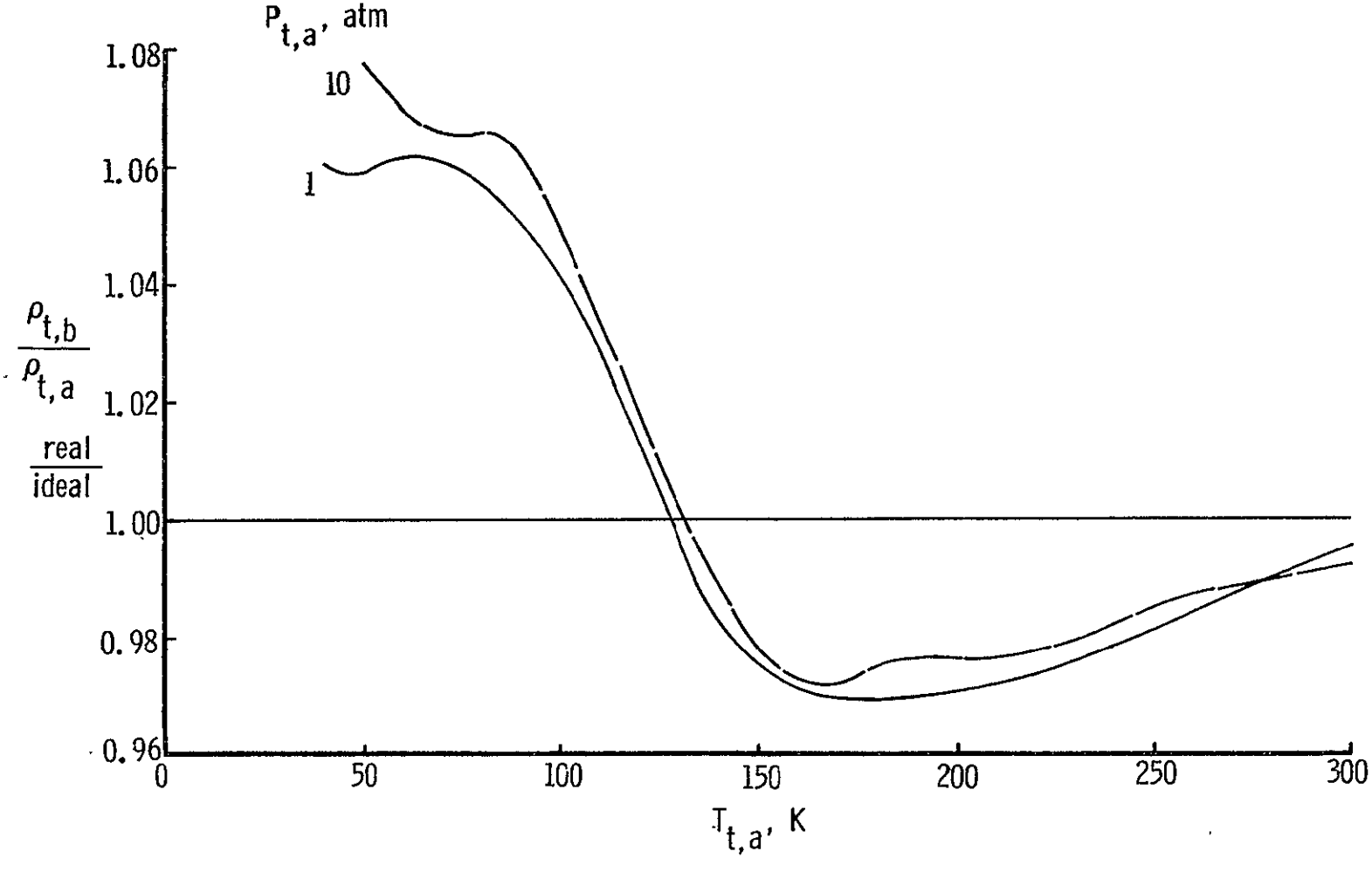

Figure 38. Total density ratio across a normal shock wave in parahydrogen relative to an ideal diatomic gas for an upstream Mach number of 2.0.

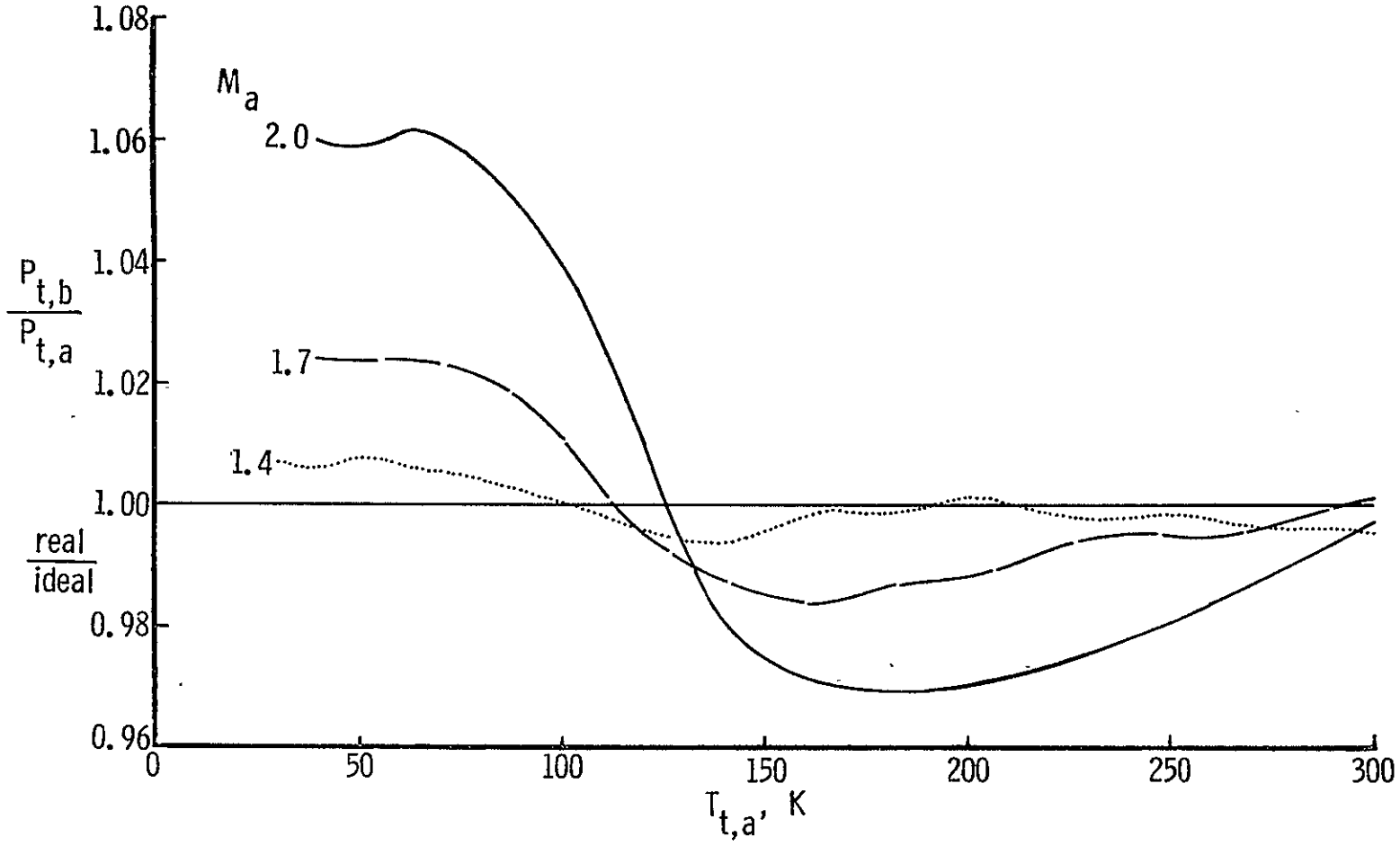

Figure 39. Total pressure ratio across a normal shock wave in parahydrogen relative to an ideal diatomic gas for an upstream total pressure of one atmosphere.

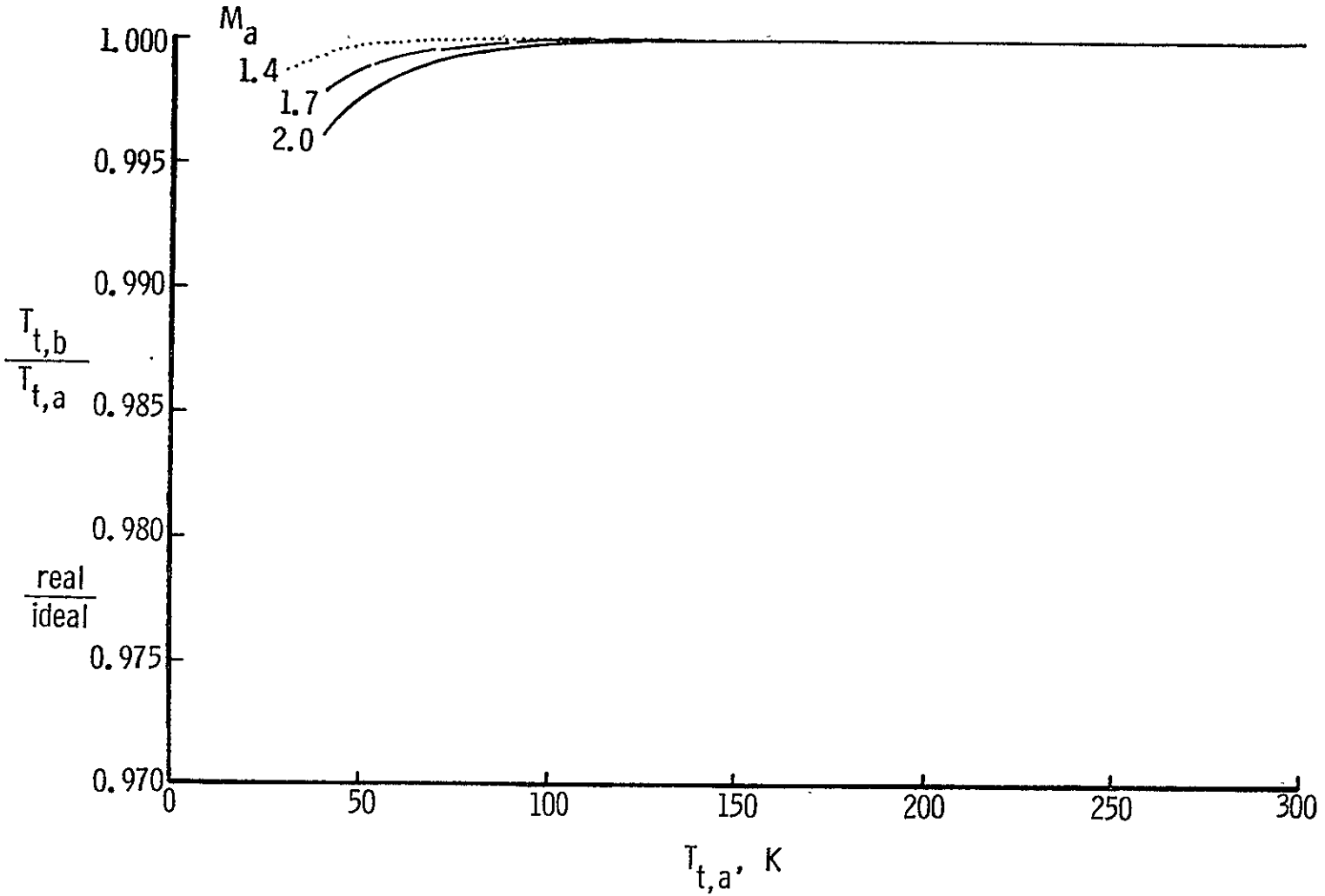

Figure 40. Total temperature ratio across a normal shock wave in parahydrogen relative to an ideal diatomic gas for an upstream total pressure of one atmosphere.

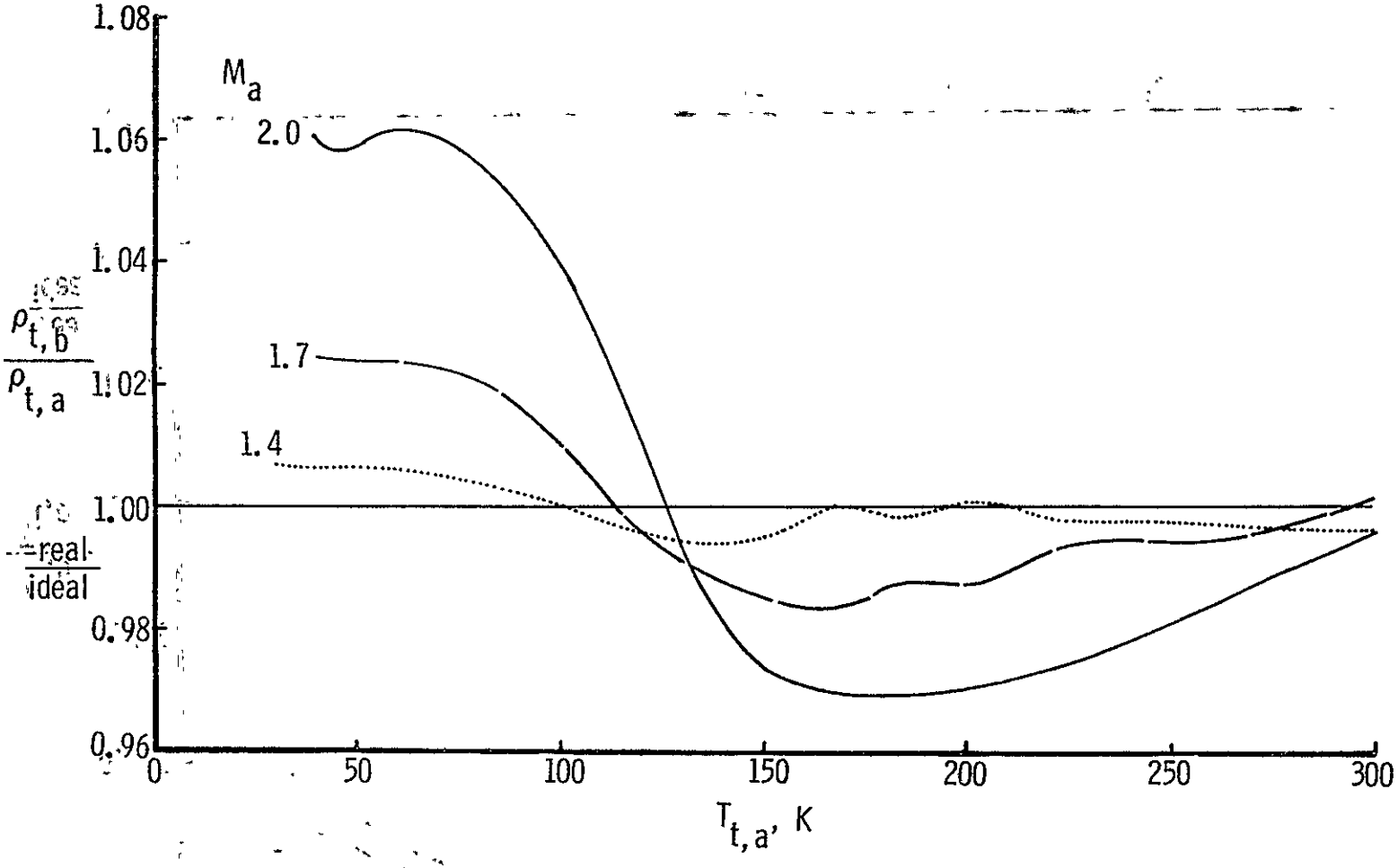

Figure 41. Total density ratio across a normal shock wave in parahydrogen relative to an ideal diatomic gas for an upstream total pressure of one atmosphere.

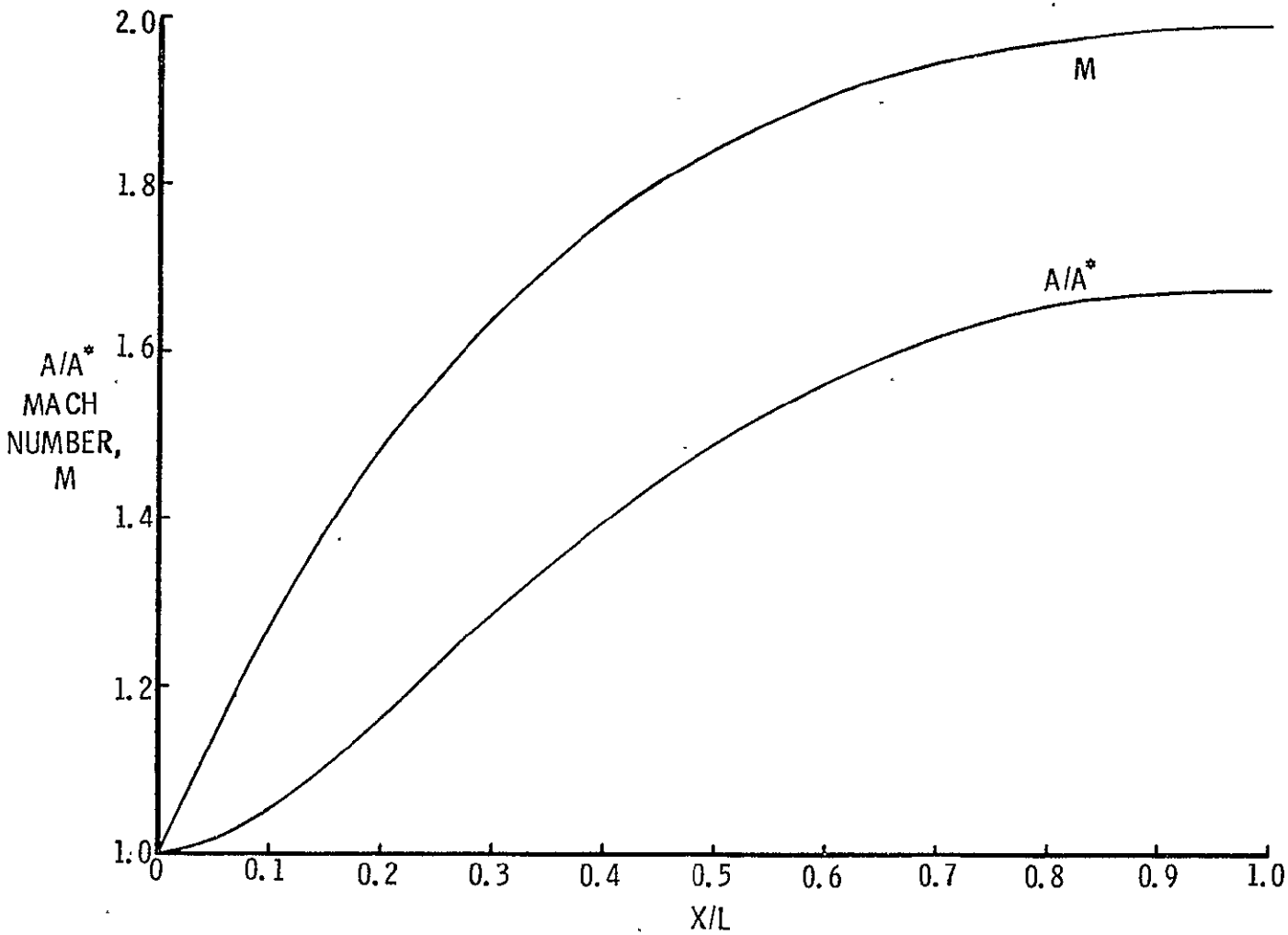

Figure 42. Ideal diatomic gas flow through the diverging section of a Mach 2.0 nozzle.

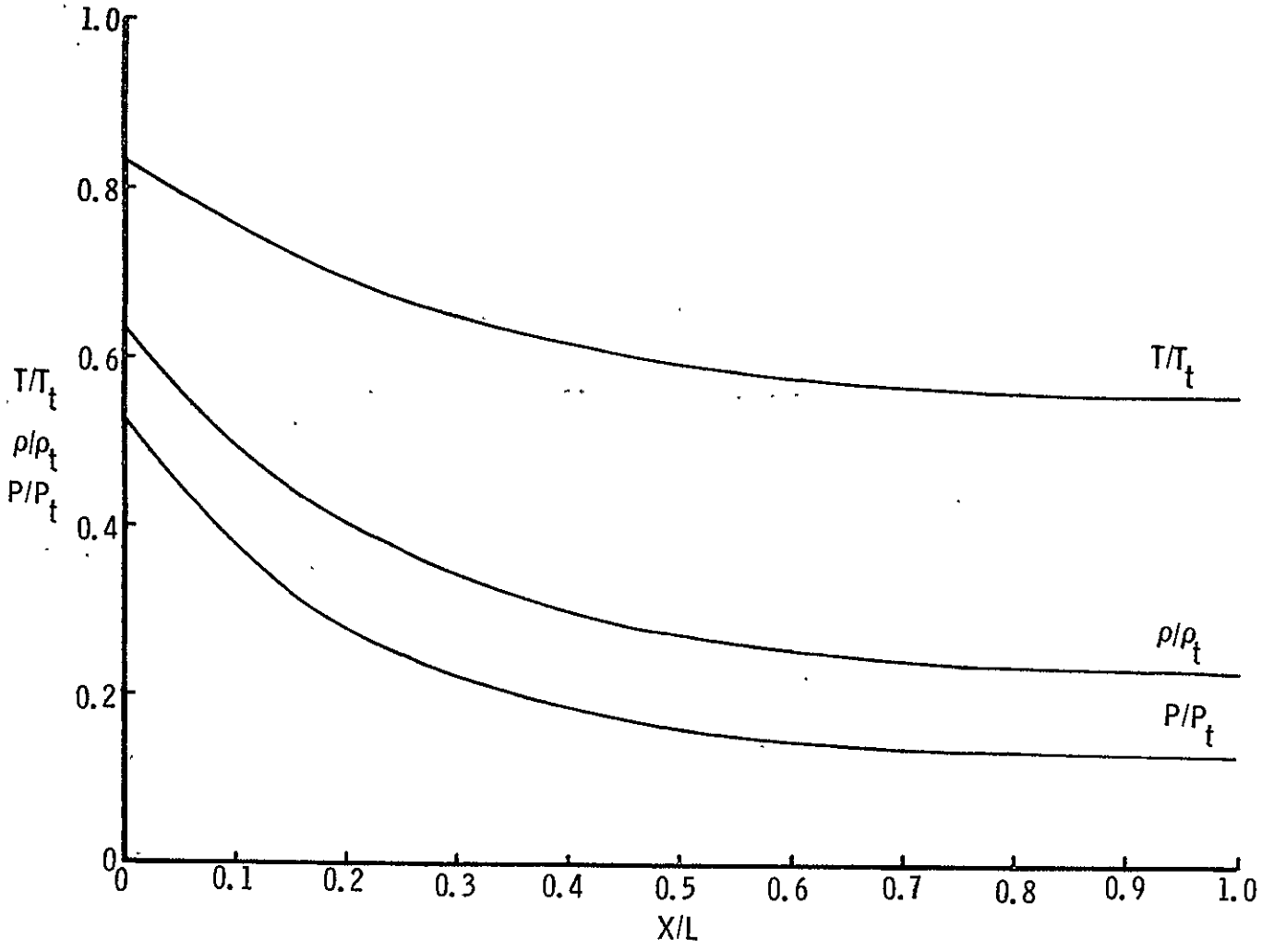

Figure 42. Concluded.

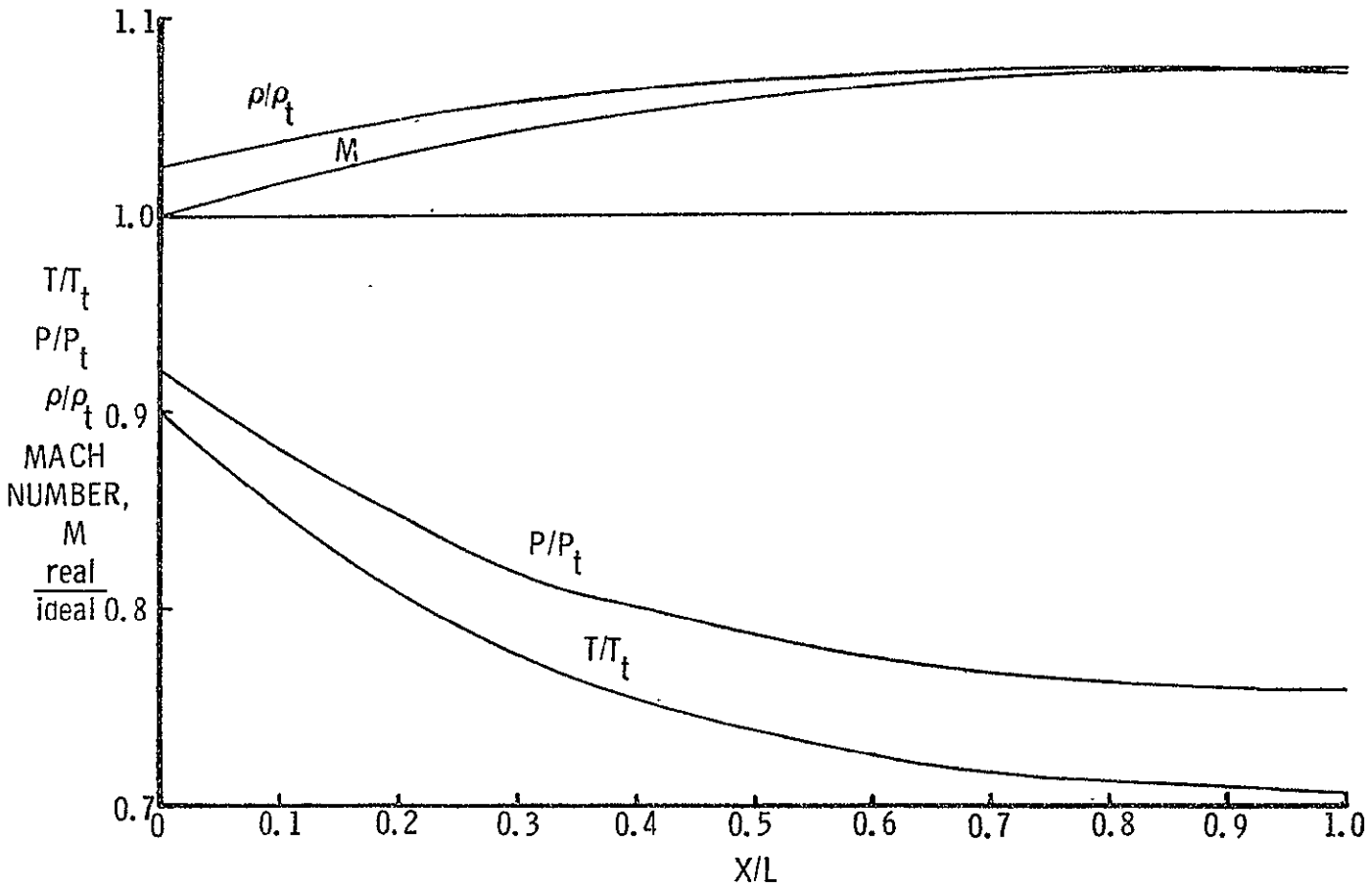

Figure 43. Deviations of parahydrogen from the ideal diatomic gas for the one-dimensional, inviscid, isentropic flow through the diverging section of a Mach 2.0 nozzle at total conditions of 45 K and one atmosphere.

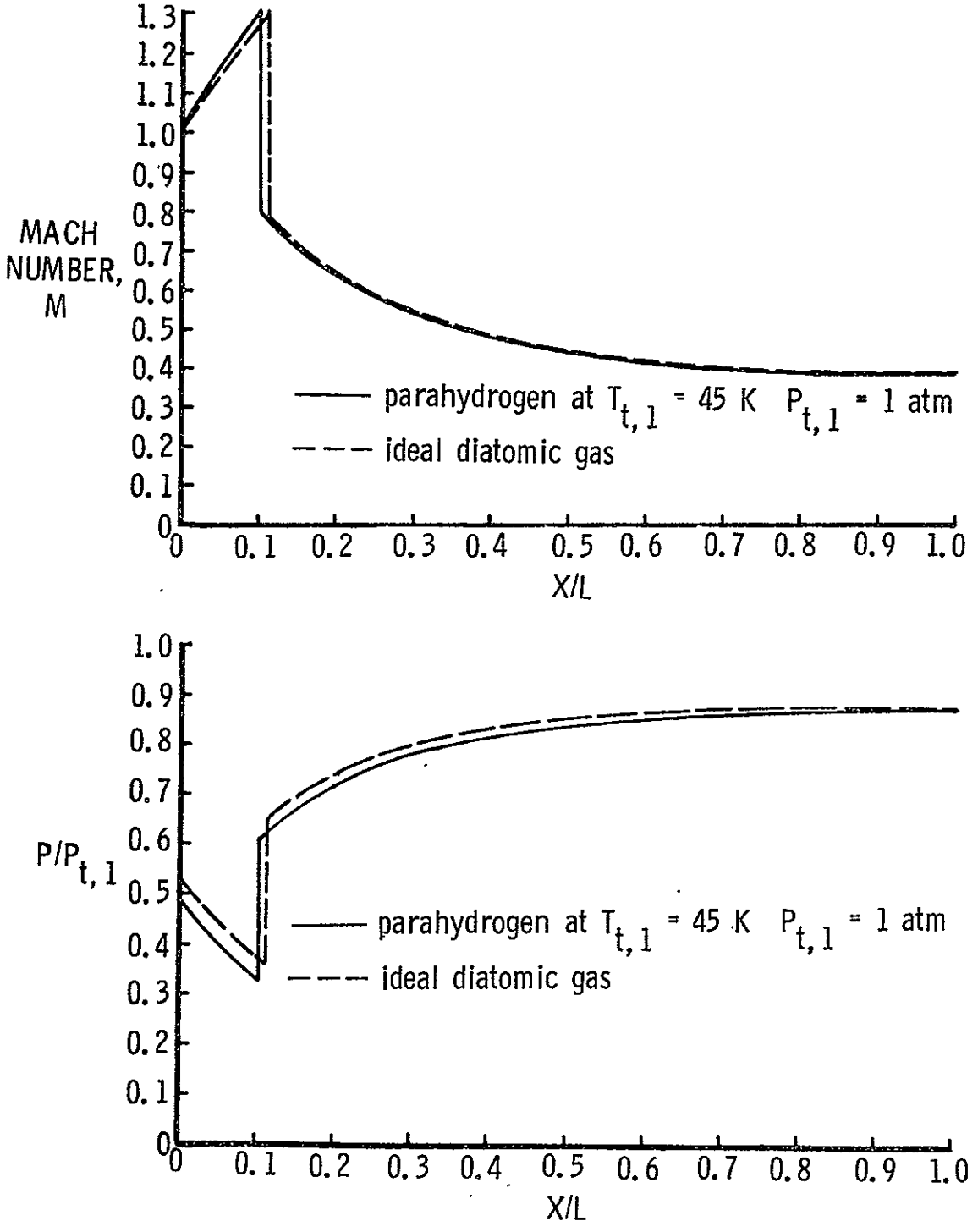

Figure 44. Mach number distribution and nozzle flow ratios for the one-dimensional, inviscid flow through the diverging section of a nozzle with a normal shock occurring at a Mach number of 1.3 at upstream total conditions of 45 K and one atmosphere.

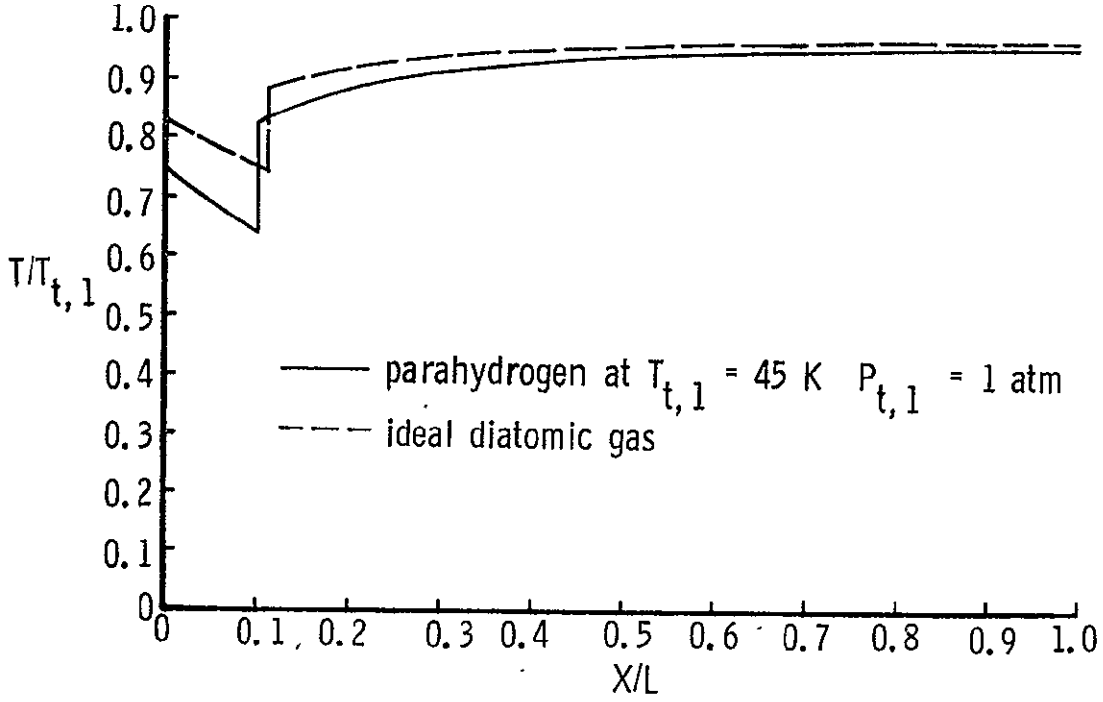

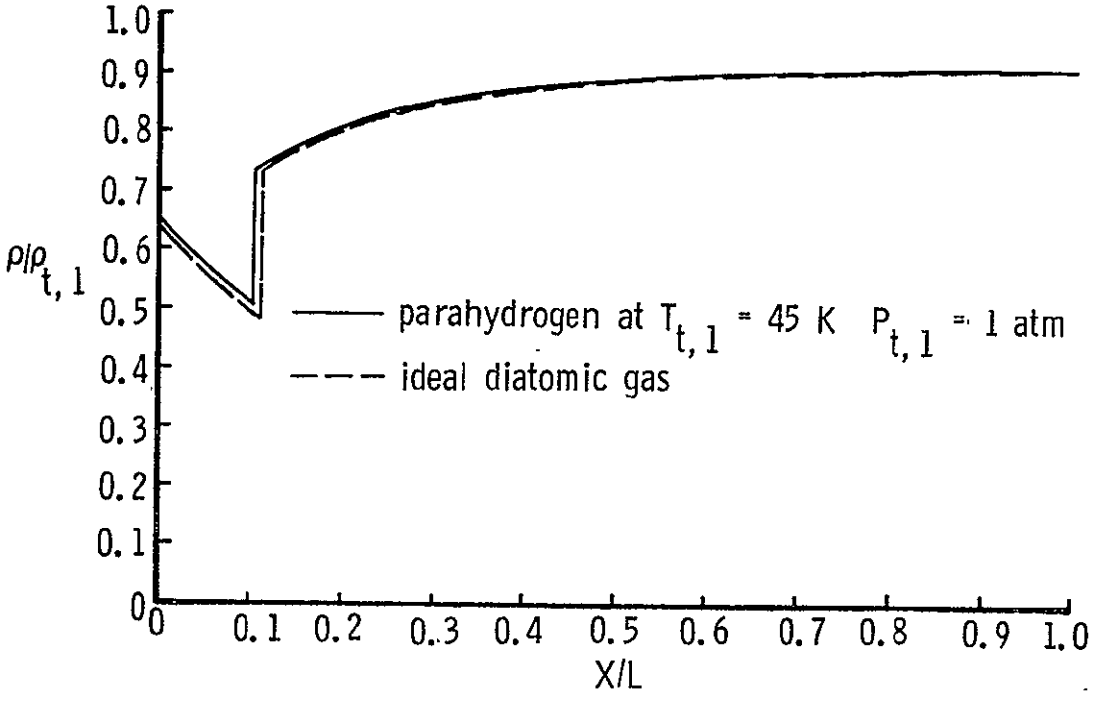

Figure 44. Concluded.

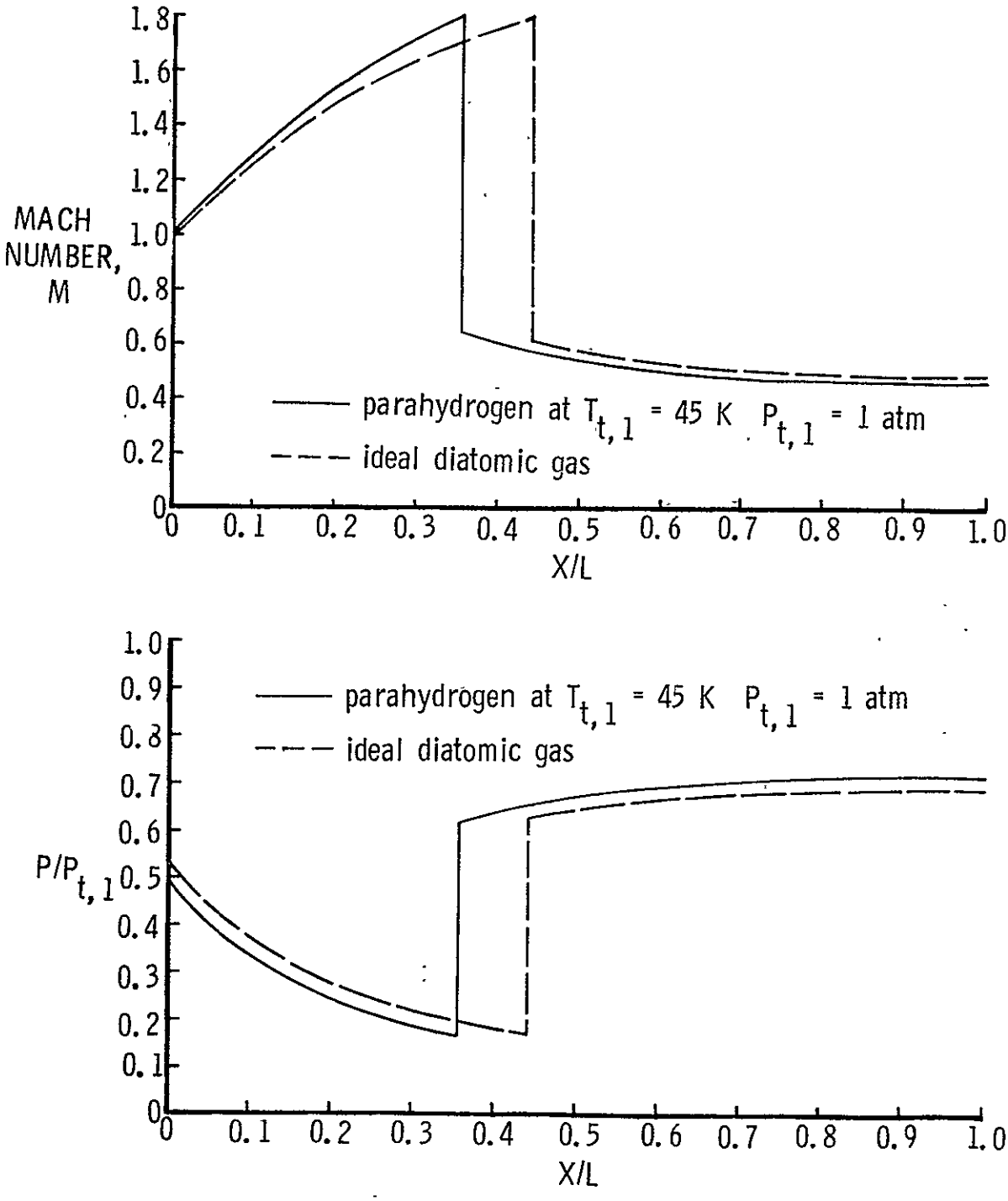

Figure 45. Mach number distribution and nozzle flow ratios for the one-dimensional, inviscid flow through the diverging section of a nozzle with a normal shock occurring at a Mach number of 1.8 at upstream total conditions of 45 K and one atmosphere.

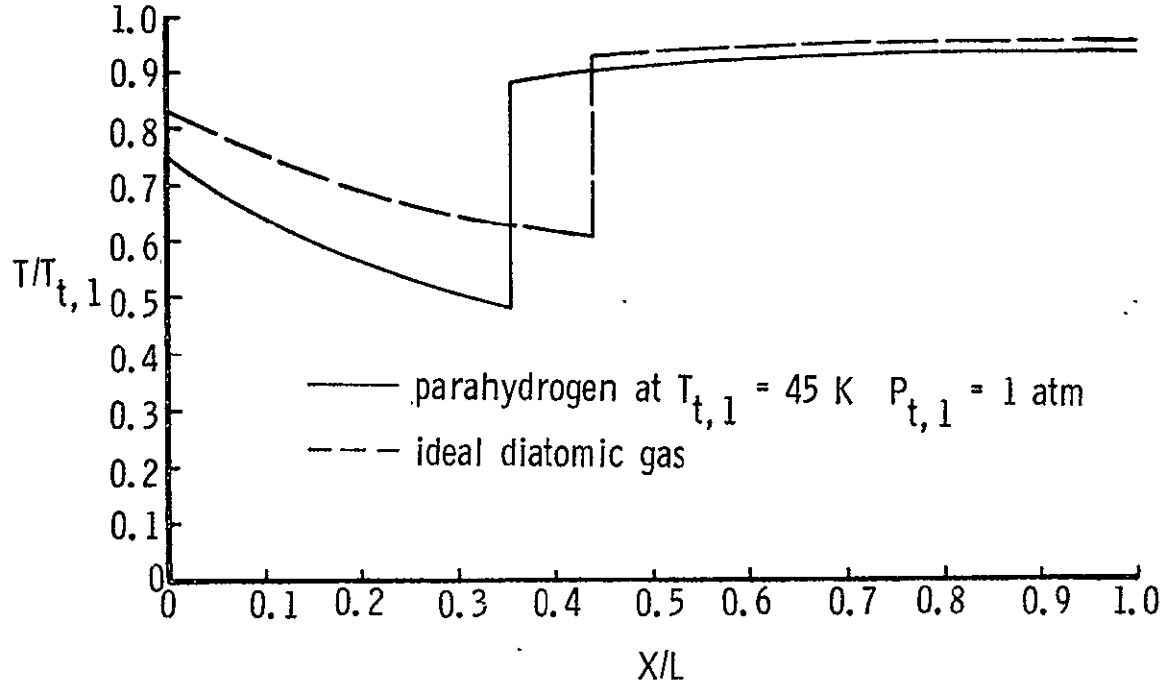

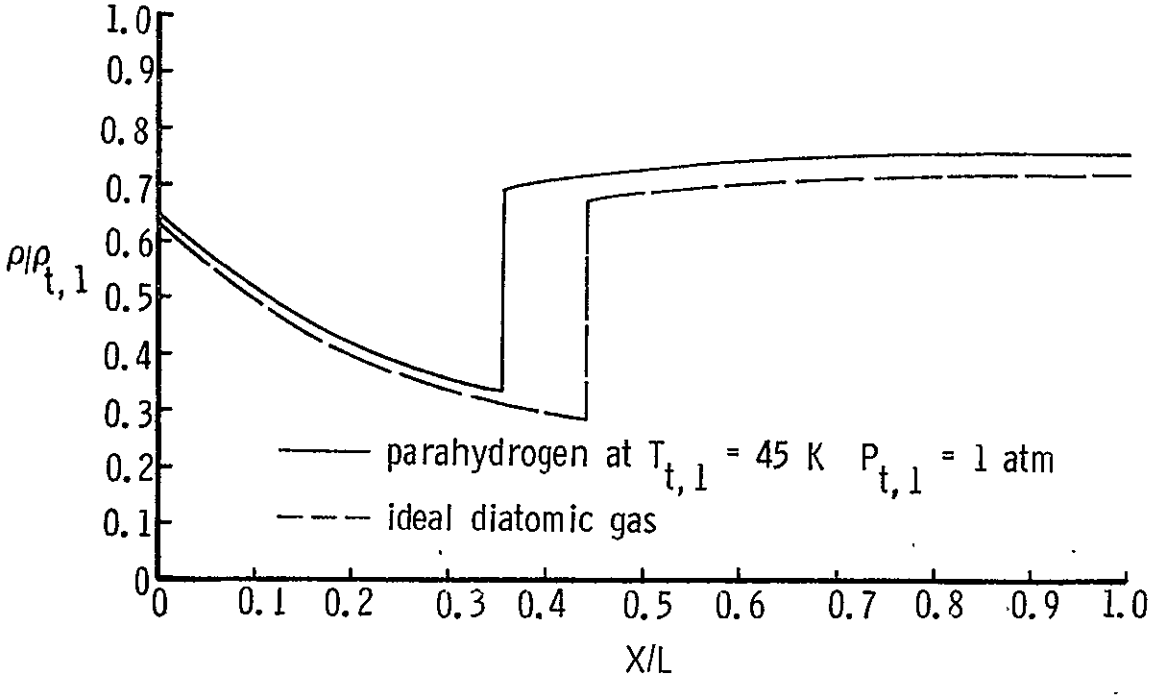

Figure 45. Concluded.

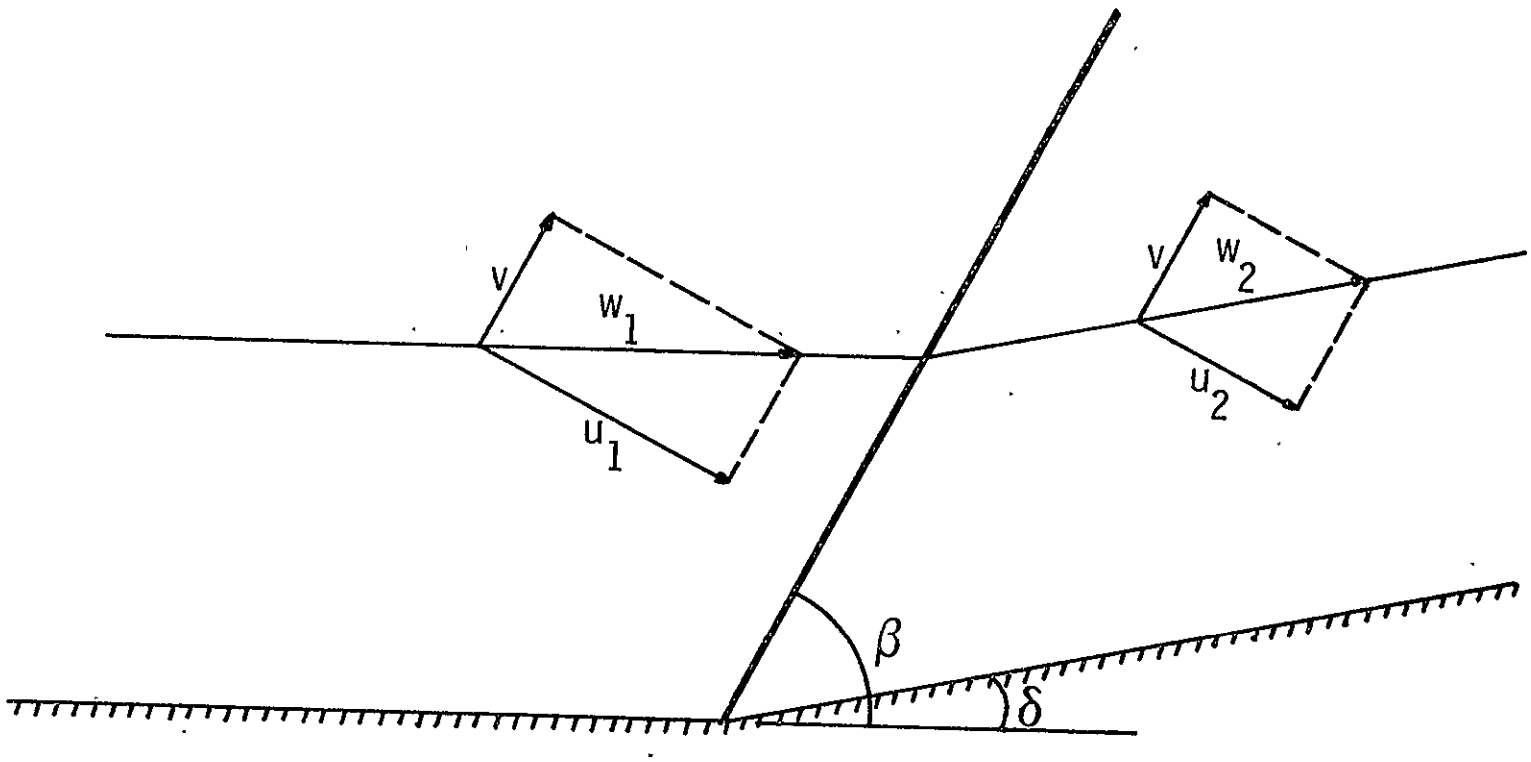

Figure 46. Oblique shock wave geometry.

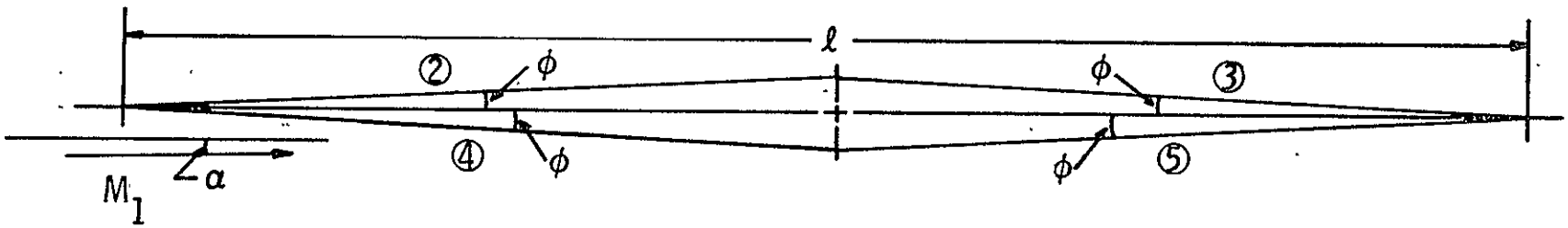

Figure 47. Diamond airfoil geometry.

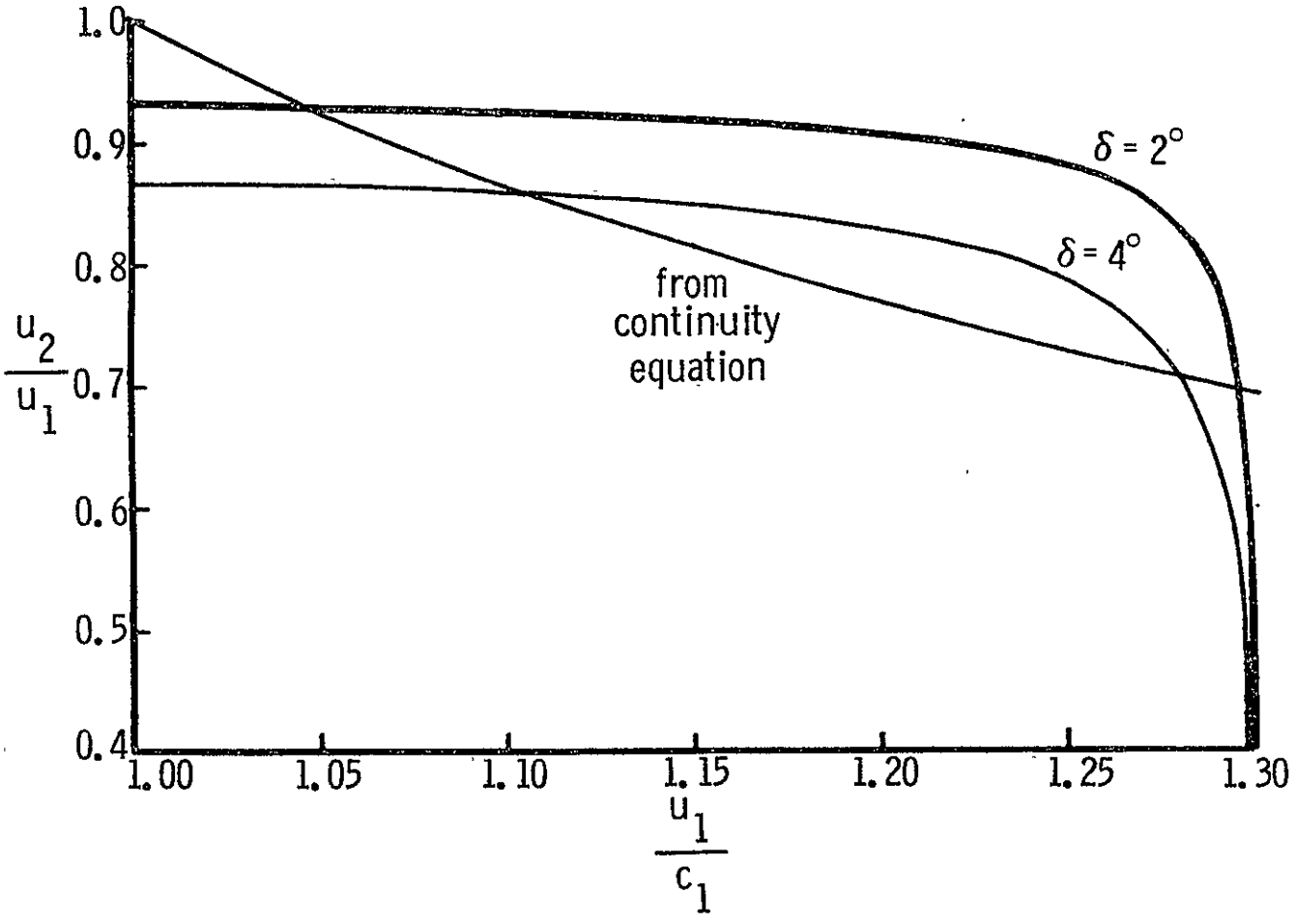

Figure 48. Oblique shock wave solution for the hydrogen case.

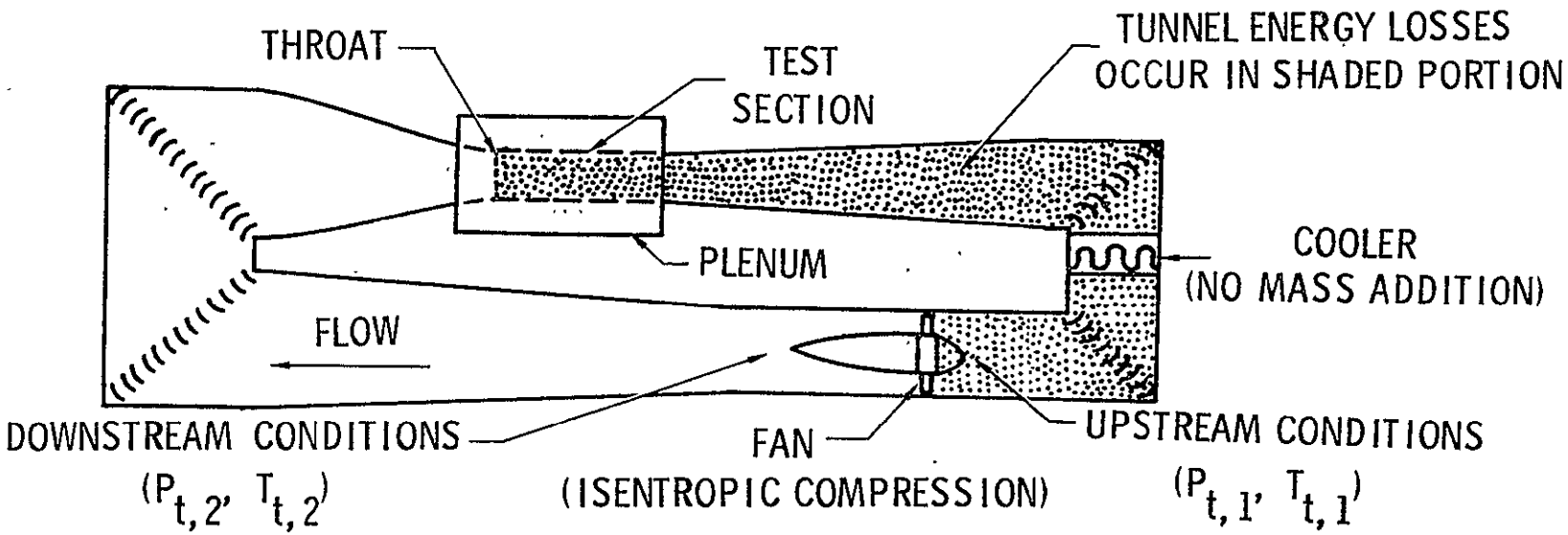

Figure 49. Analytical model of a wind tunnel.

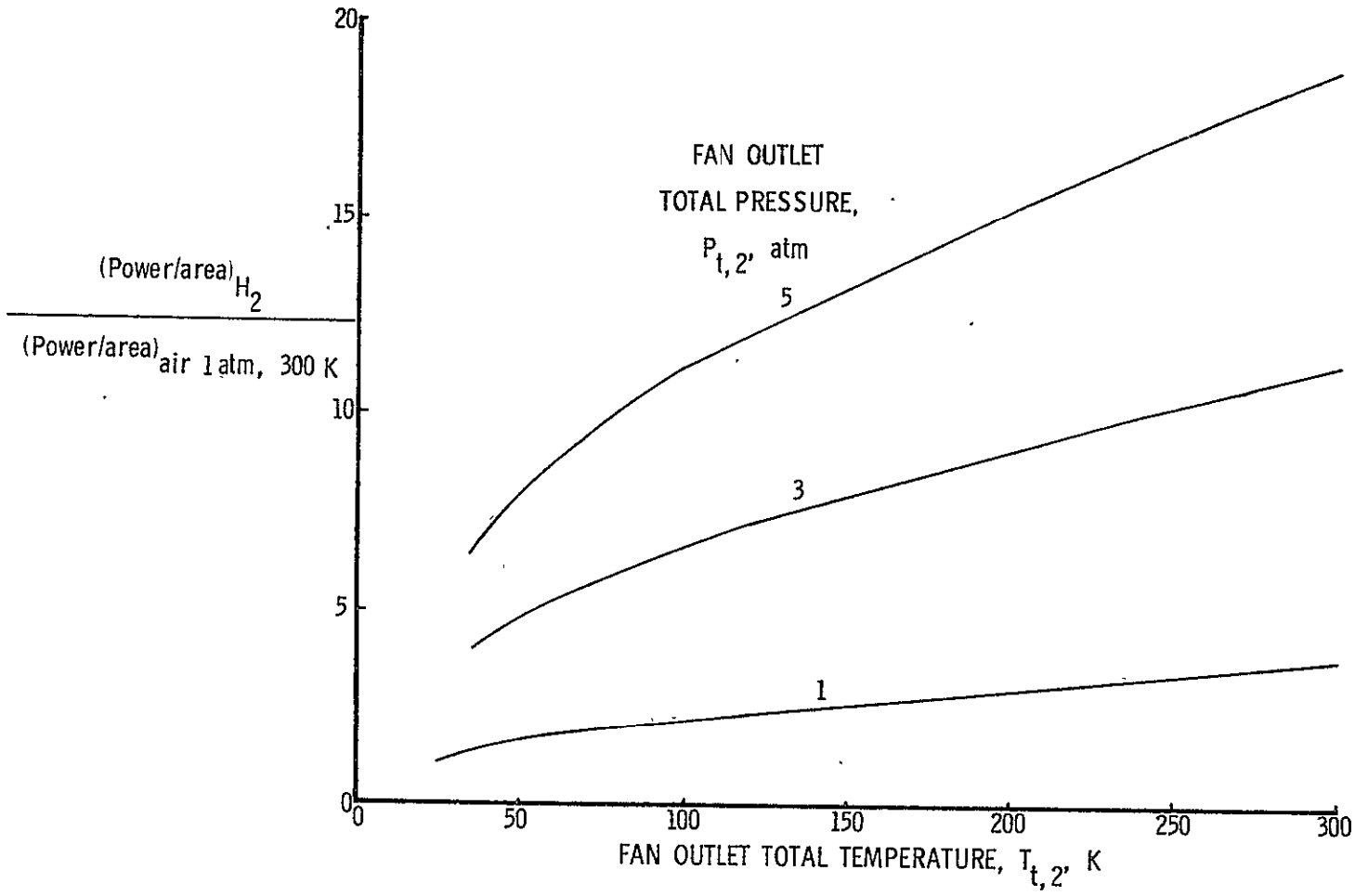

Figure 50. Hydrogen wind tunnel power requirements as a function of fan outlet total temperature.

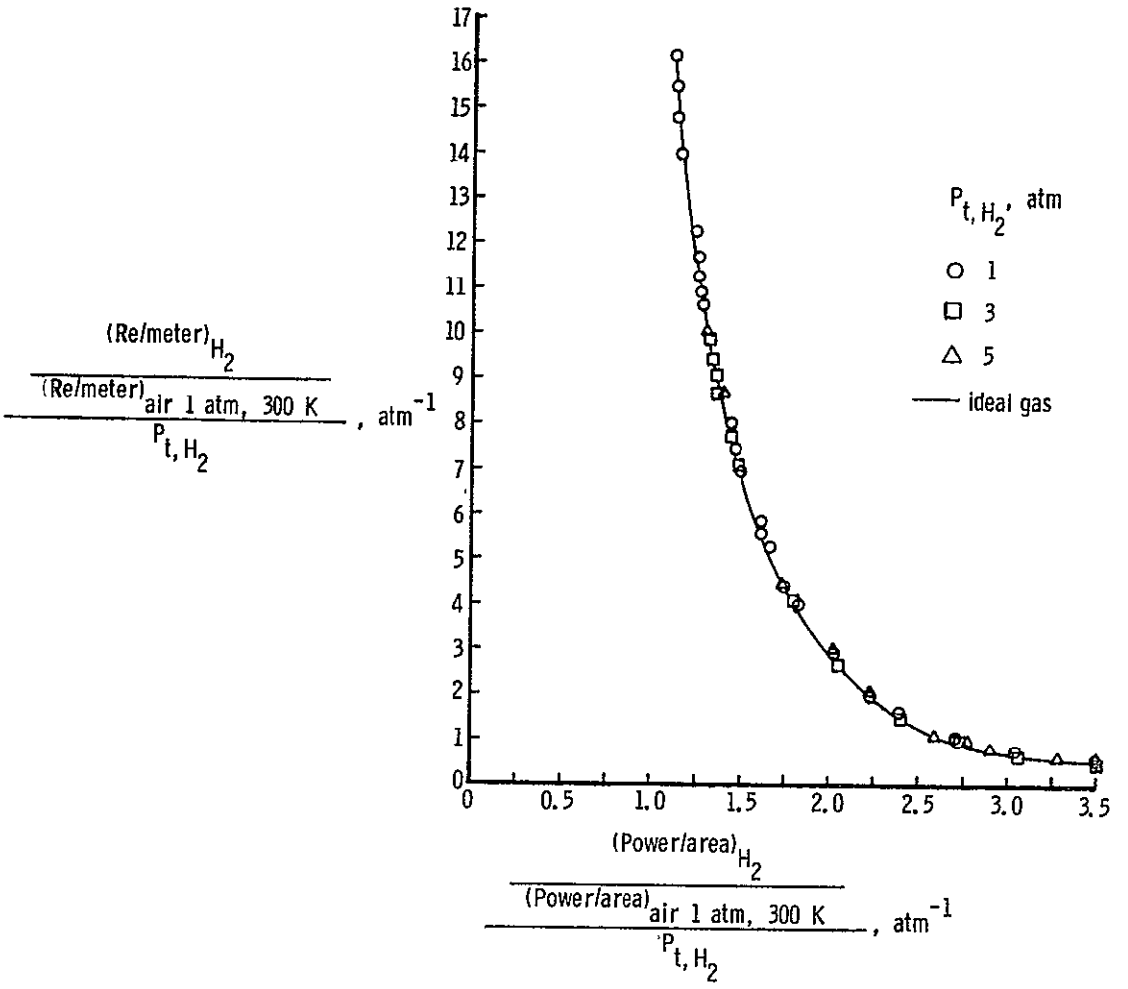

Figure 51. Hydrogen wind tunnel power requirements.

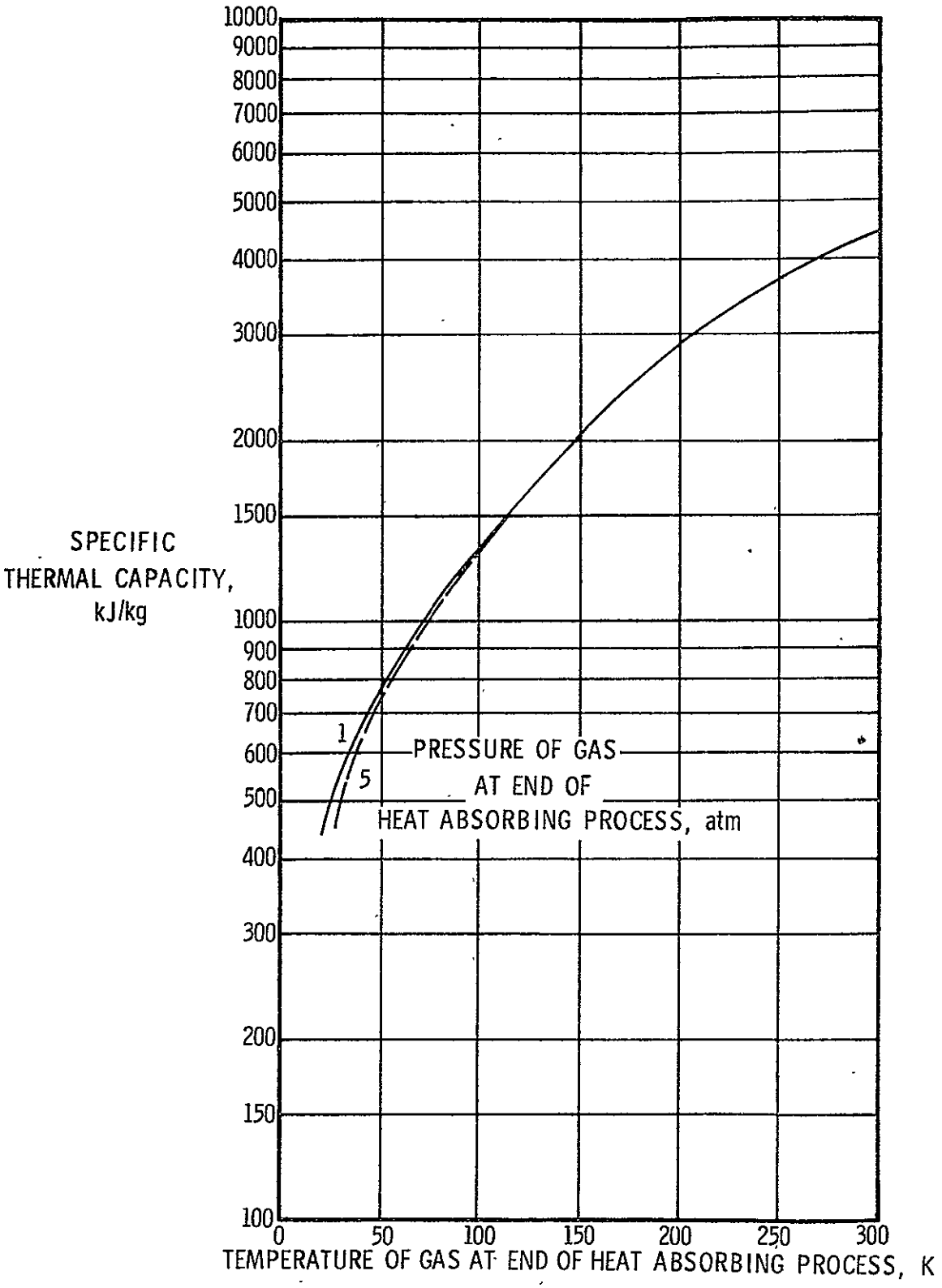

Figure 52. Heat absorbing capacity of liquid parahydrogen. Liquid initial at a pressure of one atmosphere and a temperature of 20.268 K.

APPENDIX B

Tables

M_1	ϕ	α	C_L			C_D		
			ideal	real	$\frac{\text{real-ideal}}{\text{ideal}}$	ideal	real	$\frac{\text{real-ideal}}{\text{ideal}}$
1.3	3°	1°	0.159	0.170	6.49%	0.0134	0.0136	1.34%
1.5	3°	1°	0.123	0.127	3.18%	0.0098	0.0099	0.81%
1.5	5°	1°	0.127	0.134	5.15%	0.0276	0.0280	1.33%
1.5	5°	4°	0.523	0.556	6.33%	0.0287	0.0299	4.30%
1.7	3°	1°	0.101	0.102	0.81%	0.0081	0.0080	-0.20%
1.7	5°	1°	0.100	0.110	10.07%	0.0223	0.0224	0.06%
1.7	5°	4°	0.418	0.427	2.16%	0.0228	0.0230	1.41%
1.7	10°	1°	0.119	0.128	7.12%	0.0928	0.0949	2.21%

TABLE I.

Diamond-shaped airfoil results.

Test Section Mach Number	Fan Pressure Ratio
0.10	1.019
0.15	1.022
0.20	1.025
0.25	1.028
0.30	1.031
0.35	1.034
0.40	1.037
0.50	1.043
0.60	1.050
0.80	1.068
1.00	1.100
1.20	1.200

TABLE II.

Fan pressure ratio necessary to achieve a given test section Mach number.

		AIR at 300 K		NITROGEN at free stream saturation			HYDROGEN at free stream saturation		
Mach number	Reynolds number	P_t, atm	test section area, m^2	P_t, atm	test section area, m^2	drive power relative to air	P_t, atm	test section area, m^2	drive power relative to air
1.0	50×10^6	2.5	173	2.5	9	0.052	2.5	0.73	0.011
		16.7	4	3.5	4	0.210	1.2	4	0.189
0.5	25×10^6	2.0	155	2.0	4.6	0.030	2.0	0.72	0.012
		12.5	4	2.2	4	0.176	0.2	4	0.042
0.1	6×10^6	1.0	764	1.0	16.2	0.021	1.0	1.4	0.005
		57.6	4	2.3	4	0.040	0.1	4	0.005

TABLE III.

Wind tunnel requirements for various test gases at free stream saturation.

Test gas	ε, MW-sec/kg	T_t, K	Test section area, m^2	Mass Flow rate, $\dot{m}$, kg/sec		Power, MW		
				test section	LN_2 or LH_2	drive fan	LN_2 or LH_2 production	total
AIR	—	300	173	103,600	—	777	—	777
N_2	3.5	105	9	9,090	91	23	318	341
H_2	65	30	1.2	655	16	8.5	1040	1048.5

TABLE IV.

Wind tunnel requirements for various test gases at a free stream Mach number of 1.0, a Reynolds number of 50×10^6, a total pressure of 2.5 atmospheres, and a local saturation Mach number of 1.2.

APPENDIX C

Fixed Point Properties of Parahydrogen

Below is a summary, taken from reference 11, of the P-ρ-T data at selected fixed points for parahydrogen.

Critical Point

$T = 32.976 \pm 0.05$ K

$P = 12.759$ atm

$\rho = 31.43$ kg/m^3

Normal Boiling Point

$T = 20.268$ K

$P = 1$ atm

ρ(liquid) $= 70.78$ kg/m^3

ρ(vapor) $= 1.338$ kg/m^3

Triple Point

$T = 13.803$ K

$P = 0.0695$ atm

ρ(solid) $= 86.50$ kg/m^3

ρ(liquid) $= 77.03$ kg/m^3

ρ(vapor) $= 0.126$ kg/m^3

APPENDIX D

Virial Coefficients

One equation of state for parahydrogen is given in terms of the virial coefficients. The virial coefficients are commonly defined as

$$P = RT\rho[1 + B(T)\rho + c(T)\rho^2 + \ldots] \qquad (D.1)$$

where $B(T)$ and $C(T)$ are virial coefficients of a power series expansion in density. Equation D.1 adequately describes the P-ρ-T surface for densities up to about one-half of critical. Reference 11 gives $B(T)$ and $C(T)$ as:

For temperatures below 100 K

$$B(T) = (b_1T + b_2 + b_3/T + b_4/T^2)/RT \qquad (D.2)$$

where

$$b_1 = 1.93977741 \times 10^3 \qquad b_2 = -1.9279522 \times 10^5$$
$$b_3 = -2.2890051 \times 10^6 \qquad b_4 = 1.1094088 \times 10^7$$

For $T < 55$ K

$$C(T) = (c_1T^2 + c_2T + c_3 + c_4/T + c_5/T^2 + c_6/T^3)/RT \qquad (D.3)$$

where there are two sets of the c_i coefficients. One for temperatures below $T_c = 32.95$ K

$$c_1 = 1.0541776 \times 10^5 \qquad c_2 = -1.6597141 \times 10^7$$
$$c_3 = 1.0431411 \times 10^9 \qquad c_4 = -3.2538718 \times 10^{10}$$
$$c_5 = 5.1405848 \times 10^{11} \qquad c_6 = -3.3123453 \times 10^{12}$$

and a second set for temperatures between T_c and 55 K,

$$c_1 = 1.6971294 \times 10^3 \qquad c_2 = -5.0854223 \times 10^5$$
$$c_3 = 6.7284118 \times 10^7 \qquad c_4 = -3.8045171 \times 10^9$$
$$c_5 = 1.0789413 \times 10^{11} \qquad c_6 = -1.1515642 \times 10^{12}$$

For $55 < T < 100$

$$C(T) = a_1 e^{a_2/T} \left\{ 1 - \exp \left[a_3 \left\{ 1 - \left(\frac{T}{a_4} \right)^{a_5} \right\} \right] \right\} \qquad (D.4)$$

where

$$a_1 = 388.682 \qquad a_2 = 45.5$$
$$a_3 = -0.6 \qquad a_4 = 20.0$$
$$a_5 = 4.0$$

For temperatures above 100 K

$$B(T) = \sum_{i=1}^{4} b_i x_1^{(2i-4)/4} \qquad (D.5)$$

and

$$C(T) - c_o x_2^{0.5} \left[1 + c_1 x_2^3 \right] \left[1 - \exp \left(1 - x_2^{-3} \right) \right] \qquad (D.6)$$

where

$b_1 = 42.464$ $\quad$ $b_2 = -37.1172$

$b_3 = -2.2982$ $\quad$ $b_4 = -3.0484$

$x_1 = 109.781/T$ $\quad$ $x_2 = 20.615/T$

$c_o = 1310.5$ $\quad$ $c_1 = 2.1486$

For equations D.2 through D.6 the units of temperature, T, is Kelvin, the units of B(T) are $cm^3/mole$ and the units of C(T) are $(cm^3/mole)^2$.

The uncertainty of B(T) is a maximum of about five percent at the highest and lowest temperatures. The uncertainty of C(T) is a minimum of around five percent between 55 and 100 K and as much as approximately twenty percent for temperatures below the critical temperature.

APPENDIX E

Latent Heat of Vaporization

The latent heat of vaporization is the amount of heat required to convert a unit mass of a substance from the liquid state to the vapor state at a constant pressure and may easily be obtained by subtracting the liquid enthalpy from the enthalpy of the vapor at the same temperature and pressure. From reference 11, the latent heat of vaporization for parahydrogen ranges from 448.2 Joules/gram at the triple point to 445.5 Joules/gram at the normal boiling point to 0 Joules/gram at the critical point. The uncertainty in these values is estimated to be 1.2 Joules/gram.

APPENDIX F

Thermal Conductivity of Parahydrogen

The thermal conductivity coefficient relates the transfer of heat through a material via molecular interaction caused by a temperature gradient across the material. That is

$$q = -k \text{ grad } T \tag{F.1}$$

where q is the heat flux, grad T is the temperature gradient and k is the thermal conductivity coefficient.

One of the most popular methods of correlating thermal conductivity, for example reference 11, is to separate the property into a number of additive parts

$$k = k_o(T) + k_E(\rho,T) + k_c(\rho,T) \tag{F.2}$$

where $k_o(T)$ is the dilute gas contribution (a function of temperature only, $k_E(\rho,T)$ is the excess function, and $k_c(\rho,T)$ gives the enhancement due to the critical point behavior.

The thermal conductivity of a gas may also be expressed in terms of its specific heat at constant volume, C_v, its viscosity coefficient, η, and its molecular weight, M_w, by

$$k = k_1 \eta C_v / M_w \tag{F.3}$$

where the factor k_1 allows for the fact that the mean energy of the molecules appears larger as the molecules possessing large amounts of kinetic energy travel faster and thus transfer their energy more rapidly. When the molecules possess only translational kinetic energy (i.e. in the case of hydrogen at temperatures less than 50 K) k_1 is equal to 2.5. If the rotational kinetic energy is completely available (i.e. for hydrogen above 300 K) then k_1 is equal to 1.9. In reference 4, Farkas gives an approximation of k_1 as

$$k_1 = \frac{2.25\ R + C_v}{C_v} \tag{F.4}$$

where R is the gas constant. Therefore, the thermal conductivity coefficient is given as

$$k = \frac{(2.25\ R + C_v)\eta}{M_w} \tag{F.5}$$

APPENDIX G

Viscosity of Parahydrogen

The viscosity of a fluid may be separated into two additive parts

$$\eta = \eta_o(T) + \eta_E(\rho,T) \tag{G.1}$$

where $\eta_o(T)$ is the dilute gas contribution and $\eta_E(\rho,T)$ is the excess or dense gas contribution and is a strong function of density. In the lower temperature range of $T < 100$ K, reference 7 gives

$$\eta_o(T) = a_1 \left[T^{3/2}/(T + a_2)\right]\left[(T + a_3)/(T + a_4)\right] \tag{G.2}$$

where

$$a_1 = 8.5558 \times 10^{-6} \qquad a_2 = 19.55$$
$$a_3 = 650.39 \qquad a_4 = 1175.9$$

and for the excess viscosity contribution

$$\eta_E(\rho,T) = A(\rho) \exp\left[B(\rho)/T\right] \tag{G.3}$$

where

$$A(\rho) = \frac{(A_1\rho + A_2\rho^2 + A_3\rho^3)}{(1.0 + A_4\rho + A_5\rho^2 + A_6\rho^3)} \times 10^{-6} \tag{G.4}$$

$$A_1 = 306.4636 \qquad A_2 = -3350.628$$
$$A_3 = 38680.92 \qquad A_4 = -18.4783$$
$$A_5 = 110.915 \qquad A_6 = 25.3524$$

and

$$B = B_o + B_1 \left[(\rho/B_2)^{b_1} - (\rho/B_2)^{b_2} \right] + B_3 \exp \left[B_4 (\rho/B_2)^{b_3} \right] \qquad (G.5)$$

$$B_0 = 10.0 \qquad B_1 = 7.2$$
$$B_2 = 0.07 \qquad B_3 = -17.63$$
$$B_4 = -58.75 \qquad b_1 = 6.0$$
$$b_2 = 1.5 \qquad b_3 = 3.0$$

For equations G.2 through G.5, the temperature, T, is in Kelvin, the density, ρ, is in g/cm^3, and the viscosity η, is in g/(cm-sec).

The uncertainty in the lower temperature range, using the above formula, is estimated in reference 7 to be approximately one-half percent and increases to about ten percent if the same formula is used for temperatures up to 300 K.

APPENDIX H

Vapor Pressure for Parahydrogen

The vapor pressure is the pressure, as a function of temperature, of a liquid in equilibrium with its own vapor. For parahydrogen, from reference 6,

$$P = 10^{P_o} + A_5 (T-29)^3 + A_6(T-29)^5 + A_7(T-29)^7 \qquad (H.1)$$

where

$$P_o = A_1 + \frac{A_2}{T + A_3} + A_4 T \qquad (H.2)$$

and

$$A_1 = 2.000620 \qquad A_2 = -50.09708$$

$$A_3 = 1.0044 \qquad A_4 = 1.748495 \times 10^{-2}$$

$$A_5 = \begin{cases} 0 & \text{for } T \leq 29 \text{ K} \\ 1.317 \times 10^{-3} & \text{for } T > 29 \text{ K} \end{cases}$$

$$A_6 = \begin{cases} 0 & \text{for } T \leq 29 \text{ K} \\ -5.926 \times 10^{-5} & \text{for } T > 29 \text{ K} \end{cases}$$

$$A_7 = \begin{cases} 0 & \text{for } T \leq 29 \text{ K} \\ 3.913 \times 10^{-6} & \text{for } T > 29 \text{ K} \end{cases}$$

The units of pressure, P, is atmospheres while the units on the temperature, T, is Kelvin.

APPENDIX I

Specific Cooling Capacity of Parahydrogen

The specific cooling capacity is the amount of heat which may be absorbed by a unit mass of parahydrogen in being warmed from storage conditions to the final tunnel total conditions. In this investigation the assumption is made that the liquid hydrogen is stored at atmospheric pressure. The liquid is then compressed to the operating pressure of the wind tunnel before being injected into the tunnel circuit. Assuming the compression is isentropic and assuming the vaporizing and warming of the injected hydrogen occurs at a constant pressure, the specific cooling capacity, as given in figure 52, is determined by

$$\text{specific cooling capacity} = \int_1^t T \, dS \qquad \text{(I.1)}$$

$$= H_t - H_1$$

where H_t is the enthalpy at the tunnel total conditions and H_1 is the enthalpy at the liquid initial conditions.

The specific cooling capacity for parahydrogen, in kJ/kg, may be approximated by

$$\text{specific cooling capacity} = \sum_{i=0}^{5} B_i T^i \qquad \text{(I.2)}$$

where

T = temperature, K

and where the values of B_i are given by

$$B_i = \sum_{j=0}^{2} B_{ij} P^j \qquad (I.3)$$

where

P = pressure, atmospheres

and the values of B_{ij} are as follows:

$B_{00} = 2.3362 \times 10^{2}$	$B_{01} = -2.6924 \times 10^{1}$	$B_{02} = -1.9693$
$B_{10} = 1.2591 \times 10^{1}$	$B_{11} = 7.4355 \times 10^{-1}$	$B_{12} = 7.1273 \times 10^{-2}$
$B_{20} = -7.4035 \times 10^{-2}$	$B_{21} = -8.9004 \times 10^{-3}$	$B_{22} = -9.6843 \times 10^{-4}$
$B_{30} = 9.0181 \times 10^{-4}$	$B_{31} = 5.2144 \times 10^{-5}$	$B_{32} = 6.0474 \times 10^{-6}$
$B_{40} = -3.3958 \times 10^{-6}$	$B_{41} = -1.4658 \times 10^{-7}$	$B_{42} = -1.7605 \times 10^{-8}$
$B_{50} = 4.2281 \times 10^{-9}$	$B_{51} = 1.5789 \times 10^{-10}$	$B_{52} = 1.9350 \times 10^{-11}$

The values of the specific cooling capacity calculated from equation I.2 agree with the values calculated from equation I.1 generally within two percent for pressures from one to ten atmospheres and for temperatures from saturation to 300 K.